A Novel Halogenation Protocol and Non-heme Iron Hydroxylase Mimics as Catalysts for C-H Oxidation and O₂ Activation

by

Yu He

A dissertation submitted to the Graduate Faculty of
Auburn University
in partial fulfillment of the
requirements for the
Doctor of Philosophy

Auburn, Alabama
August 8, 2012

Approved by

Christian R. Goldsmith, Chair, Assistant Professor of Chemistry and Biochemistry
David M. Stanbury, Professor of Chemistry and Biochemistry
German Mills, Associate Professor of Chemistry and Biochemistry
Orlando Acevedo, Associate Professor of Chemistry and Biochemistry
Mario Eden, Associate Professor of Chemical Engineering

Abstract

Hydrocarbons react with molar concentrations of peracetic acid and halide salts to yield predominantly monohalogenated products under optimum conditions, with chlorination being more oxidatively efficient than bromination. The alkane halogenation proceeds at ambient temperature and does not require a heavy-metal catalyst. The observed reactivity is consistent with a radical mechanism, in which the peracid initially reacts with the halide ions to yield halogen-atom radicals, which ultimately oxidize the hydrocarbon. Although the reactivity proceeds slightly more efficiently in acetonitrile, the halogenation protocol works well in water.

Iron complexes with the tetradentate N-donor ligand *N*,*N′*-di(phenylmethyl)-*N*,*N′*-bis(2-pyridinylmethyl)-1,2-cyclohexanediamine (bbpc) are reported. Despite the benzyl groups present on the amines, the iron compounds catalyze the oxygenation of cyclohexane by peroxides to an extent similar to those employing less sterically encumbered ligands. The catalytic activity is strongly dependent on the counterion, with the highest activity and the strongest preference for alkane hydroxylation correlating to the most weakly coordinating anion, SbF_6^-. The selectivity for the alcohol product over the ketone is amplified when acetic acid is present as an additive. When hydrocarbon substrates with both secondary and tertiary carbons are oxidized by H_2O_2, the catalyst directs oxidation toward the secondary carbons to a greater degree than other previously reported iron-containing homogeneous catalysts.

[Fe(bbpc)(MeCN)$_2$](SbF$_6$)$_2$ is also found to react with O$_2$ in the presence of hydrocarbons. During these reactions, a ferric hydroperoxide species is observed and identified by mass spectrometry and electron paramagnetic resonance. The rate of formation of the Fe(III)-OOH species scales with the concentration of hydrocarbon and the strength of the C-H bond, suggesting that it may be formed via a hydrogen atom abstraction by a ferric superoxo species.

Acknowledgements

This dissertation is completed under the supervision of Prof. Christian R. Goldsmith. I am very grateful for all the help I got from him. I learned and benefited a lot from his profound knowledge and experience in chemistry, his rigorous request on scientific accuracy of every single detail. I also owe thanks to Prof. David M. Stanbury, who generously provides access to a Stopped-Flow Spectrophotometer for kinetic studies, and also shares his insight in helpful discussions. I extend my thanks to Dr. Anne Gorden and Dr. John Gorden for their help with X-ray structure determinations, among much other help. I am indebted to Prof. Evert Duin for his help collecting EPR data, Dr. Yonnie Wu for his assistance with MS determinations, Dr. Meadows for his help with NMR. Prof. German Mills, Prof. Orlando Acevedo and Prof. Mario Eden spent their precious time serving on the committee and providing advice on this dissertation. I appreciate their help and care. I owe thanks to Nootan Bhattarai and Divya Prakash for their help during kinetic and EPR studies, respectively. I appreciate the friendship I got from my labmates Wenchan Jiang, Qiao Zhang and Meng Yu.

Finally, I would like to thank my wife Yan Guo, who has been supporting me through all these years and brought me the greatest joy of my life, Joyce Ho. I dedicate this dissertation to my beloved father, who shall be rejoicing upon watching me in a doctoral gown.

Table of Contents

List of Tables

List of Figures

ix

List of Schemes

Chapter 1

Introduction to C-H Activation with Focuses on Halogenation and Oxygenation Catalyzed by Non-heme Iron Enzymes and Small Molecules

Functionalizing chemically inert C-H bonds to synthetically versatile C-X (X=Cl, Br, I, OH, *etc*) bonds remains a great challenge.[1-5] With regard to modeling non-heme iron halogenases, only moderate progress has been made in terms of catalytic halogenation of aliphatic hydrocarbons.[6-8] Many non-catalytic protocols work only with electron-rich substrates.[2] For regioselective hydroxylation with non-heme iron hydroxylase mimics as catalysts, the selectivity is mainly directed towards electron-rich tertiary C-H bonds in most circumstances.[3] O_2 activation has been an intensive research topic because O_2 is cheap, easy to acquire and store compared to other commercial oxidants. However, the mechanism is not well established and the substrates are limited to hydrocarbons containing allylic or even weaker C-H bonds.[9-12] In this thesis, we report a novel protocol for halogenating aliphatic hydrocarbons (Chapter 2), a non-heme iron hydroxylase model catalyst that directs regioselective oxidation towards secondary C-H bonds (Chapter 3). In the preceding chemistry, a ferric hydroperoxo species was characterized, which could also be generated between reactions of the catalyst, O_2, and alkenes or even alkanes (Chapter 4).

1.1 Protocols for Halogenating of Aliphatic C-H Bonds

Traditionally, chlorine-containing compounds are prepared by mixing a hydrocarbon precursor with molecular chlorine (Cl_2) at high temperatures or under irradiation.[13] Either of these methods triggers a radical chain reaction through the splitting of the Cl-Cl bond. The resultant chlorine radicals serve as the oxidants, abstracting hydrogen atoms from the hydrocarbon to yield HCl and an organic radical. The organic radical abstracts a chlorine atom from Cl_2, producing organochlorides.

2

These reactions are hard to control and usually result in multiple chlorinated products. The lack of selectivity makes the method inadequate for most specialized synthetic purposes. Additionally, Cl_2 is hazardous and difficult to handle.

Naturally occurring products that contain halogens usually are organochlorides or organobromides.[1, 14] The biosyntheses of these compounds often require halogenase enzymes, which activate C-H bonds to C-Cl or C-Br functional groups.[1] The active site of the non-heme iron halogenase SyrB2 is shown in Scheme 1.1.[15] The iron is coordinated to two histidine residues, an exogenous α-ketoglutarate, and an exogenous water molecule. These three ligands are common in mononuclear non-heme iron hydroxylases.[15] The proposed mechanism of substrate halogenation is also shown in Scheme 1.1.[16] Upon binding the substrate (RCH_3), the water molecule vacates the active site, allowing O_2 to bind. The formed Fe^{III} superoxo species reacts with α-ketoglutarate to produce an Fe^{IV} oxo species, succinate, and CO_2. The $Fe^{IV}=O$, identified with Mössbauer[17] and X-ray absorption spectroscopies (XAS) [18], is powerful enough to activate aliphatic C-H bonds with high bond dissociation energies (BDEs). In the proposed catalytic cycle, this generates an $Fe^{III}(OH)(Cl)$ species and an organic radical. The chlorine atom on the Fe^{III} center subsequently transfers to the carbon radical, yielding the chlorinated product and regenerating the Fe^{II}.
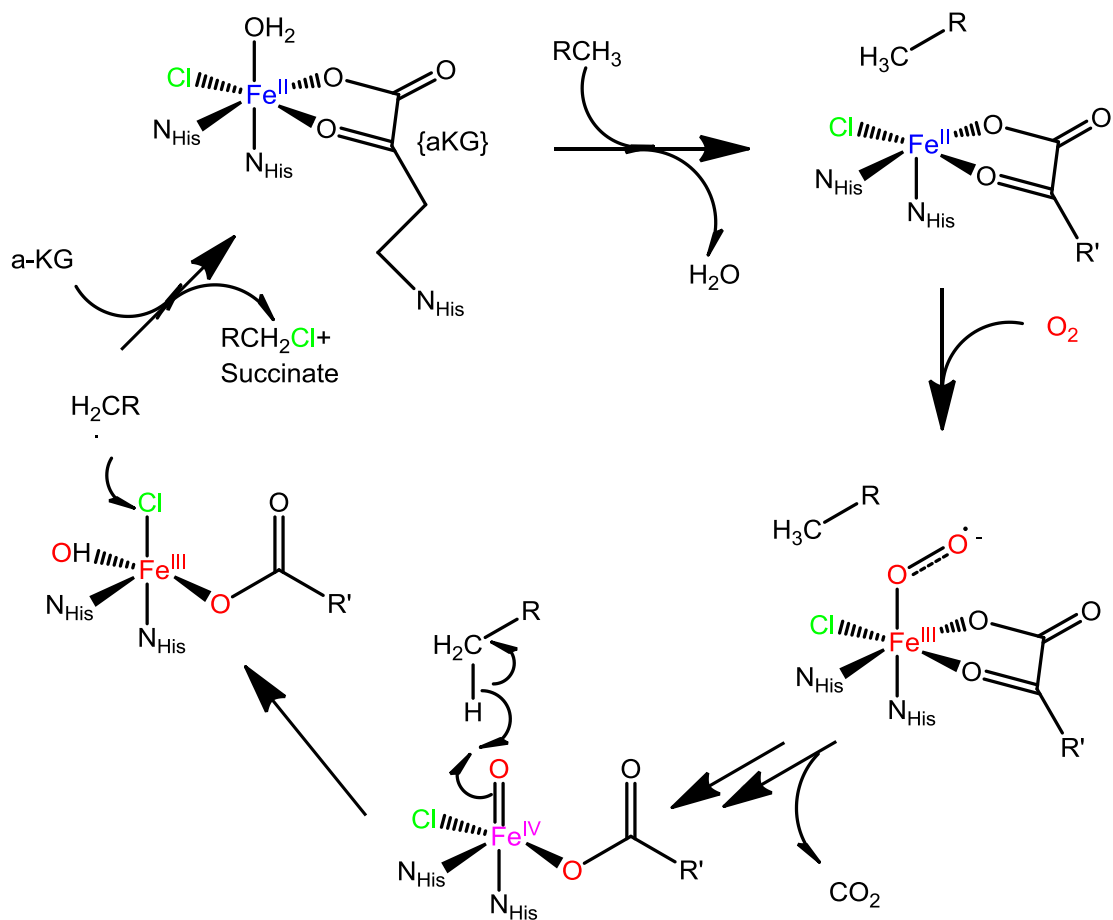
Scheme 1.1 Proposed mechanism of halogenation by halogenase SyrB2 [15]

SyrB2 and other non-heme iron halogenases have inspired synthetic inorganic chemists seeking to replicate the enzymes' catalysis of C-H chlorination. The transition-metal complex [Fe^{II}(TPA)Cl_2] (TPA = tripicolylamine, Scheme 1.3) can oxidize cyclohexane to chlorocyclohexane using *tert*-butylhydroperoxide (TBHP) as a terminal oxidant.[6-7] The chloride can be replaced by bromide, resulting in bromination. This halogenation is stoichiometric with respect to the metal complex. Even when an excess of TBHP is added, only a single equiv. of organohalide is produced; the excess TBHP results in substrate oxygenation instead of halogenation. Comba obtained catalytic chlorination using PhIO as the terminal oxidant and [Fe^{II}(L)X_2] (L = 3,7-

4

dimethyl-9-oxo-2,4-bis(2-pyridyl)-3,7-diazabicyclo[3.3.1]nonane-1,5-dicarboxylate

methyl ester, X=Cl, Br; Scheme 1.3) as the catalyst.[8] The optimum turnover number

(TON) for this system was 3.7; with other oxidants, oxygenated products are favored.[8]

Groves reported a manganese porphyrin complex capable of catalyzing the

chlorination of C-H bonds by NaOCl.[19] The ligand's steric hindrance is proposed to

direct the chlorination towards less sterically congested sites on the hydrocarbon

substrate.[19] For instance, C2 and C3 of 5α-cholestane were selectively chlorinated

because of steric effects.[19] Sawyer reported chlorination of alkanes by mixtures of Fe^{II}

salts, H_2O_2, and HCl.[20] This variation of Fenton chemistry has a low efficiency with

respect to chlorination, with the best system having a TON of 3.6.[20]

Although electron-rich substrates, such as aromatic rings and alkenes, can be

halogenated through a number of processes using cheap and environmentally benign

oxidants, such as H_2O_2 and O_2,[21] the analogous halogenation of aliphatic C-H bonds

remains elusive. For non-catalytic chlorination of aliphatic hydrocarbons, thionyl

chloride ($SOCl_2$) [22], sulfuryl chloride (SO_2Cl_2) [23], or dichloriodosobenzene ($PhICl_2$) [24]

are usually used as reagents. These reagents are either unstable or toxic, therefore

representing a questionable upgrade over Cl_2. Additionally, these reagents are difficult

to prepare and store.

1.2 Non-heme Hydroxylases and their Functional Models

Strong similarities exist between non-heme iron halogenase and hydroxylase

enzymes. The active site of a typical non-heme iron hydroxylase is illustrated in

Scheme 1.2. The active site has the iron bound to two histidine residues and an

exogenous α-ketoglutarate. The sole structural difference is that the chloride/bromide is replaced by an endogenous carboxylate ligand (from either a glutarate or aspartate residue) in the hydroxylase. The similarity of the active sites has led researchers to propose similar catalytic cycles, which both feature ferryl oxo species as the relevant oxidants.[1] In each mechanism, the rate-determining step is the abstraction of a hydrogen atom from the hydrocarbon, producing transient Fe^{III}-OH and alkyl radicals. The subsequent rebound of HO$\cdot$ to the alkyl radical yields the alcohol, in addition to the succinate and CO_2 formed from the oxidation of α-ketoglutarate (Scheme 1.2).

The most intensely studied non-heme iron hydroxylase is arguably taurine: α-ketoglutarate dioxygenase (TauD). Work with deuterated subtrates demonstrates that C-H bond cleavage is the rate determining step, since the k_H/k_D kinetic isotope effect (KIE) is approximately 37.[25] The proposed catalytic cycle proceeds though two high-valent iron species: an end-on iron(III) hydroperoxo and an iron(IV) oxo. The latter was spectroscopically characterized for TauD and prolyl 4-hydroxylase by Mössbauer spectoscopy.[26-27]

In 1990, Collins structurally characterized the first synthetic non-heme iron(IV) complex using an oxidatively resistant tetra-amido macrocyclic ligand.[28] It is noteworthy that the iron(IV) was generated from O_2 activation.[28] The pentadentate iron(IV) was coordinated by the four nitrogen atoms from the ligand and an exogenous choride.[28] Collins's complex remains the only structurally characterized high-spin iron(IV) that lacks an oxo ligand. Density functional theory (DFT) calculations suggest that the high-spin ($S = 2$) iron(IV) intermediates are more

efficient at hydrogen atom abstraction than their low-spin ($S = 1$) analogs.[29] Another crystalline high-spin iron(IV) species was reported in 2010.[30] In order to stabilize the $Fe^{IV}=O$, all the reactive hydrogens were replaced with deuterium and a mild oxidant 2-($^tBuSO_2$)C_6H_4IO was used as the O atom donor.[30] Most other reported iron(IV) species were at low-spin states. In 2003, Que reported the mononuclear non-heme iron(IV) oxo species, $[Fe^{IV}(O)(TPA)]^{2+}$.[31] Later that year, Que reported the crystal structure (Figure 1.1) of a low-spin iron complex $[Fe^{IV}(TMC)(O)(MeCN)]$ (TMC = 1,4,8,11-tetramethyl-1,4,8,11-tetraazacyclotetradecane, Scheme 1.3).[32] The complex was prepared by reacting an iron(II) precursor with iodosylbenzene (PhIO). The iron(IV) product is pale green, with an absorption maximum wavelength at 820 nm (ε = 400 M^{-1} cm^{-1}) at -40 °C.[32] Unlike previously reported iron(IV) species with neutral ligands, the TMC complex persists indefinitely, with a life-time of at least a month at − 40 °C ($t_{1/2}$ ~10 h at 25 °C).[32] A similar $Fe^{IV}=O$ species was proposed in the TMC complex's catalysis of olefin epoxidation by H_2O_2.[33] The life-time of the iron(IV) species is significantly curtailed under such conditions, and the iron(IV) only lasts for a couple of minutes at -40 °C.[33] Several other low-spin iron(IV) oxo complexes have been subsequently prepared with neutral N-donor ligands (Scheme 1.3): $[Fe^{IV}(O)N4Py]^{2+}$ (N4Py = N,N'-bis(2-pyridylmethyl)-bis(2-pyridyl)methylamine),[34] $[Fe^{IV}(O)(cyclam-acetate)]^+$ (cyclam-acetate = 1,4,8,11-tetraazacyclotetradecane-1-acetate),[33] $[Fe^{IV}(O)(\beta-bpmcn)]^{2+}$ (bpmcn = N,N'-bis(2-pyridylmethyl)-N,N'-dimethyl-*trans*-1,2-diaminocyclohexane),[35] and $[Fe^{IV}(O)(TMCS)]^{2+}$ (TMCS = 1-mercaptoethyl-4,8,11-trimethyl-1,4,8,11-tetraaza cyclotetradecane).[36]

7
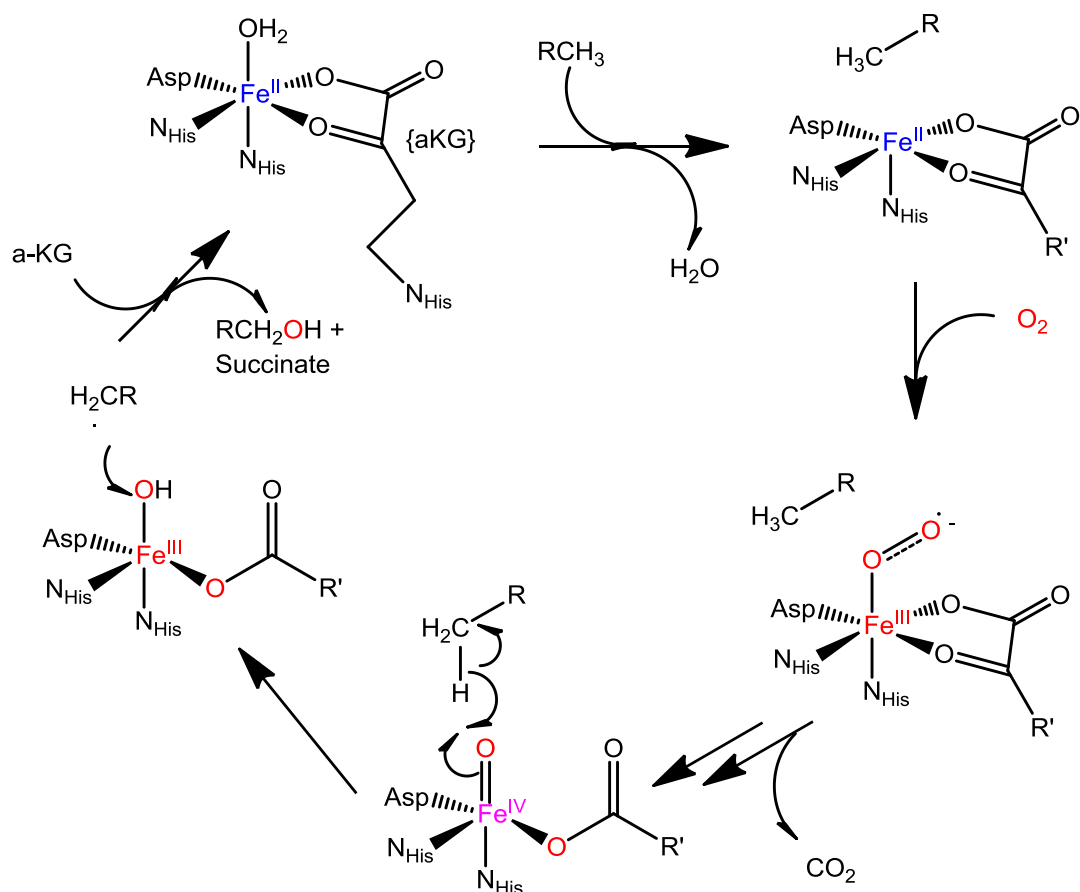
Scheme 1.2 Proposed mechanism of hydroxylation by hydroxylases [1]

Although the study of biologically relevant iron(IV) oxo species has progressed much in the recent decades, those of synthetic iron(III) superoxo, peroxo, and hydroperoxo complexes have lagged by comparison. These compounds may also be capable oxidants and in many cases are proposed as precursors to iron(IV) oxo oxidants. No crystal structures of any of these species were reported until the 2011 structure of [Fe^{III}(TMC)(O$_2$)]$^+$ by Nam (Figure 1.2).[37] Several crystal structures of enzymatic O$_2$-adducts, however, have been reported.[38-40] For the iron(III)-O$_2$ adducts, O$_2$ can bind to the iron in one of two configurations: superoxo is end-on, but peroxo is either side-on or end-on. The superoxo and peroxo formally differ by one electron. The superoxo species could potentially abstract a hydrogen atom from a hydrocarbon

8

substrate to yield an iron(III) hydroperoxo species. The related peroxo species could potentially abstract a proton from solution to form the same iron(III) hydroperoxo complex.
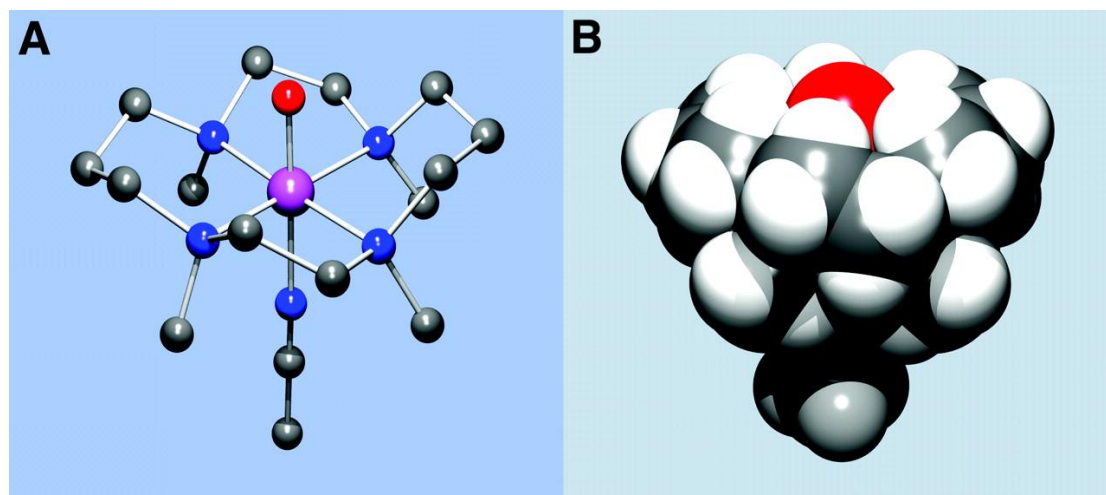
Figure 1.1 Crystal structure of [Fe(IV)(TMC)(O)(MeCN)](OTf)$_2$. (**A**) Molecular structure of the cation of *trans*-[Fe(IV)(O)(TMC)(MeCN)](OTf)$_2$ and (**B**) space-filling representation, derived from the high-resolution single-crystal structure determination. Reprint with permission from AAAS, ref 32. Copyright 2003 AAAS.

Iron(III) hydroperoxo species are believed to be relevant oxidants in a number of reactions, including the nucleophilic deformylation of aldehydes and electrophilic oxidation of C-H bonds.[37] [Fe^{III}(TMC)(O$_2$)]$^+$ was generated by reacting [Fe^{II}(TMC)(CF$_3$SO$_3$)$_2$] with 5 equiv. of H$_2$O$_2$ and 2 equiv. of triethylamine in trifluoroethanol at 0 °C.[37] X-ray quality crystals were grown from a 1:1 mixture of methanol/ether with excess NaClO$_4$ at -40 °C.[37] Peroxo bridged diiron species could also be generated directly with O$_2$ as an oxidant with [Fe^{II}BH(pz′)$_3$(O$_2$CC(O)R)] (pz′= 3,5-bis(isopropyl)-pyrazolyl, R = Me or Ph. BH(pz′)$_3$ was also denoted as Tp^{ipr2}, Scheme 1.3).[12] In other cases, a mixture of discrete electron donors, such as BPh$_4$$^-$, and proton donors are needed to generate hydroperoxo species from O$_2$ and iron(II)

precursors.[41-43] Theoretically, substrates with weak C-H BDEs, such as cyclohexene, can potentially react with a ferric superoxo species to yield a hydroperoxo species by simultaneously obtaining a proton and an electron through a hydrogen atom transfer.[10] However, no iron(III) hydroperoxide complexes have ever been observed in the reactions between iron(II) complexes, O_2, and hydrocarbons. Even though such an Fe^{III}-OOH was proposed as a key intermediate in the oxidation of cyclohexene by O_2 by the iron TMC complex, it was not stabilized and observed.[10] The formation of the hydroperoxo complex was instead inferred through the isolation of the peroxo under basic conditions.[37, 10] In the third and fourth chapters of this thesis, we report $[Fe(bbpc)(OOH)]^{2+}$, which can be generated from either H_2O_2 or O_2. Chapter 4 reports the first instance of an observable (albeit unstable) iron(III) hydroperoxide resulting from the reaction between an iron(II) precursor, O_2, and a hydrocarbon.
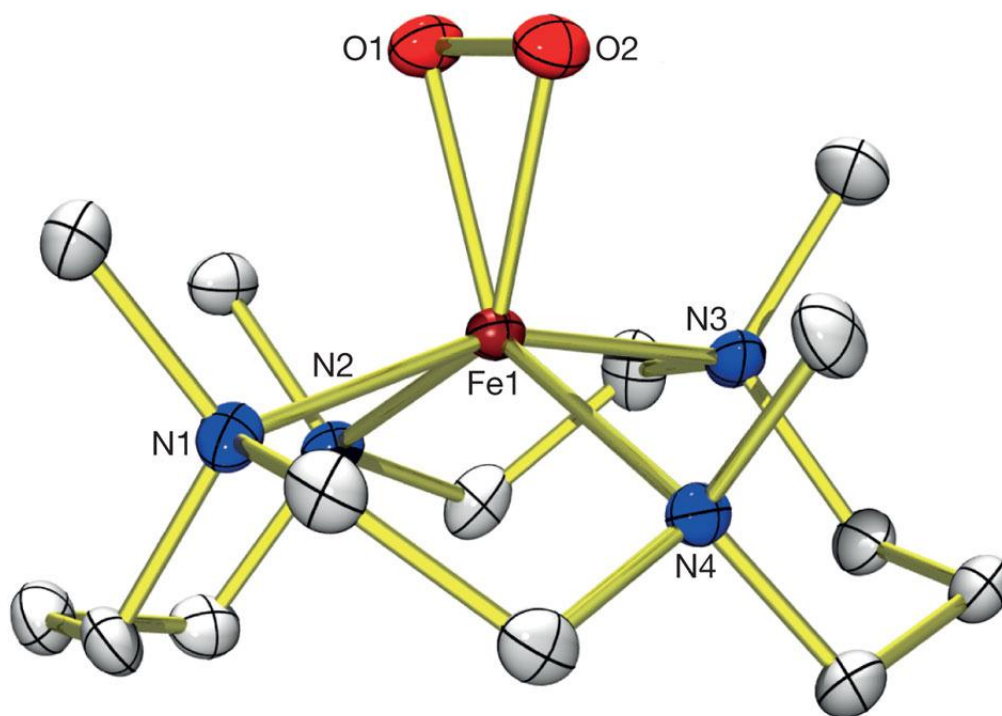
Figure 1.2 Structure of $[Fe(TMC)(OO)]^+$. Reprinted with permission from Nature Publishing Group, ref 37. Copyright 2011 Nature Publishing Group.
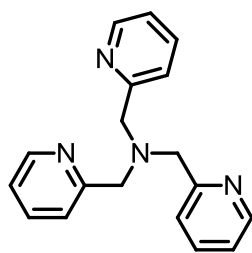
TPA
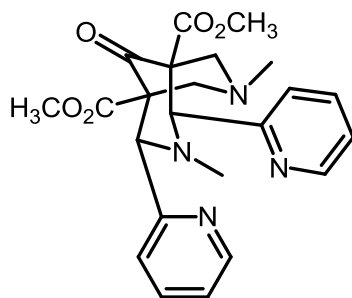
Ligand in reference 8
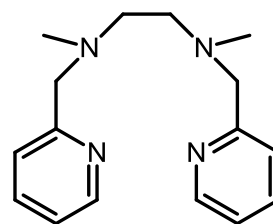
bpmen
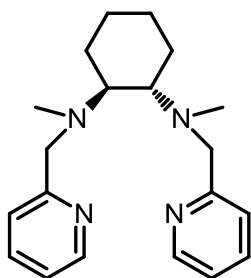
bpmcn
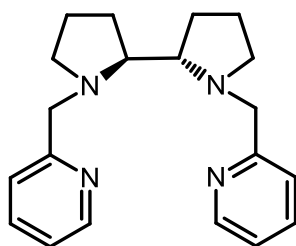
pdp
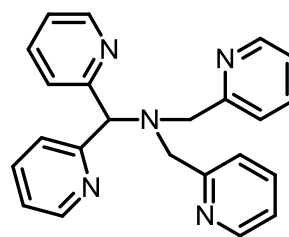
N4Py
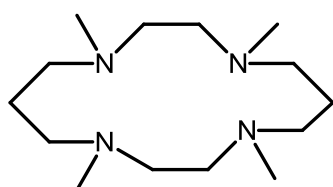
TMC
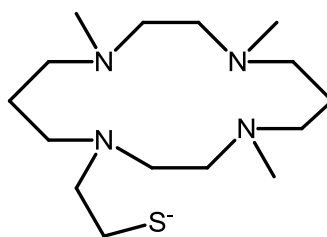
TMCS
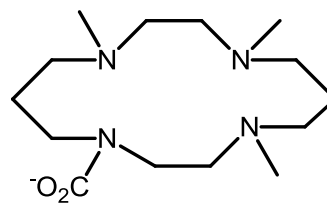
cyclam-acetate
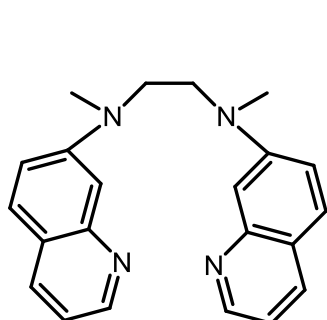
bqen
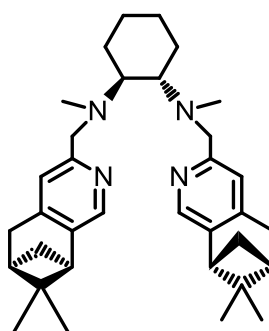
(*S*,*S*,*R*)-mcpp
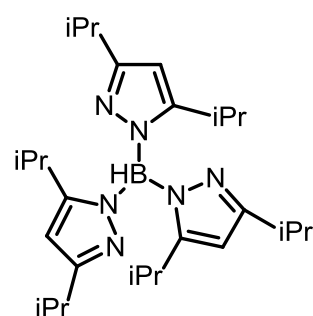
Tp^{iPr2}

Scheme 1.3 Common N-donor ligands

11

With regard to the ability of iron complexes to direct oxidation towards particular regions of the substrate, Que reported the first example of stereospecific alkane hydroxylation with a non-heme iron catalyst, $[Fe^{II}(tpa)(CH_3CN)_2](ClO_4)_2$.[44] The stereo configuration of the substrates such as *trans-* or *cis-* 1,2-dimethylcyclohexane was largely conserved in the products (>99%).[44] Nishida was the first to use a bpmen (bpmen = *N,N'*-dimethyl-*N,N'*-bis(2-pyridylmethyl)-ethane-1,2-diamine, Scheme 1.3) to prepare a non-heme iron catalyst capable of oxidizing cyclohexane to cyclohexanol and cyclohexanone.[45] Que applied $[Fe(bpmen)(OTf)_2]$ towards the oxidation of the aliphatic substrates *cis*-1,2-dimethylcylohexane and adamantane and found tertiary alcohols as the major products.[46] Nam replaced the pyridylmethyl group of bpmen with bulkier quinolyl group. He then prepared a non-heme manganese catalyst $[Mn(bqen)(OTf)_2]$ (bqen = *N,N'*-dimethyl-*N,N'*-bis(8-quinolyl)-ethane-1,2-diamine, Scheme 1.3) that selectively catalyzed tertiary C-H bonds using peracetic acid.[47] No reactivity concerning H_2O_2 was mentioned.[47]

White made modifications to the catalyst framework to shift the regioselectivity away from merely activating the weakest C-H bonds. She replaced the ethylene backbone with more rigid pyrrolidine rings resulted in the chiral ligand pdp (2-({{(*S*)-2-[(*S*)-1-(pyridin-2-ylmethyl)pyrrolidin-2-yl]pyrrolidin-1-yl}methyl)pyridine, Scheme 1.3).[49] The rigidity appears to limit intramolecular decompositions, which is often observed with the ethylenediamine-containing complexes.[48] Based on the substrates electronic, steric and stereoelectronic properties, $[Fe(pdp)(MeCN)_2](SbF_6)_2$ is able to predictably activate certain aliphatic C-H bonds within a complex

substrate.[49, 50] With simpler substrates, the ratios of secondary to tertiary carbon oxidation are higher than prior non-heme iron systems. Using a *trans* cyclohexane in place of the bpmen ethylene backbone also imparts rigidity. Costas further modified the ligand by installing pinene groups onto the ligand to limit substrate access to the active center.[51] The catalyst [Fe((*S,S,R*)-mcpp)(OTf)₂] ((*S,S,R*)-mcpp = *N,N'*-dimethyl-*N,N'*-bis[[(6*R*,8*R*)-5,6,7,8-tetrahydro-7,7-dimethyl-6,8-methanoisoquinolin-3-yl]methyl]-, (1*S*,2*S*)- 1,2-cyclohexanediamine, Scheme 1.3) exhibited high regioselectivity on some substrates relative to the pdp based catalyst.[51] For White and Costas's protocols, the high loading of catalysts (15 mol%) and acetic acid additive highlight the need to develop more efficient and green alternatives. Further, with regard to regioselectivity, electron-rich tertiary C-H bonds are still preferred for most substrates.[49, 50, 51] Developing oxidants with a preference for secondary or even primary C-H bonds remains a challenge.

References

(1)   Vaillancourt, F. H.; Yeh, E.; Vosburg, D. A.; Garneau-Tsodikova, S.; Walsh, C. T. *Chem. Rev.* **2006**, *106*, 3364–3378.

(2)   Podgorsek, A.; Zupan, M.; Iskra, J. *Angew. Chem. Int. Ed.* **2009**, *48*, 8424-8450.

(3)   Sun, C.-L.; Li, B.-J.; Shi, Z.-J. *Chem. Rev.* **2011**, *111*, 1293–1314.

(4)   White, C. M. *Science* **2012**, *335*, 807-809.

(5)   Crabtree, R. H. *Chem. Rev.* **2010**, 110, 575.

(6)   Leising, R. A.; Zang, Y.; Que, L., Jr. *J. Am. Chem. Soc.* **1991**, *113*, 8554-8555.

(7)   Kojima, T.; Leising, R. A.; Yan, S.; Que, L., Jr. *J. Am. Chem. Soc.* **1993**, *115*, 11328-11335.

(8)   Comba, P.; Wunderlich, S. *Chem. - Eur. J* . **2010**, *16*, 7293-7299.

(9)   Jaafar, H.; Vileno, B.; Thibon, A.; Mandon, D. *Dalton Trans.* **2011**, *40*, 92-106.

(10)   Lee, Y.-M.; Hong, S.; Morimoto, Y.; Shin, W.; Fukuzumi, S.; Nam, W. *J. Am. Chem. Soc.* **2010**, *132*, 10668-10670.

 (11)   Mukherjee, A.; Martinho, M.; Bominaar, E. L.; M ünck, E.; Que, L., Jr. *Angew. Chem. Int. Ed.* **2009**, *48*, 1780-1783.

(12)   Mukherjee, A.; Cranswick, M. A.; Chakrabarti, M.; Paine, T. K.; Fujisawa, K.; M ünck, E.; Que, L., Jr. *Inorg. Chem.* **2010**, *49*, 3618-3628.

(13)   Wade, L. G. J. *Organic Chemistry*, 6th Edition, 165.; Pearson Education, 2006.

(14)   Gribble, G. W. *Acc. Chem. Res.* **1998**, *31*, 141-152.

(15)   Blasiak, L. C.; Vaillancourt, F. H.; Walsh, C. T.; Drennan, C. L. *Nature* **2006**, *440*, 368-371.

(16)   Borowski, T.; Noack, H.; Radon, M.; Zych, K.; Siegbahn, P. E. M. *J. Am. Chem. Soc.* **2010**, *132*, 12887-12898.

(17)   Galonić, D. P.; Barr, E. W.; Walsh, C. T.; Bollinger, J. M., Jr; Krebs, C. *Nat. Chem. Biol.* **2007**, *3*, 113-116.

(18)   Matthews, M. L.; Krest, C. M.; Barr, E. W.; Vaillancourt, F. H.; Walsh, C. T.; Green, M. T.; Krebs, C.; Bollinger, J. M. *Biochemistry* **2009**, *48*, 4331-4343.

(19)   Liu, W.; Groves, J. T. *J. Am. Chem. Soc.* **2010**, *132*, 12847-12849.

(20)   Sawyer, D. T.; Hage, J. P.; Sobkowiak, A. *J. Am. Chem. Soc.* **1995**, *117*, 106-109.

(21)   Podgorsek, A.; Zupan, M.; Iskra, J. *Angew. Chem. Int. Ed.* **2009**, *48*, 8424-8450.

(22)   Krasniewski, J. M. Jr.; Mosher, M. W. *J. Org. Chem.*, **1974**, *39*, 1303–1306.

(23)   Kharasch, M. S.; Brown, H. C. *J. Am. Chem. Soc.* **1939**, *61*, 2142-2150.

(24)   Kojima, T.; Leising, R. A.; Yan, S.; Que, L. Jr. *J. Am. Chem. Soc.* **1993**, *115*, 11328-11335.

(25)   Price, J. C.; Barr, E. W.; Glass, T. E.; Krebs, C.; Bollinger, J. M., Jr. *J. Am. Chem. Soc.* **2003**, *125*, 13008-13009.

(26)   Krebs, C.; Price, J. C.; Baldwin, J.; Saleh, L.; Green, M. T.; Bollinger, J. M., Jr. *Inorg. Chem.* **2005**, *44*, 742-757.

(27)   Hoffart, L. M.; Barr, E. W.; Guyer, R. B.; Bollinger, J. M., Jr.; Krebs, C. *PNAS,* **2006**, *103*, 14738-14743.

(28)   Collins, T. J.; Kostka, K. L.; Münck, E.; Uffelman, E. S. *J. Am. Chem. Soc.* **1990**, *112*, 5637-5639.

(29)   Hirao, H.; Kumar, D.; Que, L., Jr.; Shaik, S. *J. Am. Chem. Soc.* **2006**, *128*, 8590-9606.

(30)   England, J.; Guo, Y.; Farquhar, E. R.; Young, V.G., Jr.; Münck, E.; Que, L., Jr. *J. Am. Chem. Soc.* **2010**, *132*, 8635-8644.

(31)   Lim, M. H.; Rohde, J.-U.; Stubna, A.; Bukowski, M. R.; Costas, M.; Ho, R. Y. N.; Münck, E.; Nam, W.; Que, L., Jr. *PNAS.* **2003**, *100*, 3665-3670.

(32)   Rohde, J. U.; In, J. H.; Lim, M. H.; Brennessel, W. W.; Bukowski, M. R.; Stubna, A.; Munck, E.; Nam, W.; Que, L., Jr. *Science* **2003**, *299*, 1037-1039.

(33)   Grapperhaus, C. A.; Mienert, B.; Bill, E.; Weyhermuller,T.; Wieghardt, K. *Inorg. Chem.* **2000**, *39*, 5306-5317.

(34)   Kaizer, J.; Klinker, E. J.; Oh, N. Y.; Rohde, J. U.; Song, J.-U.; Song, W. J.; Stubna, A.; Kim, J.; Münck, E.; Nam, W.; Que, L. Jr., *J. Am. Chem. Soc.* **2004**, *126*, 472-473.

(35)   Jensen, M. P.; Costas, M.; Ho, R. Y. N.; Kaizer, J.; Payeras, A. M.; Münck, E.; Que, L., Jr; Rohde, J. U.; Stubna, A. *J. Am. Chem. Soc.* **2005**, *127*, 10512-10525.

(36)   Bukowski, M. R.; Koehntop, K. D.; Stubna, A.; Bominaar, E. L.; Halfen, J. A.; Munck, E.; Nam, W.; Que, L., Jr. *Science* **2005**, *310*, 1000-1002.

(37)   Cho, J.; Jeon, S.; Wilson, S. A.; Liu, L. V.; Kang, E. A.; Braymer, J. J.; Lim, M. H.; Hedman, B.; Hodgson, K. O.; Valentine, J. S.; Solomon, E. I.; Nam, W. *Nature* **2011**, *478*, 502-505.

(38)   Zhang, Y.; Colabroy, K. L.; Begley, T. P.; Ealick, S. E. *Biochemistry* **2005**, *44*, 7632-7643

(39)   Karlsson, A.; Parales, J. V.; Parales, R. E.; Gibson, D. T.; Eklund, H.; Ramaswamy, S. *Science*, **2003**, *299*, 1039-1042

(40)   Kovaleva, E. G.; Lipcomb, J. D. *Science* **2007**, *316*, 453-457.

(41)   Martinho, M.; Blain, G.; Banse, F. *Dalton Trans.* **2010**, *39*, 1630-1634

(42)   Hong, S.; Lee, Y.-M.; Shin, W.; Fukuzumi, S.; Nam, W. *J. Am. Chem. Soc.* **2009**, *131*, 13910-13911

(43)   Thibon, A.; England, J.; Martinho, M.; Young, V. G., Jr.; Frisch, J. R.; Guillot, R.; Girerd, J.-J.; Münck, E.; Que, L., Jr.; Banse, F. *Angew. Chem., Int. Ed.* **2008**, *47*, 7064-7067.

(44)   Kim, C.; Chen, K.; Kim, J.; Que, L., Jr. *J. Am. Chem. Soc.* **1997**, *119*, 5964-5965.

(45)   Okuno, T.; Ito, S.; Ohba, S.; Nishida, Y. *J. Chem. Soc., Dalton Trans.* **1997**, 3547-3551.

(46)   Chen, K.; Que, L., Jr. *J. Am. Chem. Soc.* **2001**, *123*, 6327-6337.

(47)   Nehru, K.; Kim, S. J.; Kim, I. Y.; Seo, M. S.; Kim, Y.; Kim, S.; Kim, J.; Nam, W. *Chem. Commun.* **2007**, 4623-4625.

(48)   White, M. C.; Doyle, A. G.; Jacobsen, E. N. *J. Am. Chem. Soc.* **2001**, *123*, 7194-7195.

(49)   Chen, M. S.; White, M. C. *Science* **2007**, *318*, 783-787.

(50)   Chen, M. S.; White, M. C. *Science* **2010**, *327*, 566-571.

(51)   Gómez, L.; Garcia-Bosch, I.; Company, A.; Benet-Buchholz, J.; Polo, A.; Sala, X.; Ribas, X.; Costas, M. *Angew. Chem. Int. Ed.* **2009**, *48*, 5720 –5723.

Chapter 2

The Halogenation of Aliphatic C-H Bonds with Peracetic Acid and Halide Salts*

2.1 Introduction

The direct conversion of aliphatic C–H bonds to more useful functional groups is a topic of intense research.[1–4] Compounds containing C–X bonds (X = Cl, Br), in particular, are synthetically versatile and represent valuable precursors to more complex organic products due to their roles in C–C coupling reactions.[5–9] Additionally, many natural products of pharmaceutical interest contain C–Cl and C–Br functionalities; examples with antitumor activity include certain monoterpene derivatives and nostocyclophanes.[10] The installation of a halogen atom can improve an organic molecule's capability to enter cells and/or greatly impact the interaction with its biological target,[11] and the halogen functional groups may be essential for the documented medicinal benefits of these natural products.

Much progress has been made recently towards the halogenation of aromatic C–H bonds, particularly with respect to finding more environmentally benign terminal oxidants for the reactivity.[12–18] Less advancement has been made in the development of mild reactions capable of halogenating aliphatic C–H bonds.[9, 12, 19] The procedure used most commonly in industry is free-radical halogenation, in which either Cl_2 or Br_2 serve as both terminal oxidant and halogen source. The severe reactivity of Cl_2 and Br_2 complicates their use as reagents. For chlorination, iodobenzene dichloride ($PhICl_2$) sometimes serves as an alternative.[15, 20, 21] Upon irradiation, $PhICl_2$ can chlorinate cyclohexane and toluene.[20] One attractive benefit of $PhICl_2$ is that it can be prepared from ionic chloride sources; however, it is unstable to light and heat and readily decomposes during storage.[22] Furthermore, the analogous bromination with iodobenzene dibromide has not been reported. The transition-metal complex [Fe^{II}(TPA)Cl_2] (TPA = tripicolylamine) uses *tert*-butylhydroperoxide (TBHP) as a terminal oxidant to convert cyclohexane to chlorocyclohexane.[23,24] The chloride can

20

be replaced by bromide, resulting in bromination.[23, 24] The iron-mediated halogenation chemistry is stoichiometric with respect to the metal complex; adding further equivalents of TBHP leads to substrate oxygenation instead of halogenation.[23] Reported here is a novel synthetic protocol capable of converting nonactivated aliphatic C–H bonds to C–Cl and C–Br functional groups. A mixture of peracetic acid (PA) and a halide salt oxidizes cyclohexane to chloro- or bromocyclohexane selectively, with only traces of higher order halogenation products observed under optimum conditions (Scheme 2.1). A previously reported method uses *meta*-chloroperbenzoic acid (MCPBA) to perform the same transformation at a lower yield.[19] Our process has four benefits over most previously reported halogenation reactions.[9,25–27] First, PA is a relatively innocuous terminal oxidant, particularly compared to the more commonly used Cl_2 and Br_2.[9,27] Second, the halogen source is a halide salt, as opposed to an elemental halogen or a halogenated solvent, such as chloroform or carbon tetrachloride.[25] Third, the reported halogenation requires neither high temperatures nor a heavy-metal catalyst to proceed.[26] Fourth, the PA-mediated halogenation can be adapted to work in water. Despite the relatively mild conditions, the reaction can activate strong aliphatic C–H groups, such as the 95–100 kcal mol^{-1} bonds found in cyclohexane. [28]

2.2 Experimental section

Proton and carbon nuclear magnetic resonance (^{1}H NMR, ^{13}C NMR) spectra were collected on either a 400 MHz or a 250 MHz Bruker AV spectrometer. All NMR spectra were referenced to internal standards. Gas chromatography (GC) was performed on a Hewlett Packard 5890 gas chromatograph with either a flame ionization detector (FID) or a Fissons Instruments electrospray mass spectrometry detector (GC-MS). High resolution mass spectrometry (HRMS) data were acquired at

21

the Mass Spectrometry Center at Auburn University on a Microflex LT MALDI-TOF Mass Spectrometer (Bruker Corporation).

EtOH was purchased from Fluka and used as received. NaCl, NaBr, Na_2CO_3, $MgSO_4$, pentane, CH_2Cl_2, chlorobenzene, cyclohexanol, iodosobenzene (PhIO), PA (32% in AcOH), TBHP, H_2O_2, and MCPBA were bought from Sigma-Aldrich and used without further purification. The latter five chemicals were stored in a refrigerator when not in use. Anhydrous MeCN, TEACl, TEABr, toluene, adamantane, cyclohexene, and cyclohexane were purchased from Sigma-Aldrich and stored in a nitrogen atmosphere dry box to keep them free of oxygen and moisture. Anthracene was bought from Sigma-Aldrich and recrystallized twice from EtOH prior to use. - Acetonitrile-d_3 and chloroform-d ($CDCl_3$) were purchased from Cambridge Isotopes.

Each reaction was run at least three times to ensure reproducibility. The substrate and the halide salt were first put under nitrogen. After these reagents were dissolved, the oxidant was added dropwise. The system was subsequently sealed and stirred for 8 h at 22 °C. At the end of the reaction, chlorobenzene was added as an internal reference before product analysis by gas chromatography. Chlorobenzene was selected as an internal standard since it was found to be inert under the reaction conditions. Parallel reactions were run in deuterated solvents, such as MeCN-d_3, in order to confirm the identities and ratios of the products by ^{1}H NMR. This general procedure was followed for all substrate reactions except where noted otherwise. Representative reactions are discussed below.

Optimum Result- MeCN

Cyclohexane (0.200 g, 2.38 mmol) and TEACl (0.395 g, 2.38 mmol) were dissolved in 1.66 mL of MeCN under N_2. PA (0.050 mL, 0.018 g, 0.238 mmol) was then added dropwise. After the reaction mixture was stirred for 8 h at 22 °C,

chlorobenzene was added as an internal standard and analyzed by GC/FID. Chlorocyclohexane is the major product with a yield of 72% compared to PA consumed. Trace amounts of cyclohexanone (1%) and polychlorinated products (<1%) were also detected. These results correspond to entry 5 in Table 2.1.

Optimum Result- H_2O

Cyclohexane (1.118 g, 13.2 mmol) and NaCl (3.50 g, 60 mmol) were put under N_2 and dissolved in 10 mL of distilled water under N_2. To this solution, PA (0.28 mL, 0.101 g, 1.32 mmol) was added dropwise. The reaction was allowed to stir at 22 ℃ for 8 h. Three 5 mL portions of pentane were used to extract the product from the largely aqueous solution. The collected organic layers were combined, chlorobenzene was added as an internal standard, and the mixture was analyzed by GC. Chlorocyclohexane is produced in 59% yield. Trace amounts of cyclohexanone (1.7%) and polychlorinated cyclohexanes (5% total) were also found. These results correspond to entry 8 in Table 2.1.

Isolated Yield

In order to obtain the isolated yield, the aqueous reaction was increased in scale. Cyclohexane (33.6 g, 0.40 mol), NaCl (105 g, 1.80 mol), and 300 mL of distilled water were mixed in a 500 mL flask and degassed through N_2 bubbling. PA (8.4 mL, 3.02 g, 0.040 mol) was added dropwise. After the reaction was stirred at 22 ℃ for 8 h, four 100 mL portions of pentane were used to extract the organic products. The combined pentane extracts were washed with saturated Na_2CO_3 then distilled water. After the organic layer was dried over $MgSO_4$, the pentane and cyclohexane were removed under reduced pressure to yield chlorocyclohexane as a colorless liquid (1.33 g, 28% yield based on PAA consumed). ^{1}H NMR (400 MHz, $CDCl_3$): δ 4.01 (septet, 1H), 2.07 (m, 2H), 1.81 (m, 2H), 1.67 (m, 2H), 1.54 (m, 1H),

1.34 (m, 3H). ^{13}C NMR (100 mHz, CDCl$_3$): δ 60.53, 36.89, 25.32, 25.09. HR-MS (MALDI-TOF): Calcd M, 118.0549; found, 118.0573.

Cyclohexane to Bromocyclohexane

Optimum Result- MeCN

Cyclohexane (0.200 g, 2.38 mmol) and TEABr (0.250 g, 1.19 mmol) were combined in a vial, and dissolved in 1.66 mL of MeCN under N$_2$,. PA (0.10 mL, 0.036 g, 0.473 mmol) was added dropwise, and the resultant mixture was stirred at 22 ℃ for 8 h. Chlorobenzene was added as internal standard immediately prior to analysis by GC. Bromocyclohexane is the major product (30% yield, based on the amount of PA) with a trace amount of cyclohexanone (1%). These results correspond to entry 6 in Table 2.1.

Optimum Result- H$_2$O

Cyclohexane (1.118 g, 13.2 mmol) and NaBr (7.00 g, 68 mmol) were dissolved under N$_2$ in 10 mL of distilled water. PA (0.28 mL, 0.101 g, 1.32 mmol) was added dropwise to the resultant solution, which was allowed to stir at 22 ℃ for 8 h. The organic products were extracted with three 5 mL portions of pentane. Chlorobenzene was added to the combined fractions immediately prior to analysis by GC. Bromocyclohexane is the only observed product, forming in 16% yield. These results correspond to entry 9 in Table 2.1.

Cyclohexene to 1,2-Dichlorocyclohexene

PA (0.42 mL, 0.15 g, 2.0 mmol) was slowly added to a solution of TEACl (0.83 g, 5.00 mmol) in 10mL of MeCN under N$_2$. After stirring for 5 min, 0.041g of cyclohexene (0.50 mmol) was added. The reaction mixture was analyzed by GC after stirring for 2 h at 22 ℃, using chlorobenzene as an internal standard. The product was formed in 21% yield, alongside trace amounts of numerous side-products, including

3-chlorocyclohexene, and was identified by GC/MS. These results are listed in Table 2.2.

Cyclohexene to 1,2-Dibromocyclohexene

PA (0.42 mL, 0.15 g, 2.0 mmol) was slowly added to a solution of TEABr (1.05 g, 5.00 mmol) in 10 mL of MeCN. After stirring for 5 min, 0.041g of cyclohexene (0.50 mmol) was added. The reaction mixture was analyzed by GC after stirring for 2 h at 22 ℃, using chlorobenzene as an internal standard. The product was formed in 77% yield and was identified by GC/MS. A single side-product, 3-bromocyclohexene, was present in 23% yield. These results are reported in Table 2.2.

Adamantane to 1-Chloroadamantane

Isolated Yield

Adamantane (0.68 g, 5.00 mmol) and TEACl (8.3 g, 50 mmol) were dissolved in 100 mL of CH_2Cl_2 under N_2. PA (4.2 mL, 1.5 g, 20 mmol) was added dropwise to the reaction mixture. After stirring at 22 ℃ for 8 h, the CH_2Cl_2 was removed under reduced pressure. The residue was neutralized with a saturated solution of Na_2CO_3 in water. The organic products were extracted from the aqueous layer with three 50 mL portions of CH_2Cl_2, which were collected, combined, and dried over $MgSO_4$. After filtration to remove the solids, the CH_2Cl_2 was evaporated, yielding a mixture of 1-chloroadamantane and 2-chloroadamantane in a 79:21 ratio. The components were separated by column chromatography (silica gel, hexane). The 1-chloroadamantane was recrystallized from hexane to yield 0.167 g (20%) of the product as a white crystalline solid. ^{1}H NMR (400 MHz, $CDCl_3$): δ 2.14 (s, 9H), 1.68 (s, 6H). ^{13}C NMR (100 MHz, $CDCl_3$): δ 69.13, 47.94, 35.78, 31.91. HR-MS (MALDI-TOF): Calcd M, 170.0862; found, 170.0861.

Anthracene to 9,10-Dichloroanthracene

Anthracene (0.090 g, 0.50 mmol) and TEACl (0.83 g, 5.0 mmol) TEACl were dissolved in 10 mL of MeCN under N_2. PA (0.42 mL, 0.15 g, 2.0 mmol) was added slowly to the reaction vessel, and the resultant mixture was allowed to stir at 22 °C for 8 h. At the end of this duration, the MeCN was removed under reduced pressure. The products were extracted from the residue with four 10 mL portions of diethyl ether. Removal of the diethyl ether yielded 9,10-dichloroanthracene (77%) as the major product, with anthroquinone (19%) and 9,10-tetrachloro-9,10-dihydroanthracene (4%) as minor products. The ratios and identities of the products were confirmed by ^{1}H NMR and GC/MS. These results are summarized in Table 2.2.

2.3 Results and discussion

When treated with high concentrations of tetraethylammonium chloride (TEACl) and PA in acetonitrile (MeCN), cyclohexane is converted into predominantly chlorocyclohexane, with traces of cyclohexanone and negligible amounts of higher-order chlorinated products when the substrate is present in excess of the oxidant (Table 2.1, Figure 2.1). When the concentration of oxidant exceeds that of the substrate, polychlorinated products do form (Table 2.2). With 1.32 M TEACl and 0.132 M PA, the oxidative efficiency of the chlorination is 72% (Table 2.1, entry 5); the other terminal oxidants that were investigated do not promote halogenation as efficiently. Reactions with TBHP, H_2O_2, and iodosobenzene yield, at best, trace quantities of chlorocyclohexane, as assessed by GC analysis of the reaction mixtures. With 1.32 M TEACl and 0.132 M of the peracid MCPBA, the oxidative efficiency is only 21% (Table 2.1, entry 4), consistent with the results reported by Kojima et al. [10]
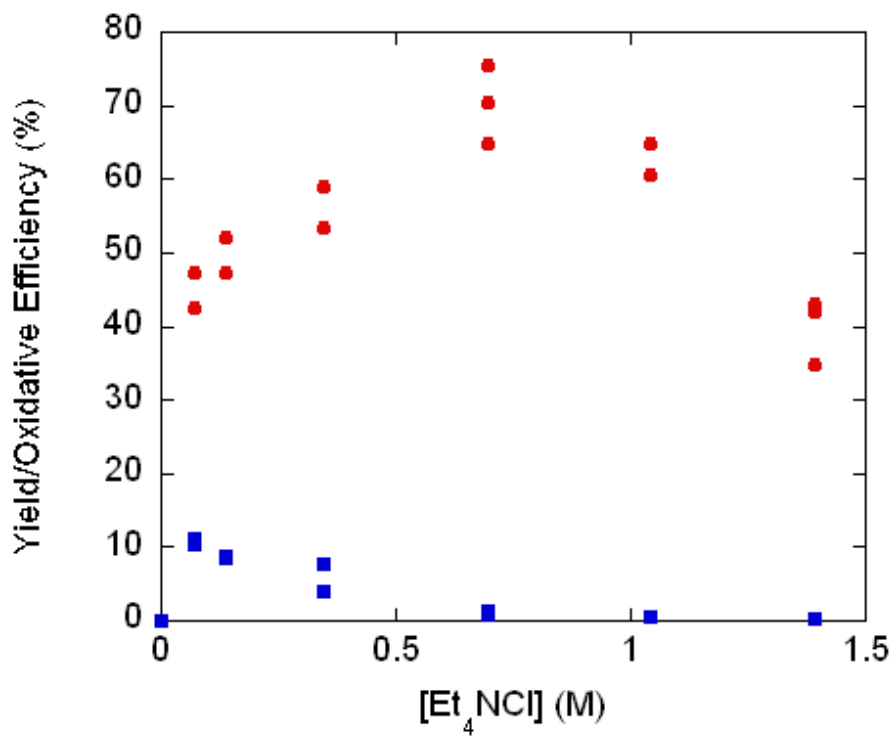
Figure 2.1 Dependence of the oxidative efficiencies for the formation of chlorocyclohexane (red dot) and cyclohexanone (blue square) on the concentration of chloride, added in the form of TEACl. The starting concentration of cyclohexane was 1.32 M, whereas the starting concentration of peracetic acid was 0.132 M.

Table 2.1 Reactivity of cyclohexane.[a]

Entry	Oxidant	Halide Salt	[Halide] (M)	Efficiency(%)	X/O Ratio
1	H_2O_2	Et$_4$NCl	1.32	<1	-- [c]
2	t-BuO$_2$H	Et$_4$NCl	1.32	<1	-- [c]
3	PhIO	Et$_4$NCl	1.32	1.3	0.08
4	MCPBA	Et$_4$NCl	1.32	21	4.8
5	PA	Et$_4$NCl	1.32	72	71
6[d]	PA	Et$_4$NBr	0.66	30	93
7[e]	PA	NaCl	1.32	36	16
8[e]	PA	NaCl	6.00	59[f]	56
9[e]	PA	NaBr	3.33	16	_ [g]
10	PA	None	0	0	_ [g]
11	PA	Et$_4$NCl	0.132	56	4.1
12	PA	Et$_4$NCl	0..266	58	5.7
13	PA	Et$_4$NCl	0.667	62	11
14	PA	Et$_4$NCl	1.32	72	71
15	PA	Et$_4$NCl	1.98	63	114
16	PA	Et$_4$NCl	2.64	40	109

[a] Standard reaction conditions: 1.32 M cyclohexane, 0.132 M oxidant, 1.8 mL total volume, 295 K, 8 h. [b] Efficiency defined as percent yield based on the oxidant.
[c] Trace amounts of cyclohexanol, cyclohexanone, and chlorocyclohexane are present.
[d] Concentration of oxidant is 0.264 M.
[e] Water used as solvent. The pH during the reaction is 4.
[f] An isolated yield of 28% is reported.
[g] No oxygenated products observed.

The oxidative efficiency of the reaction depends on the identity and concentration of the halide salt (Figure 2.1). When no TEACl or tetraethylammonium bromide (TEABr) is present, no oxidation occurs. The efficiency increases with the concentration of TEACl until it reaches 10 equivalents relative to the oxidant. Above this ratio, the yield of chlorocyclohexane decreases. The incidence of cyclohexanone, the oxygenated byproduct, steadily decreases with increasing halide concentration. With 1 equivalent of chloride relative to oxidant, roughly 20% of the PA oxidizes cyclohexane to cyclohexanone instead of the chlorinated product. At higher concentrations of chloride, this oxygenated byproduct accounts for less than 1% of the oxidized cyclohexane. Unlike the MCPBA-mediated halogenation reported by Kojima et al.,[10] PA-promoted chlorination is much more efficient than the analogous bromination. The PA-promoted bromination uses TEABr as the halide source and has an optimum efficiency of just 30%. The bromination reactions, however, generally yield less of the ketone byproduct.

The reaction also proceeds in water, albeit less efficiently. The peak efficiencies are 59% for chlorination and 16% for bromination (Table 2.1). The reduced oxidative efficiency likely results from the immiscibility of the cyclohexane substrate and water. There is precedence for aqueous halogenation reactions; a system involving H_2O_2 and HBr was reported to brominate benzylic C-H bonds.[3, 20] As with the protocol reported in this manuscript, the halogenation chemistry of the H_2O_2-HBr system proceeds at room temperature and does not require a metal catalyst. However, neither the reactivity of the H_2O_2-HBr mixture with more oxidatively robust alkanes nor attempts at chlorination were reported. [20]

Table 2.2 Reactivity of other hydrocarbon substrates.

Substrate	Efficiency (%)	Identified Products
Anthracene	100	9,10-dichloranthracene (77%), anthraquinone (19%), 9,10-tetrachloro-9,10-dihydroanthracene (4%)
Adamantane	24	1-chloroadamantane (79%), 2-chloroadamantane (21%)
Toluene	46	(*meta, para*)-chloro-methylbenzenes (94%), benzyl chloride (6%)
Cyclohexanol	100	Cyclohexanone (100%)
Cyclohexane	44	Chlorocyclohexane (92%), cyclohexanone (8%)
Cyclohexene	100	1,2-Dichlorocyclohexane (21%), 3-chlorocyclohexene (<1%)
Cyclohexene[b]	100	1,2-Dibromocyclohexane (77%), 3-bromocyclohexene (23)

[a] Standard reaction conditions: 0.050 M substrate, 0.50 M TEACl, 0.20 M PA in 10 mL MeCN, 295 K, 8 h.
[b] CH_2Cl_2 used instead of MeCN. An isolated yield of 20% is reported.
[c] 0.5 M TEABr used instead of TEACl.
[d] Dichlorocyclohexanes account for the remainder of the product.

Anthracene, toluene, cyclohexene, and adamantane were tested as alternate substrates for the chlorination reaction in order to assess its regioselectivity and its tolerance for olefins and aromatic C-H bonds (Table 2.2). Anthracene is halogenated to a mixture of mono- and polychlorinated products, demonstrating a second mode of reactivity. Under the reaction conditions, acetyl hypochlorite could potentially form and provide Cl^+ for electrophilic aromatic substitution reactions.[21-23] Since toluene contains both benzylic and aromatic C-H bonds, it was selected as a substrate in order to assess the relative speeds of the aliphatic and aromatic C-H halogenations. The products of toluene chlorination are mostly chloromethylbenzenes, and benzyl chloride accounts for only 5% of the oxidized products (Table 2.2). The product distribution demonstrates that the aromatic C-H halogenation proceeds more rapidly than the aliphatic C-H oxidation. The investigation of the aromatic C-H oxidation is ongoing in our laboratory.

Cyclohexene is oxidized to *trans*-1,2-dichlorocyclohexane with TEACl as the halide source and *trans*-1,2-dibromocyclohexane with TEABr as the halide source (Table 2.2). The bromination reaction proceeds much more cleanly than the chlorination, which yields several side products, many of which are not readily identifiable. The dihalogenated major products have previously been observed in the oxidation of cyclohexene by Cl_2 and Br_2. Adamantane is oxidized to a mixture of 1- and 2-chloroadamantanes with a preference for the activation of the C-H bonds on the tertiary carbons (Table 2.2). The observed lack of regioselectivity for the chlorination of adamantane is suggestive of a radical mechanism.

The color changes that accompany the halogenation reactions are consistent with the presence Cl_2 and Br_2 in the reactive mixture. During the chlorination reactions, the solution turns faint green before fading to pale yellow; this color completely

disappears when the reaction is put under reduced pressure, consistent with the loss of dissolved chlorine gas. During bromination, the solution turns brownish orange, suggesting the presence of Br_2. Kojima et al. observed similar spectral features in the previously reported halogenation reactions with MCPBA.[10] The observation of Cl_2 and Br_2 is intriguing since the reactions occur at room temperature and without a heavy-metal catalyst. In the absence of hydrocarbon substrates, this may represent an alternative to the Deacon process, which uses high temperatures and a copper catalyst to produce Cl_2 from chloride salts and dioxygen. [24]

Although most halogenation reactions were run under ambient light, the chlorination of cyclohexane was also found to proceed in the dark. During these latter reactions, the solutions still turn green, suggesting that the reaction between PA and the chloride salt is not initiated by photons. The oxidative efficiencies of the reactions run in the dark are identical within error to those of reactions run under ambient light.

One mechanistic possibility for the alkane oxidation is that the peracid may initially convert the alkane to an alcohol, which would then undergo acid-catalyzed nucleophilic substitution to form the organohalide product. Under the conditions used to convert cyclohexane to chlorocyclohexane, cyclohexanol was converted into cyclohexanone exclusively (Table 2.2). Additionally, the alcohol was stable in a solution of acetic acid and TEACl at the temperature and duration used for the experiments, providing further evidence that cyclohexanol is not a plausible intermediate for these reactions and that cyclohexane is oxidized directly to chlorocyclohexane.

The lack of regioselectivity in the adamantane reactions and the production of elemental halogens suggest the intermediacy of halogen atom radicals. Based on the reduction potentials of the species involved, peracetic acid (E °= 2.05 V vs. NHE) [25] is

32

thermodynamically capable of oxidizing Cl^- (Cl_2, $E°= 1.36$ V vs. NHE) and Br^- (Br_2, $E°= 1.07$ V vs. NHE) to chlorine and bromine molecules, respectively.[26, 27] Based on these data, we hypothesize that Cl^- and Br^- could be oxidized to corresponding radicals. The PA is converted into acetate and water during this process. The halogen-atom radicals are believed to be responsible for the abstraction of the hydrogen atom from the alkane. Similar chemistry was proposed for the oxidation of enones and alkenes with oxone and sodium halides, although no aliphatic C-H activation was reported.[28] When chlorination of cyclohexane is attempted in the presence of $BrCl_3C$, bromocyclohexane is observed as a side product, consistent with the intermediacy of a cyclohexyl radical.

The reliance of the halogenation chemistry on the initially generated halogen atom radicals may explain the nonlinear dependence of the oxidative efficiency on the halide concentration. We hypothesize that at higher concentrations of chloride, the elevated production of Cl radicals facilitates the formation of Cl_2. The conversion of Cl radicals to gaseous Cl_2 removes the oxidant from the reaction mixture, thereby reducing the oxidative efficiency of alkane halogenation. The greater overpotential for the oxidation of bromide relative to chloride would hasten the production of bromine radicals relative to chloride radicals. Consequently, more of the bromide may be diverted into Br_2 production instead of alkane halogenation, explaining the lower oxidative efficiency of PA-mediated bromination relative to the analogous chlorination.

2.4 Conclusions

To summarize, we report a novel procedure to halogenate hydrocarbons with nonactivated aliphatic C-H bonds that uses commercially available PA as a terminal

oxidant and a halide salt as the terminal halogen source. The synthetic protocol can be adapted to work in water, with NaCl or NaBr as the halogen source. The incidence of side products can be modulated and minimized by adjusting the concentrations of oxidant and halide. The major drawback to this method is that both aromatic C-H activation and the dihalogenation of alkenes proceed much more quickly than aliphatic C-H activation.

References

(1)   Gribble, G. W. *Acc. Chem. Res.* **1998**, *31*, 141-152.

(2)   Metrangolo, P.; Resnati, G. *Science* **2008**, *321*, 918-919.

(3)   Podgoršek, A.; Zupan, M.; Iskra, J. *Angew. Chem. Int. Ed.* **2009**, *48*, 8424-8450.

(4)   Stowers, K. J.; Sanford, M. S. *Org. Lett.* **2009**, *11*, 4584-4587.

(5)   Yang, L.; Lu, Z.; Stahl, S. S. *Chem. Commun.* **2009**, 6460-6462.

(6)   Kalyani, D.; Sanford, M. S. *J. Am. Chem. Soc.* **2008**, *130*, 2150-2151.

(7)   Xia, J.-B.; You, S.-L. *Org. Lett.* **2009**, *11*, 1187-1190.

(8)   Kakiuchi, F.; Kochi, T.; Mutsutani, H.; Kobayashi, N.; Urano, S.; Sato, M.; Nishiyama, S.; Tanabe, T. *J. Am. Chem.Soc.* **2009**, *131*, 11310-11311.

(9)   Bogdal, D.; Lukasiewicz, M.; Pielichowski, J. *Green Chem.* **2004**, *6*, 110-113.

(10)   Kojima, T.; Matsuo, H.; Matsuda, Y. *Chem. Lett.* **1998**, *27*, 1085-1086.

(11)   Banks, D. F.; Huyser, E. S.; Kleinberg, J. *J. Org. Chem.* **2002**, *29*, 3687-3692.

(12)   Breslow, R.; Link, T. *Tetrahedron Lett.* **1992**, *33*, 4145-4148.

(13)   Zielinksa, A.; Skulski, L. *Tetrahedron Lett.* **2004**, *45*, 1087-1089.

(14)   Leising, R. A.; Zang, Y.; Que, L. Jr. *J. Am. Chem. Soc.* **1991**, *113*, 8555-8557.

(15)   Kojima, T.; Leising, R. A.; Yan, S.; Que, L. Jr. *J. Am. Chem. Soc.* **1993**, *115*, 11328-11335.

(16)   Tanemura, K.; Suzuki, T.; Nishida, Y.; Horaguchi, T. *Tetrahedron Lett.* **2008**, *49*, 6419-6422.

(17)   Zhuk, T. S.; Gunchenko, P. A.; Korovai, Y. Y.; Schreiner, P. R.; Fokin, A. A. *Theor. Exp. Chem.* **2008**, *44*, 48-53.

(18)   Jiang, X.; Shen, M.; Tang, Y.; Li, C. *Tetrahedron Lett.* **2005**, *46*, 487-489.

(19)   Tian, Z.; Fattahi, A.; Lis, L.; Kass, S. R. *J. Am. Chem. Soc.* **2006**, *128*, 17087-17092.

(20)   Podgoršek, A.; Stavber, S.; Zupan, M.; Iskra, J. *Tetrahedron Lett.* **2006**, *47*, 7245-7247.

(21)   Jia, Z.; Margerum, D. W.; Francisco, J. S. *Inorg. Chem.* **2000**, *39*, 2614-2620.

(22)   El Dusouqui, O. M. H.; El Nadi, A. R. H.; Hassan, M.; Yousif, G. *J. Chem. Soc., Perkin Trans. 2* **1976**, 357-359.

(23)   El Dusouqui, O. M. H.; Hassan, M.; El Nadi, A. R. H.; Yousif, G. *J. Chem. Soc., Perkin Trans. 2* **1976**, 359-362.

(24)   Deacon, H. *J. Chem. Soc.* **1872**, *25*, 725-767.

(25)   Awad, M. I.; Denggerile, A.; Ohsaka, T. *J. Electrochem. Soc.* **2004**, *151*, E358-E363.

(26)   Atkins, P. *Physical Chemistry*, 6th Edition; W. H. Freeman and Company, New York, **1997**.

(27)   Vanýsek, P. *Handbook of Chemistry and Physics,* 88th Edition; Chemical Rubber Company, **2007**.

(28)   Dieter, R. K.; Nice, L. E.; Velu, S. E. *Tetrahedron Lett.* **1996**, *37*, 2377-2380.

Chapter 3

**Steric Modifications Tune the Regioselectivity of the Alkane Oxidation
Catalyzed by Non-heme Iron Complexes***

3.1 Introduction

The selective activation of C-H bonds within either a single substrate or a group of substrates remains an elusive goal in homogeneous catalysis.[1-5] With heterogeneous catalysts, the reactive portions can be encapsulated within a porous solid support. When these pores are sufficiently small, they can exclude substrates, or portions of substrates, on the bases of their size and shape.[6-10] In two recent studies with homogeneous catalysis, regioselective oxidation was achieved by engineering non-covalent interactions between a functional group on the substrate and a docking group on the catalyst.[11, 12] The rigidity of the catalyst-substrate adduct is essential towards directing the oxidation towards the target region of the substrate.

The development of homogeneous catalysts for the regioselective activation of non-functionalized alkanes and alkenes has had fewer successes.[13-17] One design strategy, partly influenced by the active sites of metalloenzymes,[18] is to install steric bulk onto the organic component of the catalyst, using steric repulsions to restrict the access of substrates to the reactive portion of the oxidant. If the steric bulk is of the wrong size or in the wrong position, however, its placement can severely impede or eliminate the desired reactivity.[19] In some cases, this can be beneficial, for such ligand modifications have allowed the isolation of a number of reactive species relevant to non-heme iron chemistry.[20-28] A second drawback is that the addition of steric bulk can also facilitate one or more competing modes of reactivity, for instance, promoting alkene bishydroxylation over epoxidation.[29] Despite these potential problems, this strategy has been successfully applied to modulate the selectivity of hydroxylation catalyzed by iron porphyrin compounds.[30, 31]

In order to alter the regioselectivity of non-heme iron catalysis, we have modified the bpmcn framework (Scheme 3.1),[32] replacing the methyl groups on the amine nitrogens with benzyl groups (Scheme 3.2). We prepared complexes with three

iron(II) salts: iron(II) chloride, iron(II) triflate, and iron(II) hexafluoroantimonate. All three Fe(II) complexes catalyze the oxidation of aliphatic substrates by hydrogen peroxide, with the hexafluoroantimonate salt associated with both the highest activity and the greatest selectivity for alkane hydroxylation. The bulk installed on the ligand appears to direct the oxidation toward the less sterically congested portions of substrates to an extent heretofore unobserved with mononuclear non-heme iron catalysts.
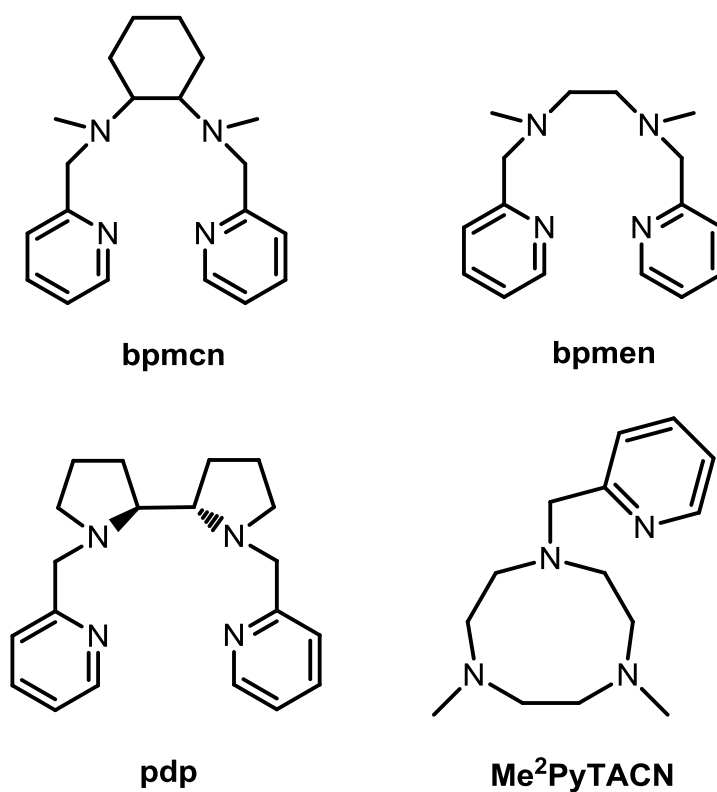
Scheme 3.1 Tetradentate N-donor ligands
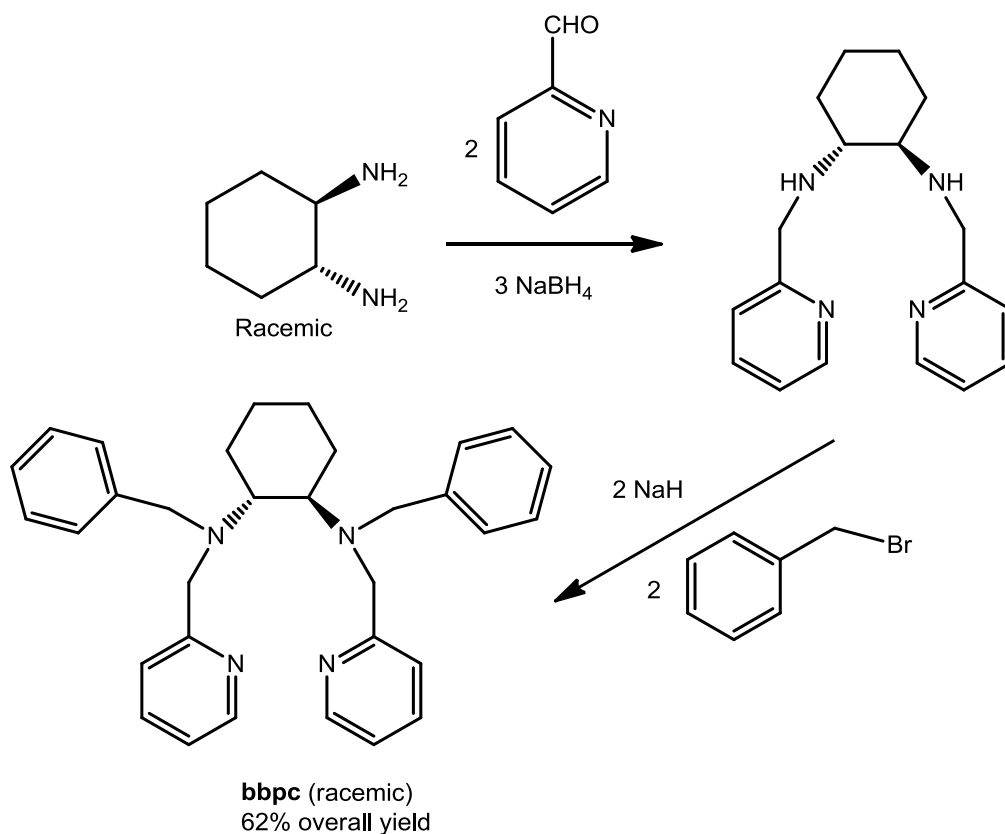
Scheme 3.2 Synthesis of bbpc ligand

3.2 Experimental Section

Materials

Unless stated otherwise, all chemicals were purchased from Sigma–Aldrich and used as received. Anhydrous acetonitrile (MeCN) was stored in a glovebox free of moisture and oxygen. Anhydrous methanol (MeOH) and tetrahydrofuran (THF) were stored over 4 Å molecular sieves. Anhydrous diethyl ether (ether), hydrogen peroxide (H_2O_2, 50% with inhibitor) and ammonium hydroxide (NH_4OH) were purchased from Fisher Scientific. Silver(I) hexafluoroantimonate ($AgSbF_6$) was stored in a dark -35 ℃ freezer in a dry, anaerobic glovebox. Chloroform-*d* ($CDCl_3$), acetonitrile-*d₃* (CD_3CN), and cyclohexane-*d₁₂* (C_6D_{12}) were bought from Cambridge Isotopes. Ethanol (EtOH) was purchased from Fluka. Iron(II) triflate ($Fe(OTf)_2$•2MeCN) was prepared through a previously reported procedure,[33] as were

N,N'-dimethyl-*N,N'*-bis(2-pyridinylmethyl)-1,2-ethanediamine (bispicen) and *N,N'*-dimethyl-*N,N'*-bis(2-pyridinylmethyl)-1,2-cyclohexanediamine (bpmcn).[34] The [Fe(bpmcn)(MeCN)$_2$](SbF$_6$)$_2$ complex was prepared from the reaction of [Fe(bpmcn)Cl$_2$] with two equiv. of AgSbF$_6$ in MeCN; the dication was confirmed to be the *cis*-isomer on the bases of its ^{1}H NMR and optical spectra.[32]

Instrumentation

^{1}H and ^{13}C nuclear magnetic resonance (NMR) spectra were recorded on either a 400 MHz or a 250 MHz AV Bruker NMR spectrometer at 22 ℃. All NMR peaks were referenced to internal standards. A Varian Cary 50 spectrophotometer was used to collect optical data, which were processed and analyzed using software from the WinUV Analysis Suite. A Johnson Matthey magnetic susceptibility balance (model MK I#7967) was used to measure the magnetic moments of solid samples. High resolution mass spectrometry (HR-MS) data were acquired at the Mass Spectrometer Center at Auburn University on a Bruker microflex LT MALDI-TOF mass spectrometer via direct probe analysis operated in the positive ion mode. Electron paramagnetic resonance (EPR) spectra were collected on a Bruker EMX-6/1 X-band EPR spectrometer operated in the perpendicular mode. All EPR spectra were analyzed with the program EasySpin.[35] All EPR samples were run as frozen MeCN solutions in quartz tubes. Crystalline samples were dried and sent to Atlantic Microlabs (Norcross, GA) for elemental analysis.

X-Ray Crystallography

X-ray diffraction data were collected at −80 °C on a Bruker SMART APEX CCD X-ray diffractometer unit using Mo Kα radiation from crystals mounted in Paratone-N oil on glass fibers. SMART (v 5.624) was used for preliminary determination of cell constants and data collection control. Determination of

integrated intensities and global cell refinement were performed with the Bruker SAINT software package using a narrow-frame integration algorithm. The program suite SHELXTL (v 5.1) was used for space group determination, structure solution, and refinement.[36] Refinement was performed against F^2 by weighted full-matrix least-square, and empirical absorption correction (SADABS) were applied.[37] Hydrogen atoms were placed at calculated positions using suitable riding models with isotropic displacement parameters derived from their carrier atoms. Crystallographic data and selected bond distances and angles are provided in Table 3.1, Table 3.2, and Table 3A.1 of the Appendix.

Table 3.1 Selected crystallographic data for the bbpc complexes.

Parameter	[Fe(bbpc)Cl$_2$] •MeCNN	[Fe(bbpc)(MeCN)$_2$] (SbF$_6$)$_2$	[Fe(bbpc)(OTf)$_2$]
Formula	C$_{34}$H$_{39}$Cl$_2$FeN$_5$	C$_{36}$H$_{42}$FeF$_{12}$N$_6$Sb$_2$	C$_{34}$H$_{34}$F$_6$FeN$_4$O$_6$S$_2$
MW	644.45	1086.13	830.66
Crystal system	Orthorhombic	Orthorhombic	Triclinic
Space group	*P2$_1$2$_1$2$_1$ (#19)*	*P2$_1$2$_1$2$_1$ (#19)*	*P$\bar{1}$ (#2)*
a (Å)	10.3299(10)	14.9875(7)	10.2508(11)
b (Å)	16.3604(16)	16.5523(8)	11.8558(12)
c (Å)	18.4921(18)	19.8461(10)	15.8754(16)
α (deg)	90	90	71.418(2)
β(deg)	90	90	85.954(2)
γ(deg)	90	90	76.263(2)
V (Å^3)	3125.2(5)	4923.4(4)	1776.4(3)
Z	4	4	2
Cryst color	Dark red	Green	Yellow
T (K)	193	193	193
Reflns collected	48351	12228	11965
Unique reflns	11128	9116	5925
R1 (F, I > 2σ(I))	0.0509	0.048	0.0585
wR2 (F^2, all data)	0.1018	0.1155	0.1879

R1 = Σ||F$_o$| - |F$_c$||/Σ||F$_o$|; wR2 = [Σw(F$_o^2$-F$_c^2$)^2/Σw(F$_o^2$)^2]$^{1/2}$.

Table 3.2 Selected bond lengths for Fe(II) complexes with the bbpc ligand, $[Fe(bbpc)X_2]^{n+}$ (Å)

X =	Cl⁻	MeCN	OTf⁻
Fe-N(1)	2.2224(15)	2.146(4)	2.146(3)
Fe-N(2)	2.1798(16)	2.182(4)	2.132(3)
Fe-N(3)	2.3286(15)	2.227(3)	2.234(3)
Fe-N(4)	2.4391(16)	2.256(3)	2.225(3)
Fe-X(1)	2.3608(5)	2.147(4)	2.270(2)
Fe-X(2)	2.4708(6)	2.164(4)	2.107(3)

Donor atoms have been relabeled from their CIF designations to facilitate comparison. N(1) and N(2) correspond to pyridine nitrogens, N(3) and N(4) correspond to amine nitrogens.

A.   B.
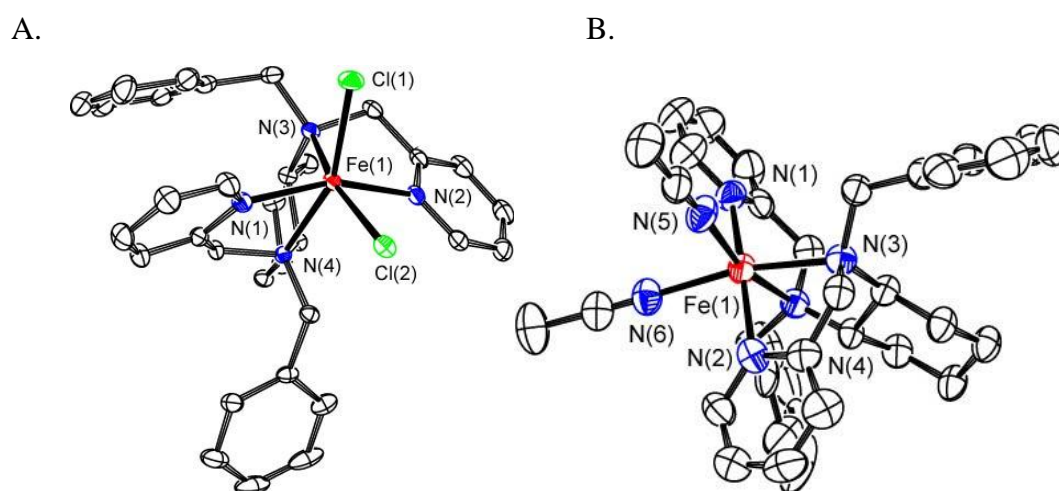
Figure 3.1 ORTEP representations of (A) $[Fe(bbpc)Cl_2]$ and (B) $[Fe(bbpc)(MeCN)_2]^{2+}$. The hydrogen atoms, counteranions, and outer-sphere acetonitrile molecules have been omitted for clarity. All thermal ellipsoids are drawn at 50% probability. Note that the donor atoms have been relabeled from their original CIF designations to facilitate comparison of the crystallographic data.

Synthesis

N,N′-bis(phenylmethyl)-N,N′-bis(2-pyridinylmethyl)-1,2-cyclohexanediamine

(bbpc). 2-Pyridinecarboxaldehyde (4.551 g, 42.5 mmol) was added to a solution of (±)-*trans*-1,2-diaminocyclohexane (2.422 g, 21.2 mmol) in 40 mL of dry MeOH. The reaction mixture was stirred at 60 ℃ for 2 h, at which point sodium borohydride (NaBH$_4$, 4.848 g, 128 mmol) was added as a solid. The resultant mixture was heated at reflux for 16 h, at which point the reaction was cooled and the MeOH removed under reduced pressure, yielding crude *N,N'*-bis(2-pyridinylmethyl)-1,2-cyclohexanediamine. The crude material was dissolved in distilled H$_2$O, at which point the precursor was extracted with 4 × 100 mL portions of CH$_2$Cl$_2$. These extracts were dried over Na$_2$SO$_4$. Removal of the CH$_2$Cl$_2$ under reduced pressure yielded the purified *N,N'*-bis(2-pyridinylmethyl)-1,2-cyclohexanediamine as a yellow oil (5.556 g, 18.8 mmol, 88%). The compound's purity and identity were confirmed by ^{1}H NMR.[38] The precursor (1.603 g, 5.42 mmol) was dissolved in 60 mL of dry THF. The solution was cooled to 0 ℃, at which point, sodium hydride (2.067 g, 51.7 mmol) was added as a solid. After stirring for 20 min, benzyl bromide (1.949 g, 11.4 mmol) was added at 0 ℃. The reaction was warmed to room temperature and stirred for an additional 48 h. Water was added dropwise to quench the reaction. Subsequently, 3 M HCl was added dropwise until the pH of the aqueous layer fell beneath 2. The organic layer was removed under vacuum, and the remaining acidic layer was washed with 3 × 40 mL aliquots of ether. The aqueous solution was made basic (pH > 10) through the addition of 3 M NaOH, at which point, the product was extracted with 3 × 100 mL portions of ethyl acetate (EtOAc). The collected EtOAc layers were dried over Na$_2$SO$_4$, filtered, and concentrated to yield the crude product as brown oil. The pure ligand may be obtained through flash chromatography on silica with a 20:4:1 mixture

45

of EtOAc/EtOH/NH$_4$OH as the elutant (R$_f$ = 0.89). Alternatively, the ligand can be obtained in a crystalline form by cooling a saturated solution of the crude in MeCN. The latter process affords a higher yield of the light yellow product (1.814 g, 3.81 mmol, 70%). ^{1}H NMR (CDCl$_3$, 400 MHz): δ 8.50 (m, 2H), 7.71 (m, 2H), 7.49 (t, 2H), 7.34 (m, 4H), 7.18-7.09 (m, 8H), 3.73 (q, 4H), 3.49 (q, 4H), 2.70 (m, 2H), 2.14 (m, 2H), 1.72 (m, 2H), 1.06 (4H). ^{13}C NMR (CDCl$_3$, 62.5 MHz): δ 161.32, 148.84, 140.11, 136.10, 129.11, 128.12, 126.87, 123.28, 121.77, 59.08, 55.49, 53.93, 26.03, 24.49. HR-MS (ESI): Calcd MH$^+$: 477.3018; Found: 477.3017.

cis-**Dichloro-(*N,N′*-bis(phenylmethyl)-*N,N′*-bis(2-pyridinylmethyl)-1,2-cyclohexanediamine)manganese(II) ([Mn(bbpc)Cl$_2$]).** The bbpc ligand (0.510 g, 1.07 mmol) and MnCl$_2$ (0.130 g, 1.03 mmol) were dissolved in 10 mL of MeCN and stirred for 16 h under N$_2$, during which time a white solid deposited. The addition of ether (5 mL) yielded more precipitate. The product was isolated through filtration as a white powder (0.310 g, 50%). Crystals suitable for analysis by X-ray diffraction were obtained through the vapor diffusion of ether into a saturated solution of the manganese complex in MeCN. Solid-state magnetic susceptibility (294 K): μ $_{eff}$ = 5.8 μ $_B$. Optical spectroscopy (MeCN, 294 K): 310 nm (shoulder), 390 M^{-1} cm^{-1}. Elemental Analysis: Calcd for C$_{32}$H$_{36}$N$_4$MnCl$_2$ CH$_3$CN: C, 63.45%; H, 6.11%; N, 10.88%; Found: C, 63.31%; H, 6.23%; N, 10.81%.

cis-**Dichloro-(*N,N′*-bis(phenylmethyl)-*N,N′*-bis(2-pyridinylmethyl)-1,2-cyclohexanediamine)iron(II) ([Fe(bbpc)Cl$_2$]).** The bbpc ligand (1.07 g, 2.25 mmol) was dissolved in 5 mL of MeCN and combined with a solution of FeCl$_2$ (0.284 g, 2.23 mmol) in 5 mL of MeCN. Upon stirring for 16 h under an anaerobic atmosphere, a yellow solid began to precipitate. Ether (5 mL) was added, depositing more of the product. The product was isolated through filtration as a yellow powder (0.874 g,

65%). Crystals suitable for X-ray diffraction were grown through vapor diffusion of ether into a saturated solution of the iron complex in MeCN. Solid-state magnetic susceptibility (294 K): μ_{eff} = 4.9 μ_{B}. Optical spectroscopy (MeCN, 294 K): 380 nm, 1400 M^{-1} cm^{-1}. Elemental Analysis: Calcd for $C_{32}H_{36}N_4FeCl_2$ CH_3CN $0.5H_2O$: C, 62.49%; H, 6.17%; N, 10.72%; Found: C, 62.65%; H, 6.09%; N, 10.69%.

***trans*-Ditriflato-*(N,N′*-bis(phenylmethyl)-*N,N′*-bis(2-pyridinylmethyl)-1,2-cyclohexanediamine)iron(II) ([Fe(bbpc)(OTf)₂]).** The bbpc ligand (0.852 g, 1.79 mmol) and $Fe(OTf)_2 \cdot 2MeCN$ (0.782 g, 1.79 mmol) were dissolved in 5 mL of MeCN, resulting in a dark red brown solution. The reaction stirred under N_2 for 30 min at which point the volume of MeCN was reduced through vacuum. The addition of ether precipitated the product as a light yellow powder (0.696 g, 45%). Crystals suitable for X-ray diffraction were obtained through the slow addition of ether to a solution of the powder in CH_2Cl_2. ^{1}H NMR (CD_3CN, 250 MHz): δ 58.0, 57.7, 54.6, 52.7, 37.7, 22.3, 21.1, 16.0, 13.7, 10.9, 10.2, 6.4, 5.5, 5.1, 4.7, 4.4, 3.9, 3.5, 3.2, 1.0, 0.5, -0.2, -1.3, -8.0, -21.3. Solid-state magnetic susceptibility (294 K): μ_{eff} = 4.6 μ_{B}. Optical spectroscopy (MeCN, 294 K): 350 nm, 1600 M^{-1} cm^{-1}. Elemental Analysis: Calcd for $C_{34}H_{36}N_4FeF_6O_6S_2$ CH_3CN $0.5H_2O$: C, 48.64%; H, 4.44%; N, 6.67%; Found: C, 48.36%; H, 4.27%; N, 6.74%.

***cis*-Diacetonitrilo-*(N,N′*-bis(phenylmethyl)-*N,N′*-bis(2-pyridinylmethyl)-1,2-cyclohexanediamine)iron(II) hexafluoroantimonate ([Fe(bbpc)(CH₃CN)₂](SbF₆)₂).** The synthesis is based on a literature procedure.[13] Solid [Fe(bbpc)Cl₂] (0.503 g, 0.835 mmol) was suspended in 10 mL of MeCN under N_2. As the suspension was vigorously stirred, $AgSbF_6$ (0.574 g, 1.67 mmol) was added. The mixture continued to stir in the dark for 24 h, with the reaction vessel covered with aluminum foil to further limit the exposure of the silver salts to light. At the conclusion of the reaction, the

suspension was filtered through a packed celite plug. Removal of the solvent under reduced pressure yielded a purple powder. The purple solid was redissolved in MeCN and filtered through a 0.2 μm Acrodisc LC PVDF filter (HPLC certified). The MeCN was removed through evaporation. The purple residue was treated to two more dissolution/filtration/concentration cycles to ensure the complete removal of the silver salts. The purple solid was dried under a nitrogen stream to yield [Fe(bbpc)(CH$_3$CN)$_2$](SbF$_6$)$_2$ (0.805 g, 89% yield). ^{1}H NMR (CD$_3$CN, 250 MHz): δ 62.4, 58.5, 52.5, 50.5, 26.2, 25.4, 23.6, 18.9, 14.0, 4.99, 3.7, -5.3, -12.6. Solid-state magnetic susceptibility (294 K): $\mu_{eff} = 4.4 \, \mu_B$. Optical spectroscopy (MeCN, 294 K): 340 nm, 1050 M^{-1} cm^{-1}. Elemental Analysis: Calcd for C$_{36}$H$_{42}$N$_6$FeF$_{12}$Sb$_2$: C, 39.81%; H, 3.90%; N, 7.74%; Found: C, 40.26%; H, 3.98%; N, 8.06%.
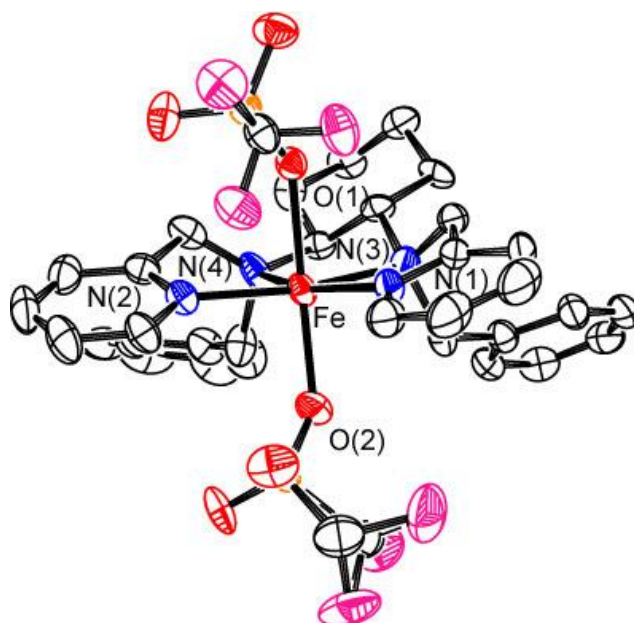
Figure 3.2 ORTEP representation of [Fe(bbpc)(OTf)$_2$]. Hydrogen atoms have been omitted for clarity, as have the ellipsoids for the disordered triflate and cyclohexane backbone corresponding to molecular configuration b. The disordered triflate binds to the Fe(II) ion through O(2). All thermal ellipsoids are drawn at 50% probability. Note that the donor atoms have been relabeled from their original CIF designations to facilitate comparison of the structures.
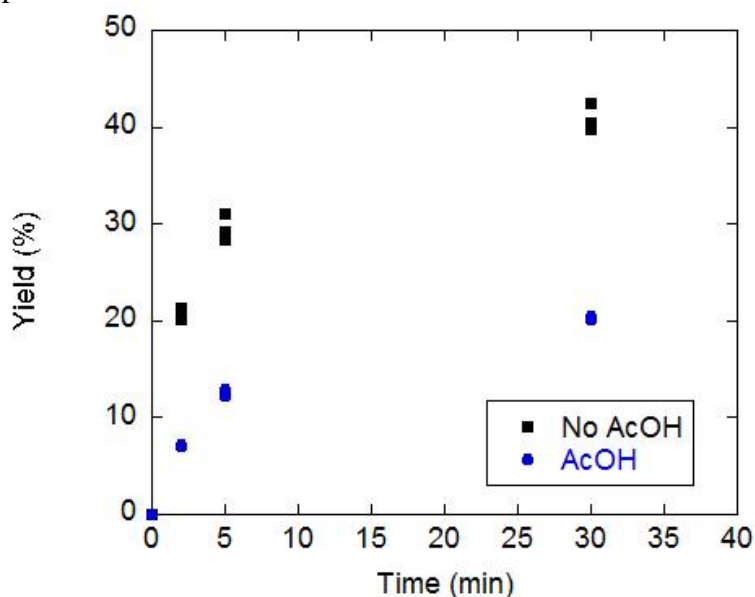
Figure 3.3 Oxidation of cyclohexanol in the presence and absence of acetic acid (AcOH) as a function of time. The initial concentrations of reagents were as follows: 1.0 mM [Fe(bbpc)(MeCN)](SbF$_6$)$_2$, 100 mM cyclohexanol, 100 mM H$_2$O$_2$, 670 mM AcOH (when present). All reactions were run in MeCN at 298 K. The yield is the amount of cyclohexanol that has been oxidized to cyclohexanone; no other organic products were observed.

3.3 Results

Synthesis

The bbpc ligand can be prepared in moderate yield (62% over two steps) through the procedure outlined in Scheme 3.2. The two-step synthesis proceeds through the previously characterized *N,N'*-bis(2-pyridinylmethyl)-1,2-cyclohexanediamine.[38] Since the synthesis begins with a racemic mixture of *trans*-1,2-cyclohexanediamine, the bbpc product is also racemic. Scheme 3.2 shows only the *R,R* enantiomers in order to improve clarity. The final organic product can either be purified through chromatography or through direct crystallization from a solution of the crude material dissolved in MeCN. The obtained crystals are suitable for X-ray diffraction (Figure 3A.1).

The [M(bbpc)Cl$_2$] compounds (M = Mn, Fe) were prepared by mixing MeCN solutions of bbpc and either MnCl$_2$ or FeCl$_2$. Both the Mn(II) and Fe(II) products precipitate readily from the reaction mixture. The [Fe(bbpc)(SbF$_6$)$_2$] complex resulted from the reaction of [Fe(bbpc)Cl$_2$] with AgSbF$_6$. In MeCN, acetonitrile molecules displace the weakly bound hexafluoroantimonate anions, and the isolated product is [Fe(bbpc)(MeCN)$_2$](SbF$_6$)$_2$. Although triflate ions are also widely perceived to be weakly coordinating ligands, it was the [Fe(bbpc)(OTf)$_2$] complex that was isolated from the reaction between bbpc and Fe(OTf)$_2$•2MeCN, as assessed by crystallography and elemental analysis.

Structural and Solid-State Characterization

The bbpc ligand and its Mn(II) and Fe(II) complexes crystallize readily from MeCN solutions (Table 3.1, Table 3A.1). For [Mn(bbpc)Cl$_2$], [Fe(bbpc)Cl$_2$], and [Fe(bbpc)(MeCN)$_2$]$^{2+}$, the tetradentate ligand coordinates to the metal in a *cis*-α conformation, in which the two pyridine rings are *trans* to each other and the two

chloride ligands are *cis* to each other (Figure 3.1). Unexpectedly, the bbpc ligand is found in the *trans* conformation in the structure of the [Fe(bbpc)(OTf)$_2$] complex (Figure 3.2). In this structure, one of the triflate anions and the cyclohexane backbone are disordered over two sets of positions; the disorder of the cyclohexane component corresponds to a mixture of (*R,R*) and (*S,S*) chiralities at carbons 1 and 2 of the ring. The chiralities of the amine nitrogens is (*R,S*) for both molecular configurations, resulting in a mixture of diastereomers in the crystal. The *trans* conformation has not been observed previously for *N,N'*-bis(2-pyridinylmethyl)-1,2-cyclohexanediamine or its close derivatives,[32] although it has been observed recently for a ligand with a 1,2-ethanediamine backbone.[39] Despite the presence of the benzyl groups, the tertiary amines remain bound to the metal ions in all four complexes.

The metal-ligand bond distances in the Fe(II) complexes are consistent with high-spin iron centers (Table 3.2).[40] These spin-state assignments are corroborated by solid-state magnetic susceptibility measurements. The Fe-N bond distances are notably shorter for the [Fe(bbpc)(MeCN)$_2$]$^{2+}$ and [Fe(bbpc)(OTf)$_2$] complexes. In the [Fe(bbpc)Cl$_2$] complex, the two Fe-Cl bond lengths differ by 0.11 Å. Similarly, Fe-N(4) is 0.08 Å longer than Fe-N(3) in this structure. The disparities in these bond lengths can be attributed to the different steric interactions between the two chlorides and the benzyl groups of the bbpc ligand. The benzyl group on N(4) is nearly eclipsed with the Fe-Cl(2) bond, with a dihedral angle of 11.2°. The heightened steric repulsion that results from this configuration elongates both Fe-Cl(2) and Fe-N(4). Conversely, the benzyl group on N(3) is in a staggered conformation relative to the Fe-Cl(1) bond, with a dihedral angle of 43.2°. The shorter Fe-Cl(1) and Fe-N(3) bonds are compatible with the lesser strain. The Fe-O bonds in the structure of [Fe(bbpc)(OTf)$_2$] differ by 0.17 Å. In this structure, Fe-O(1) and the benzyl groups

are on the same side of the plane defined by the four N-donors. The increased steric repulsions between the O(1)-containing triflate and the benzyl groups likely explains why Fe-O(1) is longer than Fe-O(2).

Solution Characterization

Each iron complex has a single ligand-to-metal charge transfer (LMCT) band with λ_{max} between 300 and 400 nm. The energies and relatively low intensities of these bands are typical for high-spin Fe(II) complexes.[41] Solutions of all three Fe(II) compounds in CD_3CN were found to be paramagnetic by ^1H NMR, further confirming the spin-states of the Fe(II) complexes (Figure 3A.5, Figure 3A.6). The spectra for the $[Fe(bbpc)(MeCN)_2]^{2+}$ and $[Fe(bbpc)(OTf)_2]$ are consistent with the solid-state structures, with the latter containing two diastereomers. The numbers and sharpness of the peaks suggest that the conformation of the bbpc ligand is static on the NMR time-scale. The $[Fe(bbpc)Cl_2]$ complex was not sufficiently soluble in CD_3CN to unambiguously support the same conclusions. The optical spectra of the triflate and hexafluoroantimonate complexes are not identical, contrary to what would be anticipated if both counteranions were non-coordinating. In conjunction with the structural data, these results may suggest either that the *trans* conformation of $[Fe(bbpc)(OTf)_2]$ is retained in solution or that the triflates retain their stronger affinity for the Fe(II) centers in solution.

Reactivity Studies- Cyclohexane

The abilities of the three Fe(II) compounds to catalyze the oxidation of alkanes by H_2O_2 were assayed with cyclohexane in MeCN at 298 K (Table 3.3). The iron catalyst with the hexafluoroantimonate counteranions has the highest reactivity (TON = 27.4) and preferentially produces the alcohol product, cyclohexanol, over the ketone, cyclohexanone (A:K = 7.3). When the reactions were run under air, the results were

52

identical within error to those run under a dry N_2 atmosphere. Higher loadings of the terminal oxidant decrease the A:K ratio, consistent with earlier reports on related systems.[42-45] The addition of a stoichiometric amount of acetic acid (AcOH) into the system increases the selectivity for the alcohol but decreases the overall oxidative activity. This effect is not seen with a catalytic amount of AcOH. Triethylamine was also explored as an additive. When 0.40 M of the base is present, cyclohexanone is the preferred product (A:K = 0.17), but the catalytic activity is almost completely lost (TON = 1.4).

The oxidation of cyclohexanol to cyclohexanone in the presence and absence of AcOH was monitored over 30 min (Figure 3.3). When AcOH is added, the number of turnovers completed in 30 min decreases from 41 to 20. The lifetimes of the catalytic activities under these conditions appear to be similar, with estimated half-lives of 2.4 min (AcOH absent) and 3.5 min (AcOH present).

A kinetic isotope effect of 2.4 was measured from competition studies between protonated and deuterated cyclohexane (C_6D_{12}). When C_6D_{12} is run as a substrate with 100 mM of H_2O_2, 9.6 turnovers are observed with a A:K ratio of 3.1. The lower A:K ratio suggests that the deuteration of the substrate slows the primary oxidation to the alcohol to a greater extent than the secondary step in the oxidation, which converts the alcohol to the ketone.

Table 3.3 Catalyzed oxidation of cyclohexane by hydrogen peroxide.

Catalyst	[H$_2$O$_2$] (mM)	[CH$_3$CO$_2$H]	TON[a]	A:K[b]
[Fe(bbpc)(Cl)$_2$]	100	0	12.4	0.7
[Fe(bbpc)(OTf)$_2$]	100	0	12.8	2.6
[Fe(bbpc)(MeCN)$_2$](SbF$_6$)$_2$	10	0	4.0	7.3
[Fe(bbpc)(MeCN)$_2$](SbF$_6$)$_2$	100	0	27.4	4.8
[Fe(bbpc)(MeCN)$_2$](SbF$_6$)$_2$	100	1.0	19.0	4.7
[Fe(bbpc)(MeCN)$_2$](SbF$_6$)$_2$	10	670	2.8	12.1
[Fe(bbpc)(MeCN)$_2$](SbF$_6$)$_2$	100	670	10.9	6.8

Standard reaction conditions: The starting concentrations of the iron(II) catalyst and the cyclohexane substrate in all reactivity assays were 1.0 mM and 1.0 M, respectively. All reactions were run at 295 K. A solution of H$_2$O$_2$ diluted in MeCN was added dropwise over the course of 1 min. The final volume of each reaction solution was 2.50 mL. The duration of each reaction was 30 min. After this time, the solution was filtered through silica gel and analyzed via GC. [a]Turnover number, defined as the number of moles of cyclohexanol and cyclohexanone generated per mole of Fe(II) catalyst. [b]The products were identified by GC/MS and comparison of the retention times with those of authentic samples of cyclohexanol (A) and cyclohexanone (K). The concentrations of each organic product were calibrated relative to that of an internal standard (dichlorobenzene) with a known concentration.

Reactivity Studies- 1,2-Dimethylcyclohexanes and Other Sterically Complicated
Alkanes

The two benzyl groups can potentially limit substrate access to the reactive portion of the oxidant, which we believe is a higher-valent iron complex (*vide infra*). The steric bulk represented by these benzyl groups could potentially hinder the oxidation of more sterically congested C-H bonds. The regioselectivity of $[Fe(bbpc)(MeCN)_2]^{2+}$ was tested using a protocol developed by Chen and White, which employs *cis*- and *trans*-1,2-dimethylcyclohexanes as diagnostic substrates.[13] The key output in these experiments is the relative prevalence of oxidation at the secondary and tertiary carbons of the two substrates. Equatorial C-H bonds tend to be more readily oxidized than axial C-H bonds in cyclohexane rings.[46] The *trans* isomer of 1,2-dimethylcyclohexane contains axial C-H bonds on the two tertiary carbons in its most stable chair conformation. This hinders the approach of external molecules and consequently leads to more oxidation on the secondary carbon atoms relative to the *cis* isomer.

The previously reported catalyst $[Fe(bpmen)(OTf)_2]$ was also investigated on the basis of its similarly strong preference for hydroxylation.[29, 45, 47-51] The bpmen compound promotes the oxidation of C-H bonds on tertiary carbons over those on secondary carbons when the substrate is *cis*-1,2-dimethylcyclohexane (Table 3.4). This result is anticipated from consideration of the bond dissociation energies (BDEs). The C-H bonds on tertiary carbons should have BDEs approximately 3 kcal mol^{-1} lower than those on secondary carbons;[52] the bonds on the tertiary carbons should and often do react more quickly as a consequence.[43, 51, 53-55] Upon reaction with the *trans* isomer, activation of the C-H bonds on secondary carbons is favored, albeit slightly. Similar results are observed for $[Fe(bpmcn)(MeCN)_2]^{2+}$, which has methyl groups in

place of the bbpc ligand's benzyl groups. The bpmcn catalyst is less active under these conditions but exhibits a noticeably higher preference for the C-H bonds on secondary carbons. When the ligand is switched to pdp, the preference for oxidizing the bonds on secondary carbons is likewise stronger than that of the bpmen system (Table 3.4).[13] The bbpc complex with Fe(II) favors the oxidation of secondary carbons over tertiary carbons to a greater extent than the other three Fe(II) compounds with both the *cis* and *trans*-1,2-dimethylcyclohexane substrates. With both alkanes, the reactivity of $[Fe(bbpc)(MeCN)_2]^{2+}$ is lower than that of the pdp complex, which is the most active of the four. The reactivity at the tertiary carbons is, however, curtailed to a much larger extent.

The same trend is observed for adamantane (Scheme 3.3, Table 3A.2). Although the observed 5:1 ratio of tertiary:secondary oxidation is unimpressive relative to those found for the 1,2-dimethylcyclohexane reactions, such ratios are commonly much higher for reactions catalyzed by mononuclear non-heme iron complexes.[51] 1,1-Dimethylcyclohexane and *tert*-butylcyclohexane were also investigated using Chen and White's protocol (Scheme 3.3, Table 3A.2). With *tert*-butylcyclohexane, oxidation is observed at neither the tertiary carbon nor the secondary carbons α to the tertiary carbon. With 1,1-dimethylcyclohexane, the plurality of the oxidation occurs at the γ carbon, as opposed to the β carbon for the pdp oxidant.[13] A preference for activating the C-H bonds on primary over secondary carbons is not observed. Oxidation of the methyl groups of the dimethylcyclohexane substrates is not seen. Additionally, when n-hexane is used as a substrate, oxygenation occurs exclusively on the secondary carbon atoms in the chain (Table 3A.2).

Table 3.4 Catalytic oxidation of *cis-* and *trans-*1,2-dimethylcyclohexane

Substrate	Catalyst	Overall Yield, Individual Product Yields
cis-	[Fe(bpmen)(OTf)$_2$]	45%, *trans*-1,2-dimethylcyclohexanol 31.9% *cis*-1,2-dimethylcyclohexanol 1.1% *cis*-2,3-dimethylcyclohexanone 5% *cis*-3,4-dimethylcyclohexanone 7% **[tertiary : secondary] = 2.9 : 1**
trans-	[Fe(bpmen)(OTf)$_2$]	30%, *cis*-1,2-dimethylcyclohexanol 11.3% *trans*-1,2-dimethylcyclohexanol 0.7% *trans*-2,3-dimethylcyclohexanone 11% *trans*-3,4-dimethylcyclohexanone 7% **[tertiary : secondary] = 1 : 1.5**
cis-	[Fe(bpmcn)(MeCN)$_2$] (SbF$_6$)$_2$	37%, *trans*-1,2-dimethylcyclohexanol 24% *cis*-2,3-dimethylcyclohexanone 5% *cis*-3,4-dimethylcyclohexanone 8% **[tertiary : secondary] = 1.8 : 1**
trans-	[Fe(bpmcn)(MeCN)$_2$] (SbF$_6$)$_2$	20%, *cis*-1,2-dimethylcyclohexanol 7% *trans*-2,3-dimethylcyclohexanone 6% *trans*-3,4-dimethylcyclohexanone 7% **[tertiary : secondary]=1 : 1.9**

Table 3.4 continued

cis-	[Fe(pdp)(MeCN)₂](SbF₆)₂	70%, *trans*-1,2-dimethylcyclohexanol 55% *cis*-2,3-dimethylcyclohexanone 9% *cis*-3,4-dimethylcyclohexanone 6% **[tertiary : secondary] = 4 : 1**
trans-	[Fe(pdp)(MeCN)₂](SbF₆)₂	79%, *cis*-1,2-dimethylcyclohexanol 29% *trans*-2,3-dimethylcyclohexanone 22% *trans*-3,4-dimethylcyclohexanone 28% **[tertiary : secondary]=1 : 2**
cis-	[Fe(bbpc)(MeCN)₂](SbF₆)₂	32%, *trans*-1,2-dimethylcyclohexanol 16.1% *cis*-1,2-dimethylcyclohexanol 0.9% *cis*-2,3-dimethylcyclohexanone 7% *cis*-3,4-dimethylcyclohexanone 5% **[tertiary : secondary] = 1.2 : 1**
trans-	[Fe(bbpc)(MeCN)₂](SbF₆)₂	29%, *cis*-1,2-dimethylcyclohexanol 4.4% *trans*-1,2-dimethylcyclohexanol 0.6% *trans*-2,3-dimethylcyclohexanone 11% *trans*-3,4-dimethylcyclohexanone 13% **[tertiary : secondary]=1 : 5**

Standard reaction conditions: the general procedure was adapted from Reference 13 in order to facilitate direct comparison of the data. The substrate (0.056 g, 0.50 mmol, 1 equiv) was dissolved in 1.0 mL of MeCN. The iron catalyst and the terminal oxidant, H_2O_2, were added to this solution in three portions. For each addition, the H_2O_2 was added dropwise over the course of 90 s. After the first additions, the concentrations were as follows: [Fe] = 4.26 M, [substrate] = 85.2 M, [H_2O_2] = 0.102 mM. 10 min after the first portion of H_2O_2 was added, further equivalents of catalyst and oxidant were added, yielding the following concentrations: [Fe] = 4.65 M, [substrate] = 46.5 M, [H_2O_2] = 0.112 mM. 20 min after the first portion of H_2O_2 was added, the third portions of catalyst and oxidant were added, yielding the following concentrations: [Fe] = 4.80 M, [substrate] = 32.0 M, [H_2O_2] = 0.115 mM. At 30 min, the reaction solution was filtered through a short plug of silica gel to remove the metal complexes. Cyclohexanone was added as internal standard and the products were analyzed by GC. The products were identified by comparison of the GC retention times and mass spectra (GC/MS) to those of commercially available or previously prepared standards.[13, 43, 51] All data are the averages of three independent runs.

58

Characterization of a Reactive Intermediate

When 4 equiv of H_2O_2 are allowed to react with $[Fe(bbpc)(MeCN)_2]^{2+}$ in MeCN in the absence of a hydrocarbon substrate, the solution turns green with an optical feature at 690 nm (Figure 3.4). At room temperature, the solution quickly turns blue, concomitant with the appearance of a new absorbance band at 640 nm. The compound associated with the 640 nm species has not yet been fully characterized. The addition of 20 equiv of $HClO_4$ to the solution prolongs the lifetime of the green species; whereas, the addition of Et_3N immediately leads to the loss of the 690 nm band. EPR analysis of a sample quenched during the decay process shows two signals (Figure 3.5). One has a *g* value equal to 4.3, which is indicative of a high-spin Fe(III) species. The other signal is consistent with a low-spin Fe(III) complex, with *g* values at 2.36, 2.22, and 1.92 (Figure 3.5). A mass spectrum of the complex has a major m/z peak consistent with $[Fe(bbpc)(O_2)]^+$ (Figure 3A.8, Figure 3A.9). Based on the reactivity of the 690 nm species with the acid and base and comparison of the spectroscopic features to previously reported species, we tentatively assign the green species associated with the 690 nm band as $[Fe(bbpc)(OOH)]^{2+}$.

3.4 Discussion

The ligand *N,N′*-bis(phenylmethyl)-*N,N′*-bis(2-pyridinylmethyl)-1,2-cyclohexanediamine (bbpc) was prepared as a bulkier analog of bpmcn and bpmen (Scheme 3.1), which were previously reported to support non-heme iron C-H activation chemistry.[29, 32, 45, 47-50, 55-57] Large quantities of crystalline bbpc (Figure 3A.1) can be prepared within a reasonable timeframe without the need for chromatography. The ligand chelates metals ions readily, despite the additional steric bulk, and complexes with both Mn(II) and Fe(II) can be obtained in moderate yield (45-65%).

Much like bpmcn, the ligand can chelate transition metal ions in multiple fashions.[32] In two of the Fe(II) structures (Figure 3.1) and the lone Mn(II) structure (Figure 3A.2), the *cis*-α conformation is observed. The nearly eclipsed conformation between Fe-Cl(2) and the benzyl group on N(4) is associated with the much longer Fe-Cl(2) and Fe-N(4) bonds within [Fe(bbpc)Cl$_2$] (Table 3.2). The *trans* conformer is observed in the disordered structure of [Fe(bbpc)(OTf)$_2$] (Figure 3.2). To the best of our knowledge, this is the first instance of this particular conformation in the coordination chemistry of bpmcn or its close derivatives, which were previously found to coordinate metal ions in *cis*-α and *cis*-β conformations.[34, 58-63] The novel mode of coordination may be facilitated by the larger substituents on the amines, but the energetic rationale is not obvious from a precursory inspection of the structure. The conformation of the ligand in [Fe(bbpc)(OTf)$_2$] places the benzyl groups on the same side of the plane defined by the four N-donors. With this configuration, the benzyl groups strongly repel the disordered triflate, as indicated by the longer Fe-O(1) bond. This would be anticipated to destabilize the structure, although this may be counterbalanced by the reduced steric interactions around the second triflate.

The [Fe(bbpc)(MeCN)$_2$](SbF$_6$)$_2$ and [Fe(bbpc)(OTf)$_2$] compounds have different UV/vis spectra in MeCN (Figure 3A.3), indicating that the same iron complex is not present in solution. That the spectra differ is likely a consequence of the two different ligand conformations, which appear to be static on the NMR timescale. Another contributing factor may be the possibility of the triflate ions' continued coordination to the Fe(II) center in solution. These ions are capable of binding to the Fe(II), as seen in Figure 3.2 and the crystal structures of other ferrous complexes with neutral ligands.[45, 64]

The three Fe(II) compounds were investigated as catalysts for alkane oxidation, using the oxidation of cyclohexane by H_2O_2 as a standard reaction (Table 3.3). The [Mn(bbpc)Cl$_2$] complex was also investigated but was not found to be a competent catalyst for the reaction. The catalytic activities of the iron compounds scale inversely with the binding affinities of the non-bbpc ligands, and the most strongly coordinating ligand, Cl$^-$, leads to the weakest activity. Similar counteranion dependencies have been previously observed in the hydrocarbon oxidation catalyzed by non-heme iron compounds.[65-68] The most straightforward explanation for this behavior is that the counterions are competing with the terminal oxidant for coordination sites on the metal, slowing the metal oxidation step of the relevant catalytic cycle or cycles. The continued presence of an anionic ligand on the iron may also serve to destabilize any higher-valent oxidants which form during the catalysis.[69] As observed by Costas and Que, the ligand conformation can impact the reactivity profile.[32] That the catalytic activity of [Fe(bbpc)(OTf)$_2$] (*trans*) is intermediate to those of [Fe(bbpc)Cl$_2$] and [Fe(bbpc)(MeCN)$_2$]$^{2+}$ (*cis-α*) may therefore be coincidental.

With cyclohexane as a substrate, the ratio of alcohol (A) to ketone (K) products is relatively high for [Fe(bbpc)(MeCN)$_2$]$^{2+}$, particularly at lower loadings of the terminal oxidant, H_2O_2.[42, 43] Although the preference for hydroxylation is strong relative to most non-heme iron catalysts, higher A:K ratios are found for [Fe(bpmen)(OTf)$_2$], [Fe(^{Me2}PyTACN)(OTf)$_2$], and an iron complex with an electronically modified bpmen ligand.[32, 44, 54, 70, 71] When acetic acid (AcOH) is added as a stoichiometric additive, the A:K ratio increases from 7.3 to 12.1 with 10 equiv of H_2O_2 (Table 3.3). Under these conditions, [Fe(bbpc)(MeCN)$_2$]$^{2+}$ essentially matches [Fe(^{Me2}PyTACN)(OTf)$_2$] with respect to the selectivity for hydroxylation, although the latter system is about twice as active, with a 65% oxidative efficiency relative to the 28% for the bbpc system.

Although AcOH has been previously found to improve both the selectivity of iron-mediated epoxidation reactions[47] and the regioselectivity of iron-mediated hydrocarbon oxidation reactions,[13, 43] the ability to hinder the formation of ketones in alkane oxygenation reactions had not been noted. The loss of overall activity upon the addition of AcOH contrasts with a previously reported titanium catalyst, which was found to catalyze the oxidation of cyclohexane by hydrogen peroxide to a much higher degree when the reaction was run in AcOH,[72] as well as a non-heme iron system reported by Chen and White.[17]

The addition of AcOH slows the oxidation of cyclohexanol to cyclohexanone as shown in Figure 3.3, accounting for the higher A:K ratio. Analysis of the curve yields a surprising result in that AcOH actually prolongs the lifetime of the catalytic activity (Figure 3A.7), with the estimated half-life increasing by approximately 1 min. We therefore hypothesize that the AcOH is either decreasing the intrinsic reactivity of the generated oxidant(s) or reversibly deactivating it, as opposed to hastening the irreversible degradation of one or more species in the catalytic cycle. Whether the loss of activity is a consequence of the acidity or the metal-binding properties of AcOH remains unresolved. The protonation of M(IV) oxo species has recently been found to slow their C-H activation chemistry.[57, 73]

The increased steric bulk was designed to direct oxidation towards the less sterically congested portions of hydrocarbon substrates. In order to test this, we adopted a protocol developed by Chen and White to test the regioselectivity of the alkane oxidation catalyzed by $[Fe(pdp)(MeCN)_2]^{2+}$.[13] Under these conditions, which use a lower loading of substrate, the C-H bonds on secondary carbons are oxidized predominantly to the ketone instead of the alcohol; when cyclohexane is used as a substrate, 22% of the substrate is converted to a 1: 9 mixture of cyclohexanol and

cyclohexanone. We analyzed both $[Fe(bbpc)(MeCN)_2]^{2+}$ and $[Fe(bpmen)(OTf)_2]$, with the intention of determining whether there was a correlation between the A:K ratio in the previously described cyclohexane reactivity (Table 3.3) and the regioselectivity observed with the 1,2-dimethylcyclohexanes (Table 3.4). We also analyzed $[Fe(bpmcn)(MeCN)_2]^{2+}$ in order to assess how much of the tuned regioselectivity was a consequence of the benzyl-for-methyl substitution.

The Fe(II) complex with bbpc has the strongest preference of the four catalysts for activating C-H bonds on secondary carbons over the thermodynamically weaker ones on tertiary carbons (Table 3.4). As anticipated, this preference is most pronounced with *tert*-butylcyclohexane and *trans*-1,2-dimethylcyclohexane.[46] With both 1,2-dimethylcyclohexane substrates, the overall reactivity decreases upon switching from the pdp ligand to the bbpc. The oxidation at the tertiary carbons, however, decreases to a much higher degree, going from 55% to 17% conversion for the *cis* isomer and from 29% to 5% for the *trans*. The results are consistent with steric repulsions between the substrate and catalyst regulating and restricting substrate access to the reactive portions of the active oxidant, which we hypothesize to be a higher-valent iron species, such as a ferryl oxo species.[56, 74-78] When adamantane is used as a substrate, the ratio of tertiary to secondary oxidation is 5:1, likely due to the greater accessibility of the tertiary C-H bonds relative to those in the cyclohexane derivatives. This ratio is lower than those observed for other mononuclear non-heme iron catalysts, with the exception of $[Fe(N4Py)(MeCN)]^{2+}$, which has a 3.3:1 ratio.[51, 79] A similar decrease in the ability to activate tertiary C-H bonds was observed in the oxidation chemistry of iron complexes with methylated derivatives of tris(pyridyl)amine (tpa).[51]

The bpmcn system has a stronger preference for secondary carbon oxidation than [Fe(bpmen)(OTf)$_2$], suggesting that the substitution of a cyclohexane ring for the ethylene linkage does impact the regioselectivity of the oxidation. However, the benzyl-for-methyl substitution also has a significant impact as assessed by the lower ratios of tertiary to secondary carbon oxidation for the bbpc system relative to [Fe(bpmcn)(MeCN)$_2$]$^{2+}$. The relative importance of these two perturbations appears to be substrate-dependent. With *cis*-1,2-dimethylcyclohexane, the cyclohexane ring in the bbpc appears to account for the bulk of the altered regioselectivity, for secondary carbon oxidation accounts for 35% of the oxidized products for [Fe(bpmcn)(MeCN)$_2$]$^{2+}$ versus 38% for [Fe(bbpc)(MeCN)$_2$]$^{2+}$. With the *trans* substrate, the benzyl substituents appear to have the stronger influence, with secondary carbon oxidation accounting for 60%, 65%, and 83% of the organic products in the systems using bpmen, bpmcn, and bbpc ligands, respectively.

adamantane   *tert*-butylcyclohexane   1,1-dimethylcyclohexane
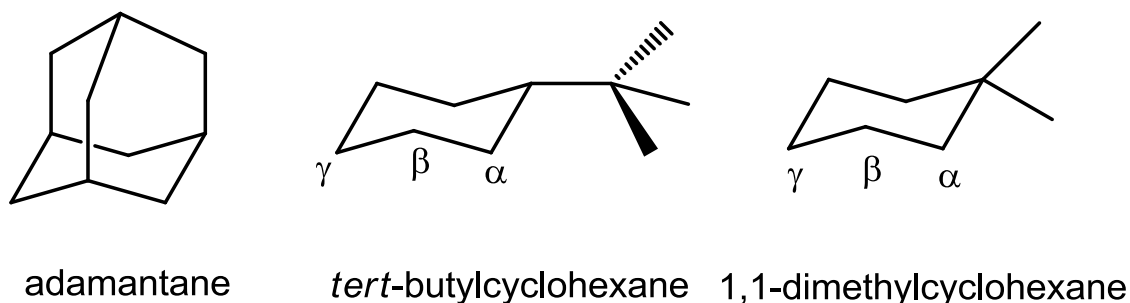
Scheme 3.3 Other substrates for regioselective oxidation

The ability of steric repulsions to block oxidation at positions α and β to the installed group is more limited (Scheme 3.3, Table 3A.2). The oxidation catalyzed by [Fe(bbpc)(MeCN)$_2$]$^{2+}$ tends to occur at sites farther from the bulkier portions of the substrates than that catalyzed by [Fe(pdp)(MeCN)$_2$]$^{2+}$. With *tert*-butylcyclohexane, no oxidation is seen on the secondary carbons α to the *tert*-butyl group. Oxidation on the β carbons is preferred, with a 3.7:1 ratio of β to γ oxidation, but not to the same extent

as in Chen and White's pdp system (4.9:1).[13] With 1,1-dimethylcyclohexane, oxidation is observed at the carbons α, β, and γ to the quaternary carbon. With the bbpc ligand, oxidation is favored on the γ, with a α:β:γ ratio of 1:1.3:2.3. This contrasts with the pdp system, which oxidizes the β position of 1,1-dimethylcyclohexane preferentially, with a α:β:γ ratio of 1:1.5:0.8.[13]

The steric repulsions do not appear to be sufficient to similarly favor the oxidation of C-H bonds on primary carbons over those on secondary carbons, as illustrated by lack of primary alcohol and aldehyde products in the oxidations of 1,2-dimethylcyclohexanes and n-hexane. The results bolster the previously presented concept that judicious ligand modification can direct the oxidation catalyzed by non-heme iron catalysts towards specific regions of structurally complicated substrates.[13]

There does not appear to be a straightforward correlation between the A:K ratio for cyclohexane oxygenation and the regioselectivity of the 1,2-dimethylcyclohexane oxidation. The [Fe(bpmen)(OTf)$_2$] complex is slightly more selective for hydroxylation (A:K = 8) than [Fe(bbpc)(MeCN)$_2$]$^{2+}$ yet activates the C-H bonds on tertiary carbons much more readily (Table 3.4). Additionally, [Fe(^{Me2}PyTACN)(OTf)$_2$] has an even stronger tendency to hydroxylate alkanes (A:K = 12), but only tertiary alcohol products are reported for its oxidation of *cis*-1,2-dimethylcyclohexane.[54] The results suggest that the geometric structure of the catalyst is not solely responsible for the observed preference for hydroxylation.

The tertiary alcohol products display 88-95% stereochemical retention (Table 3.4). These are comparable to numbers reported for other recently studied non-heme iron systems,[43, 51] and are inconsistent with a Fenton-style manner of oxidation.[80] In the 2001 paper from Chen and Que, the retention of configuration was found to decrease as the catalyst's ligand was methylated.[51] That the bulkier bbpc ligand leads

to less stereochemical retention than bpmen or less sterically hindered derivatives of tpa [51] may suggest that the additional bulk on the ligand may slow oxygen atom rebound steps in the catalytic cycle(s), which would allow intermediate organic radicals more time to rearrange.[56]

The reactivity appears to proceed through a Fe(III)-OOH species that has an absorption band at 690 nm (Figure 3.4) and both high-spin and low-spin Fe(III) EPR signals at 77 K (Figure 3.5). These are similar to spectroscopic features reported for other ferric hydroperoxide species.[78, 79, 81-83] Although the mass spectrum has a major m/z peak consistent with $[Fe(bbpc)(O_2)]^+$ (Figure 3A.8, Figure 3A.9), we find this assignment to be implausible based on the reactivity of the intermediate with $HClO_4$ and Et_3N.[83] Instead, we hypothesize that the m/z feature results from the deprotonation of $[Fe(bbpc)(OOH)]^{2+}$ to a less positively charged species; ferric hydroperoxide species have previously displayed similar instability under ESI conditions.[29] The mixture of high-spin and low-spin signals may be indicative of a spin-crossover. Neutral N-donor ligands have supported both high-spin and low-spin Fe(III)-OOH species,[78, 81-83] and a recent study with ferric alkylperoxo complexes found that a relatively minor ligand modification could convert a low-spin Fe(III)-OOR species to a high-spin one.[84] Ferric hydroperoxide species have been previously hypothesized and reported to spontaneously convert to higher-valent iron species, such as ferryl oxo complexes.[49, 51, 54, 75, 76, 85] These more highly oxidized iron species are more likely to be the actual oxidants in the alkane oxygenation reactions.[86]

3.5 Conclusions

The bbpc ligand is presented as a more sterically encumbered analog of previously reported tetradentate N-donor ligands that supported non-heme iron oxidative catalysis. The catalytic capabilities of Fe(II) compounds with bbpc are

strongly dependent on the counterions employed, with the most active alkane oxidation associated with the most weakly binding counteranion, SbF_6^-. The $[Fe(bbpc)(MeCN)_2]^{2+}$ complex also displays the strongest preference for alkane hydroxylation of the three bbpc complexes, and its selectivity for hydroxylation is on par with that of $[Fe(bpmen)(OTf)_2]$, which has been described as "the prototypical example of an efficient stereospecific alkane hydroxylation catalyst."[54] The preference for hydroxylation is amplified in the presence of stoichiometric acetic acid, albeit with a loss of activity. Lastly, the benzyl groups and the cyclohexane ring on the catalyst both appear to impede the oxidation of sterically congested C-H bonds. Although the C-H bonds on secondary carbons are still activated readily, those on tertiary carbons are oxidized less avidly than in other reported non-heme iron systems. Further modifications could potentially preclude oxidation at tertiary carbons or even direct oxidation towards primary carbons.
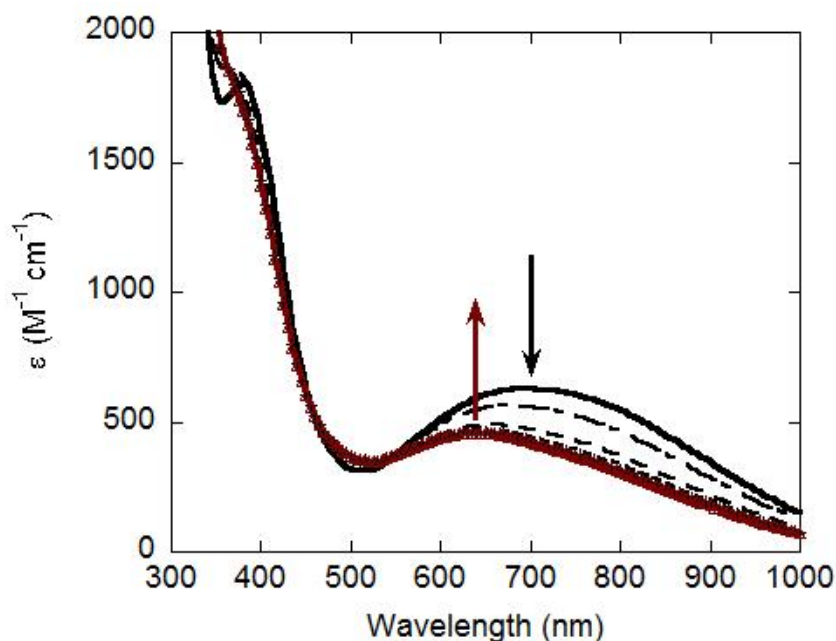
Figure 3.4 Decay of the green intermediate, tentatively assigned as [Fe(bbpc)(OOH)]$^{2+}$, over time in MeCN at 295 K. The intermediate was generated from the reaction of 1.0 mM [Fe(bbpc)(MeCN)$_2$](SbF$_6$)$_2$ with 4.0 equiv of H$_2$O$_2$. The lower limit for the ε of the 690 nm feature is 650 M^{-1} cm^{-1}; when 20 equiv of HClO$_4$ are added, the ε increases to 740 M^{-1} cm^{-1} (not shown). Six spectra are displayed; from top to bottom, these were acquired at t = 24 s (solid black), 60 s, 120 s, 180 s, 240 s, and 300 s (dark red), with t = 0 s corresponding to the initial reaction between H$_2$O$_2$ and Fe(II).
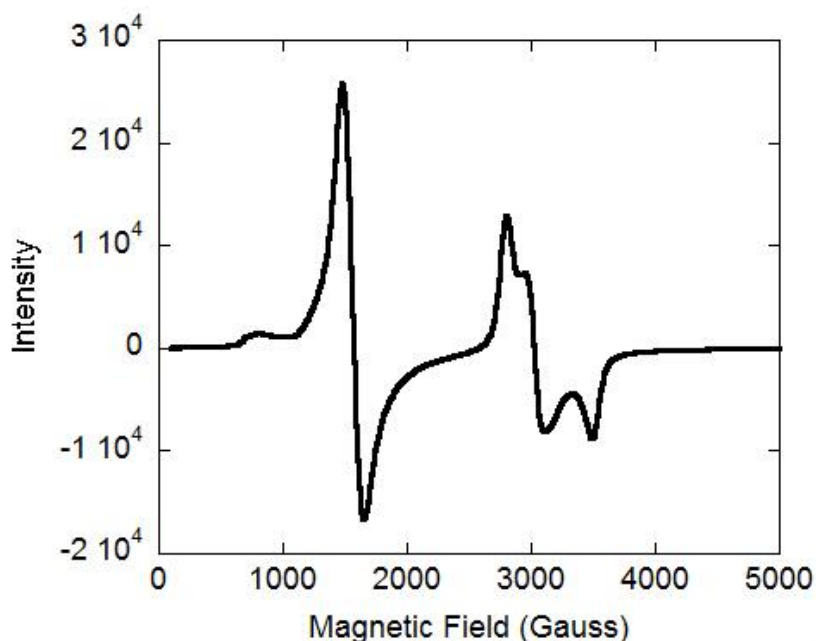
Figure 3.5 X-band EPR spectrum of the green intermediate, tentatively assigned as [Fe(bbpc)(OOH)]$^{2+}$, as a frozen MeCN solution at 77 K. The sample was prepared from the reaction between 1.0 mM [Fe(bbpc)(MeCN)$_2$](SbF$_6$)$_2$ and 4 equiv of H$_2$O$_2$. At 25 s, the reaction mixture was frozen in liquid N$_2$ and analyzed.

68

Appendix

Table 3A.1 Selected crystallographic data for bbpc and [Mn(bbpc)Cl$_2$].

Parameter	bbpc	[Mn(bbpc)Cl$_2$]•MeCN
Formula	C$_{32}$H$_{36}$N$_4$	C$_{34}$H$_{39}$Cl$_2$MnN$_5$
MW	476.65	643.54
Crystal system	Monoclinic	Orthorhombic
Space group	*C2/c (#15)*	*P2$_1$2$_1$2$_1$ (#19)*
a (Å)	17.1486(16)	10.3334(6)
b (Å)	11.4474(11)	16.4848(9)
c (Å)	14.5026(14)	18.6221(10)
(deg)	90	90
(deg)	109.012(2)	90
(deg)	90	90
V (Å^3)	2691.7(4)	3172.2(3)
Z	4	4
Cryst color	Yellow	Colorless
T (K)	193	193
Reflns collected	8963	49045
Unique reflns	2343	6673
R1 (F, I > 2σ(I))	0.08	0.0391
wR2 (F^2, all data)	0.2093	0.0700

$R1 = \Sigma||F_o| - |F_c||/\Sigma||F_o||$; $wR2 = [\Sigma w(F_o{}^2 - F_c{}^2)^2/\Sigma w(F_o{}^2)^2]^{1/2}$.
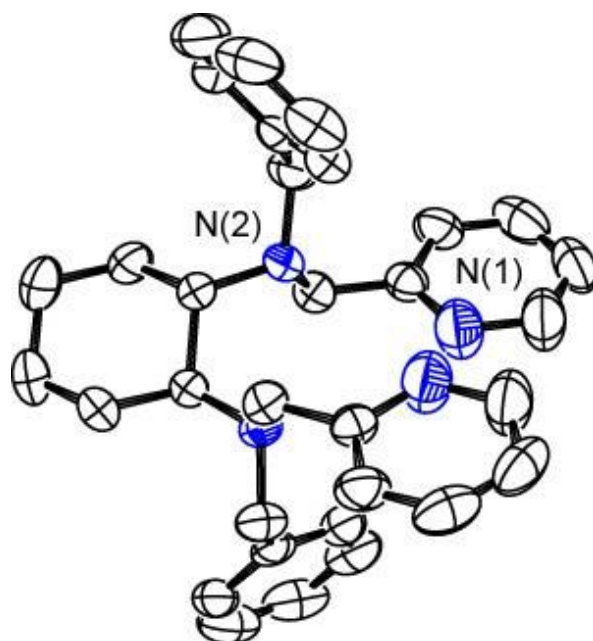
Figure 3A.1 ORTEP representation of the bbpc ligand. Hydrogen atoms have been omitted for clarity. All thermal ellipsoids are drawn at 50% probability.
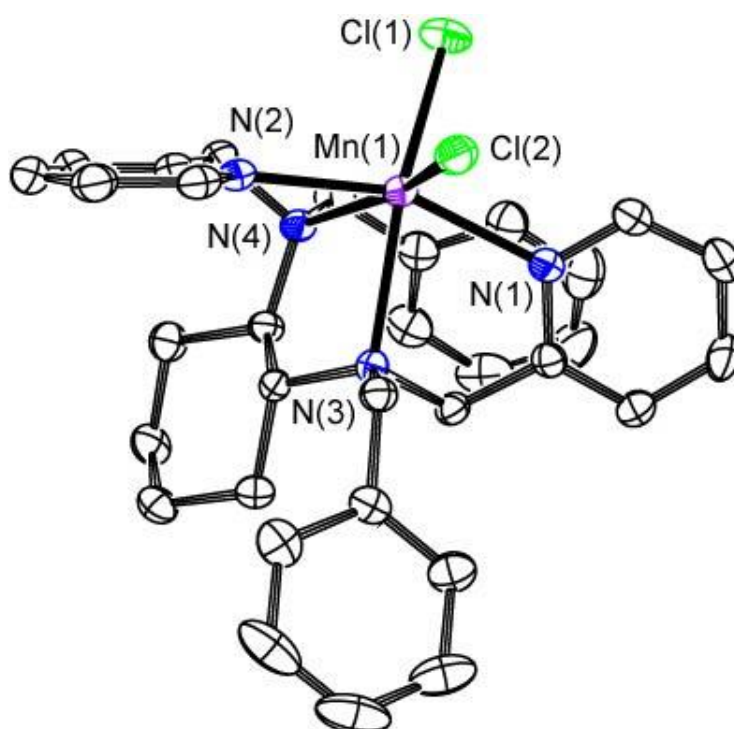
Figure 3A.2 ORTEP representation of [Mn(bbpc)Cl$_2$]. Hydrogen atoms have been omitted for clarity. All thermal ellipsoids are drawn at 50% probability.
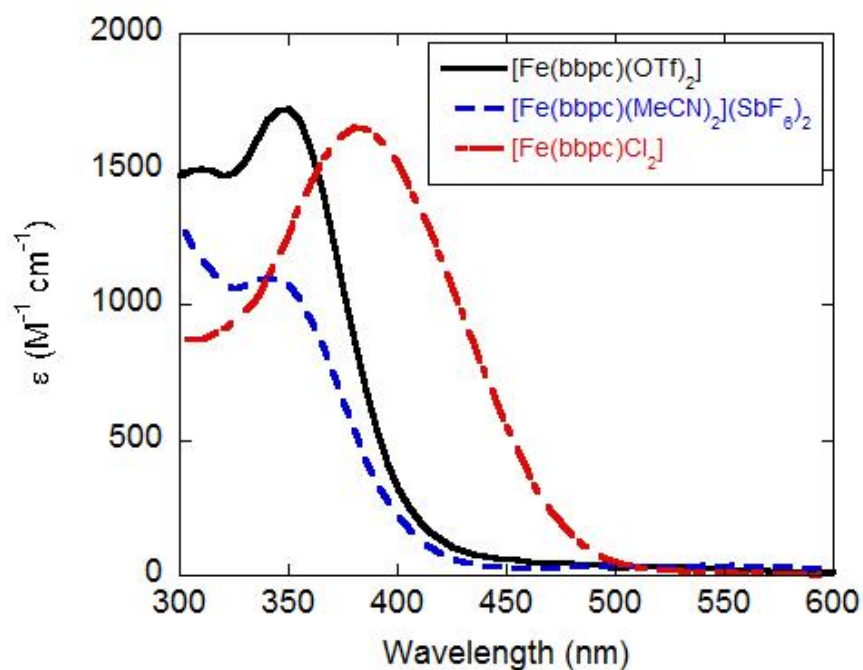
Figure 3A.3 Comparison of the UV/vis spectra of [Fe(bbpc)(OTf)$_2$], [Fe(bbpc)(MeCN)$_2$](SbF$_6$)$_2$, and [Fe(bbpc)Cl$_2$]. The above data were taken from 0.12 mM solutions of the Fe(II) compounds in MeCN. Each spectrum was acquired at 295 K.
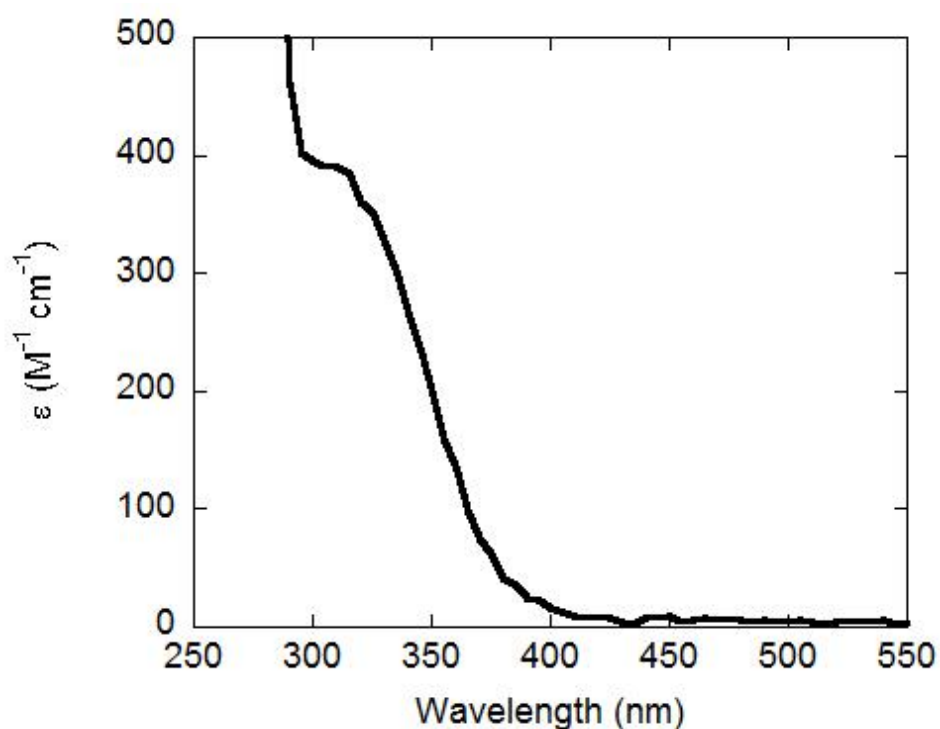
Figure 3A.4 UV/vis spectrum of [Mn(bbpc)Cl$_2$] in MeCN at 295 K. The sample concentration was 0.20 mM. The shoulder feature at 310 nm has $\varepsilon = 390$ M^{-1} cm^{-1}.
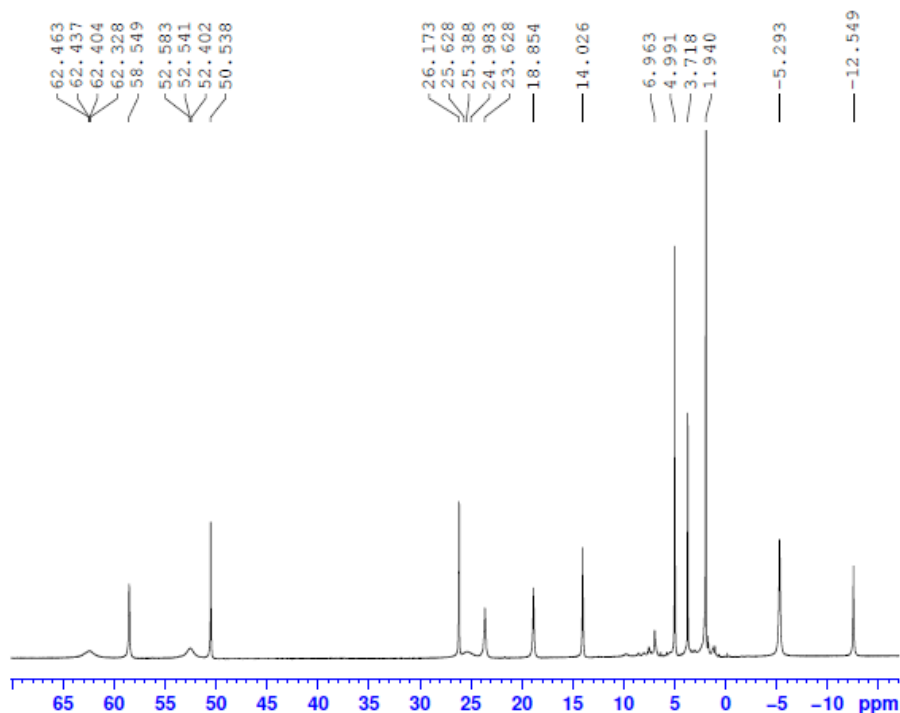
Figure 3A.5 ^{1}H NMR spectrum of a 0.10 M solution of [Fe(bbpc)(MeCN)$_2$](SbF$_6$)$_2$ in CD$_3$CN at 295 K. The peak at 1.94 ppm corresponds to MeCN.
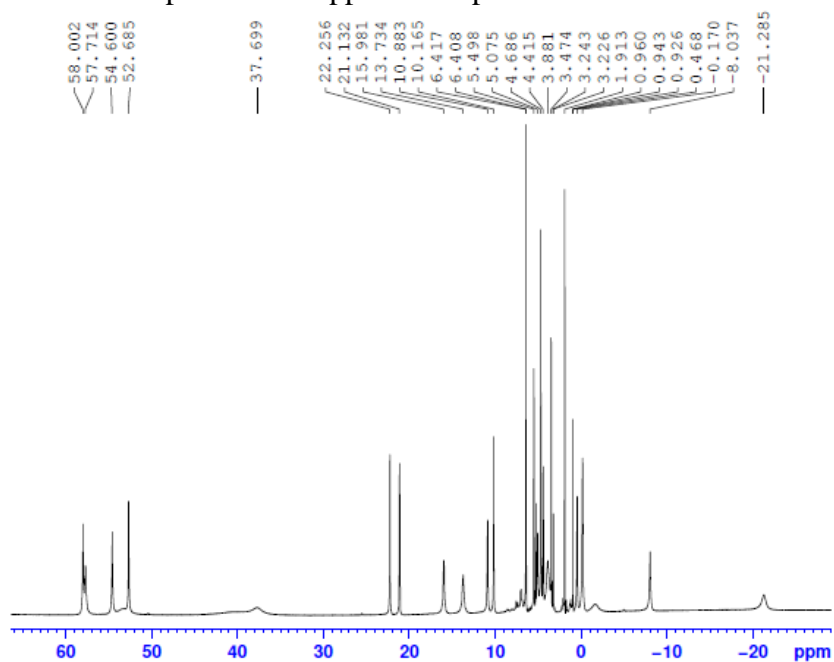
Figure 3A.6 ^{1}H NMR spectrum of a 0.10 M solution of [Fe(bbpc)(OTf)$_2$] in CD$_3$CN at 295 K. The peak at 1.91 ppm corresponds to MeCN. Note that there are two diastereomers present in the crystal structure, leading to a large number of peaks in the 0-7 ppm range relative to [Fe(bbpc)(MeCN)$_2$](SbF$_6$)$_2$.

Table 3A.2 Oxidation of hydrocarbon substrates catalyzed by [Fe(bbpc)(MeCN)$_2$](SbF$_6$)$_2$.

Substrate	Protocol[a]	[H$_2$O$_2$] (mM)	TON[b]	Product Yields[c]
n-hexane	A	100	16.2	3-hexanol (6.0%) 3-hexanone (2.1%) 2-hexanol (5.8%) 2-hexanone (2.1%)
tert-butylcyclohexane	B	0.102→0.115	6.7	3-tert-butylcyclohexanone (22%)
1,1-dimethylcyclohexane	B	0.102→0.115	8.6	2,2-dimethylcyclohexanone (8%) 3,3-dimethylcyclohexanone (10%) 4,4-dimethylcyclohexanone (18%)
adamantane	C	10	3.5	1-adamantanol (29%) 2-adamantanol/2-adamantanone (6%)[d]

All reactions were run at 295 K in MeCN. All numbers are the average of three independent reactions.

[a]Three different procedures were followed:

Protocol A) The starting concentrations of the [Fe(bbpc)(MeCN)$_2$]$^{2+}$ and the substrate were 1.0 mM and 1.0 M, respectively. A solution of H$_2$O$_2$ diluted in MeCN was added dropwise over the course of 1 min. The final volume of each reaction solution was 2.50 mL. After 30 min, the solution was filtered through silica gel and analyzed.

Protocol B) The general procedure was adapted from Reference 13 in order to facilitate comparison of the data. The substrate (0.50 mmol, 1 equiv) was dissolved in 1.0 mL of MeCN. The iron catalyst and the terminal oxidant, H$_2$O$_2$, were added to this solution in three portions. For each addition, the H$_2$O$_2$ was added dropwise over the course of 90 s. After the first additions, the concentrations were as follows: [Fe] = 4.26 M, [substrate] = 85.2 M, [H$_2$O$_2$] = 0.102 mM. 10 min after the first portion of H$_2$O$_2$ was added, further equivalents of catalyst and oxidant were added, yielding the following concentrations: [Fe] = 4.65 M, [substrate] = 46.5 M, [H$_2$O$_2$] = 0.112 mM. 20 min after the first portion of H$_2$O$_2$ was added, the third portions of catalyst and oxidant were added, yielding the following concentrations: [Fe] = 4.80 M, [substrate] = 32.0 M, [H$_2$O$_2$] = 0.115 mM. At 30 min, the reaction solution was filtered through a short plug of silica gel prior to analysis.

Protocol C) Identical to Protocol A except that the starting concentration of adamantine was 10 mM, due to the lesser solubility of this alkane in MeCN.

[b]Defined as the number of moles of oxidized organic products generated per mole of Fe(II) catalyst.
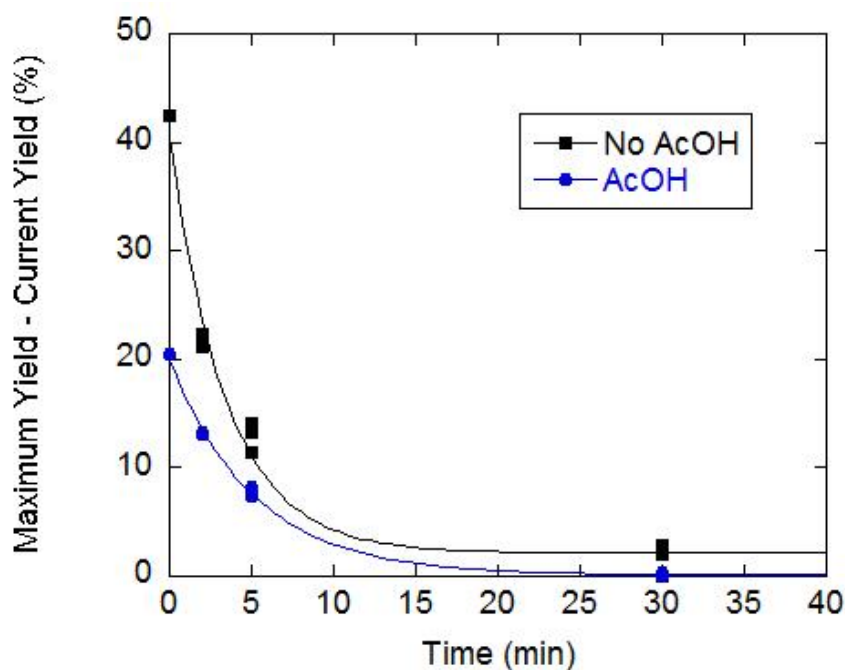
Figure 3A.7 Oxidation of cyclohexanol to cyclohexanone in the presence and absence of acetic acid (AcOH). The data are from **Figure 3**. In order to assess the lifetime of the catalyst, the differences between the maximum observed yield and the current yield as a function of time were plotted and fit to exponential decay functions of the form: $y = a + be^{-ct}$. For the reactions run in the absence of acetic acid, $c = 0.29$ (± 0.03) min^{-1}, with an $R = 0.98796$ for the overall fit. For the reactions run in the presence of acetic acid, $c = 0.20$ (± 0.01) min^{-1}, with an $R = 0.99866$ for the overall fit. The results may suggest that the catalyst derived from $[Fe(bbpc)(MeCN)]^{2+}$ is slightly hardier but less active when AcOH is present.
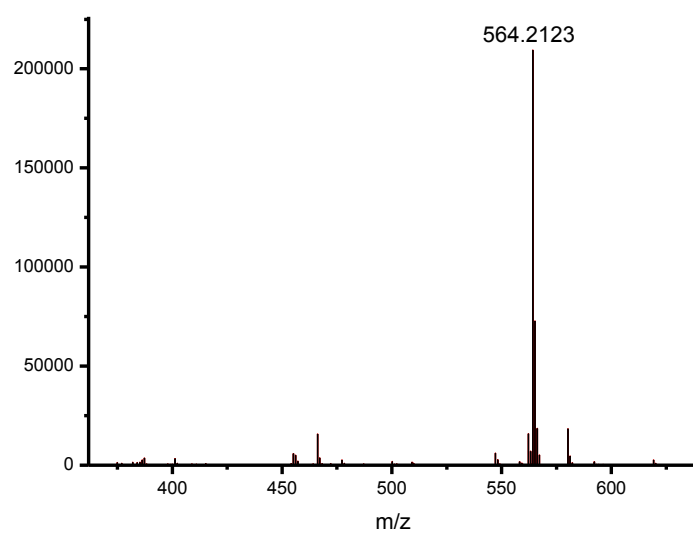
Figure 3A.8 ESI Mass spectrum of the green species formed when 4 equiv of H_2O_2 reacts with 1.0 mM [Fe(bbpc)(MeCN)$_2$](SbF6)$_2$ in MeCN at 295 K. The major m/z peak is at 564.2123.
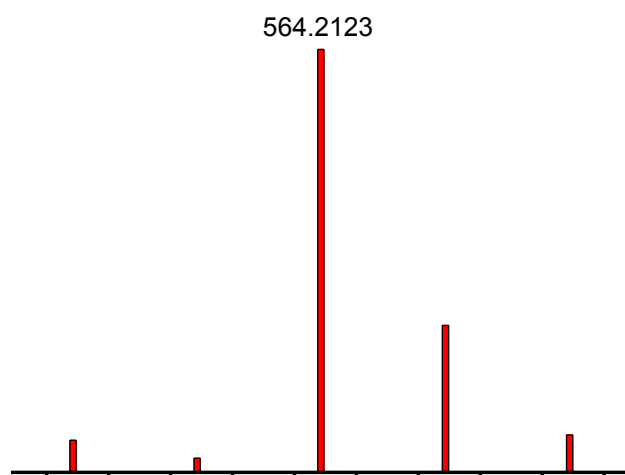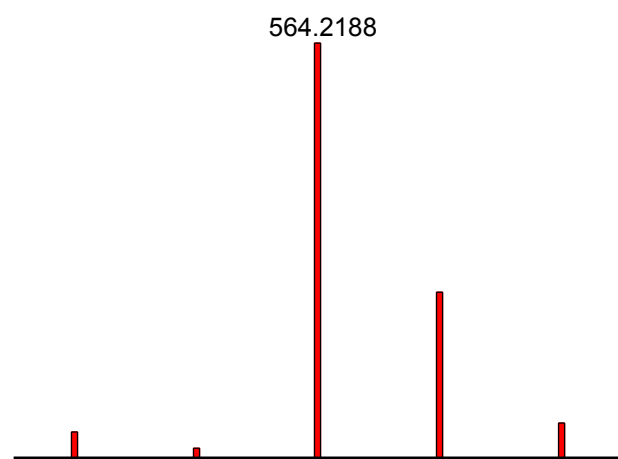
Figure 3A.9 Isotopic pattern predicted for [Fe(bbpc)(O$_2$)]$^+$ (top) compared to the expanded region around the m/z peak at 564.2123 from **Figure 3.A8** (bottom).

References

(1)   Shilov, A.E.; Shul'pin, G. B. *Chem. Rev.*, **1997**, *97*, 2879-2932.

(2)   Lersch, M.; Tilset, M. *Chem. Rev.* **2005**, *105*, 2471-2526.

(3)   Davies, H.M.L.; Beckwith, R.E.J. *Chem. Rev.* **2003**, *103*, 2861-2904.

(4)   Jia, C.; Kitamura, T.; Fujiwara, Y. *Acc. Chem. Res.* **2001**, *34*, 633-639.

(5)   Crabtree, R.H. *Chem. Rev.* **2010**, *110*, 575.

(6)   Bhan, A.; Iglesia, E. *Acc. Chem. Res.* **2008**, *41*, 559-567.

(7)   De Vos, D. E.; Dams, M.; Sels, B. F.; Jacobs, P. A. *Chem. Rev.* **2002**, *102*, 3615– 3640.

(8)   Ernst, S.; Disteldorf, H.; Yang, X. *Microporous Mesoporous Mater.* **1998**, *22*, 457– 464.

(9)   Lee, S. J.; Lin, W.Acc. *Chem. Res.* **2008**, *41*, 521-537.

(10)   Fiedler, D.; Leung, D. H.; Bergman, R. G.; Raymond, K. N. *Acc. Chem. Res.* **2004**, *38*, 349– 358

(11)   Fackler, P.; Berthold, C.; Voss, F.; Bach, T. *J. Am. Chem. Soc.* **2010**, *132*, 15911– 15913.

(12)   Das, S.; Incarvito, C. D.; Crabtree, R. H.; Brudvig, G. W. *Science* **2006**, *312*, 1941– 1943.

(13)   Chen, M. S.; White, M. C. Science **2010**, *327*, 566– 571.

(14)   Goldsmith, C. R.; Coates, C. M.; Hagan, K.; Mitchell, C. A. *J. Mol. Catal. A* **2011**, *335*, 24– 30.

(15)   Chen, J.; Che, C.-M. *Angew. Chem., Int. Ed.* **2004**, *43*, 4950– 4954.

(16)   Zhang, J.-L.; Che, C.-M. *Chem. —Eur. J.* **2005**, *11*, 3899– 3914.

(17)   Chen, M. S.; White, M. C. *Science* **2007**, *318*, 783– 787.

(18)   Holm, R. H.; Kennepohl, P.; Solomon, E. I. *Chem. Rev.* **1996**, *96*, 2239– 2314.

(19)   Mirica, L. M.; Ottenwaelder, X.; Stack, T. D. P. *Chem. Rev.* **2004**, *104*, 1013–1046.

(20)   Gupta, R.; Borovik, A. S. *J. Am. Chem. Soc.* **2003**, *125*, 13234– 13242.

(21)   Borovik, A. S. *Acc. Chem. Res.* **2005**, *38*, 54– 61

(22)   Gupta, R.; MacBeth, C. E.; Young, V. G., Jr.; Borovik, A. S. *J. Am. Chem. Soc.* **2002**, *124*, 1136– 1137.

(23)   Parsell, T. H.; Behan, R. K.; Green, M. T.; Hendrich, M. P.; Borovik, A. S. *J. Am. Chem. Soc.* **2006**, *128*, 8728– 8729.

(24)   MacBeth, C. E.; Golombek, A. P.; Young, V. G., Jr.; Yang, C.; Kuczera, K.; Hendrich, M. P.; Borovik, A. S. *Science* **2000**, *289*, 938– 941

(25)   Lacy, D. C.; Gupta, R.; Stone, K. L.; Greaves, J.; Ziller, J. W.; Hendrich, M. P.; Borovik, A. S. *J. Am. Chem. Soc.* **2010**, *132*, 12188– 12190.

(26)   Klinker, E. J.; Kaizer, J.; Brennessel, W. W.; Woodrum, N. L.; Cramer, C. J.; Que, L., Jr. *Angew. Chem., Int. Ed.* **2005**, *44*, 3690– 3694.

(27)   England, J.; Guo, Y.; Farquhar, E. R.; Young, V. G., Jr.; Münck, E.; Que, L., Jr. *J. Am. Chem. Soc.* **2010**, *132*, 8635– 8644.

(28)   Rohde, J.-U.; In, J.-H.; Lim, M. H.; Brennessel, W. W.; Bukowski, M. R.; Stubna, A.; Münck, E.; Nam, W.; Que, L., Jr. *Science* **2003**, *299*, 1037– 1039.

(29)   Chen, K.; Costas, M.; Kim, J.; Tipton, A. K.; Que, L., Jr. *J. Am. Chem. Soc.* **2002**, *124*, 3026– 3035.

(30)   Cook, B. R.; Reinert, T. J.; Suslick, K. S. *J. Am. Chem. Soc.* **1986**, *108*, 7281– 7286.

(31)   Groves, J. T.; Viski, P. *J. Am. Chem. Soc.* **1989**, *111*, 8537– 8538.

(32)   Costas, M.; Que, L., Jr. *Angew. Chem., Int. Ed.* **2002**, *41*, 2179– 2181.

(33)   Haynes, J. S.; Sams, J. R.; Thompson, R. C. *Can. J. Chem.* **1981**, *59*, 669– 678.

(34)   Glerup, J.; Goodson, P. A.; Hazell, A.; Hazell, R.; Hodgson, D. J.; McKenzie, C. J.; Michelsen, K.; Rychlewska, U.; Toftlund, H. *Inorg. Chem.* **1994**, *33*, 4105– 4111.

(35)   Stoll, S.; Schweiger, A. *J. Magn. Reson.* **2006**, *178*, 42– 55.

(36)   Sheldrick, G. M. *SHELXTL*, 6.12 ed.; Siemens Analytical X-ray Instruments, Inc.: Madison, WI, **2001**.

(37)   Sheldrick, G. M. *SADABS*; Bruker Analytical X-ray Systems: Madison, WI, **1996**.

(38)   Fenton, R. R.; Vagg, R. S.; Jones, P.; Williams, P. A. *Inorg. Chim. Acta.* **1987**, *128*, 219– 229.

(39)   Coates, C. M.; Hagan, K.; Mitchell, C. A.; Gorden, J. D.; Goldsmith, C. R. *Dalton.Trans.* **2011**, *40*, 4048– 4058.

(40)   Shannon, R. D. *Acta Crystallogr.* **1976**, *A32*, 751– 767

(41)   Goldsmith, C. R.; Jonas, R. T.; Cole, A. P.; Stack, T. D. P. *Inorg. Chem.* **2002**, *41*, 4642– 4652.

(42)   Tanase, S.; Marques-Gallego, P.; Browne, W. R.; Hage, R.; Bouwman, E.; Feringa, B. L.; Reedijk, *J. Dalton Trans.* **2008**, 2026– 2033.

(43)   Gómez, L.; Garcia-Bosch, I.; Company, A.; Benet-Buchholz, J.; Polo, A.; Sala, X.; Ribas, X.; Costas, M. *Angew. Chem., Int. Ed.* **2009**, *48*, 5720– 5723.

(44)   England, J.; Britovsek, G. J. P.; Rabadia, N.; White, A. J. P. *Inorg. Chem.* **2007**, *46*, 3752– 3767.

(45)   Britovsek, G. J. P.; England, J.; White, A. J. P. *Inorg. Chem.* **2005**, *44*, 8125– 8134.

(46)   Newhouse, T.; Baran, P. S. *Angew. Chem., Int. Ed.* **2011**, *50*, 3362– 3374.

(47)   Mas-Ballesté, R.; Que, L., Jr. *J. Am. Chem. Soc.* **2007**, *129*, 15964– 15972

(48)   Qui ñonero, D.; Musaev, D. G.; Morokuma, K. *Inorg. Chem.* **2003**, *42*, 8449–8455.

(49)   Qui ñonero, D.; Morokuma, K.; Musaev, D. G.; Mas-Ballest é, R.; Que, L., Jr. *J. Am. Chem. Soc.* **2005**, *127*, 6548– 6549.

(50)   Kim, S. O.; Sastri, C. V.; Seo, M. S.; Kim, J.; Nam, W. *J. Am. Chem. Soc.* **2005**, *127*, 4178– 4179.

(51)   Chen, K.; Que, L. Jr. *J. Am. Chem. Soc.* **2001**, *123*, 6327-6337.

(52)   McMillen, D. F.; Golden, D. M. Annu. *Rev. Phys. Chem.* **1982**, *33*, 493– 532.

(53)   Goldsmith, C. R.; Jonas, R. T.; Stack, T. D. P. J. *Am. Chem. Soc.* **2002**, *124*, 83– 96.

(54)   Company, A.; G ómez, L.; G üell, M.; Ribas, X.; Luis, J. M.; Que, L., Jr.; Costas, M. *J. Am. Chem. Soc.* **2007**, *129*, 15766– 15767.

(55)   Kaizer, J.; Klinker, E. J.; Oh, N. Y.; Rohde, J.-U.; Song, W. J.; Stubna, A.; Kim, J.; M ünck, E.; Nam, W.; Que, L., Jr. *J. Am. Chem. Soc.* **2004**, *126*, 472– 473.

(56)   Nam, W. *Acc. Chem. Res.* **2007**, *40*, 522– 531.

(57)   Fiedler, A. T.; Que, L., Jr. *Inorg. Chem.* **2009**, *48*, 11038– 11047.

(58)   Murphy, A.; Dubois, G.; Stack, T. D. P. *J. Am. Chem. Soc.* **2003**, *125*, 5250–5251.

(59)   Costas, M.; Tipton, A. K.; Chen, K.; Jo, D.-H.; Que, L., Jr. *J. Am. Chem. Soc.* **2001**, *123*, 6722– 6723.

(60)   Costas, M.; Rohde, J.-U.; Stubna, A.; Ho, R. Y. N.; Quaroni, L.; M ünck, E.; Que, L., Jr. *J. Am. Chem. Soc.* **2001**, *123*, 12931– 12932.

(61)   Wu, M.; Wang, B.; Wang, S.; Xia, C.; Sun, W. *Org. Lett.* **2009**, *11*, 3622–3625.

(62)   Birse, E. F.; Cox, M. A.; Williams, P. A.; Stephens, F. S.; Vagg, R. S. *Inorg. Chim. Acta.* **1988**, *148*, 45– 56.

(63)   Reynolds, M. F.; Costas, M.; Ito, M.; Jo, D.-H.; Tipton, A. A.; Whiting, A. K.; Que, L., Jr. J. Biol. *Inorg. Chem.* **2003**, *8*, 263– 272.

(64)   Mas-Ballesté, R.; Costas, M.; van den Berg, T.; Que, L., Jr. *Chem.—Eur. J.* **2006**, *12*, 7489– 7500.

(65)   White, M. C.; Doyle, A. G.; Jacobsen, E. N. *J. Am. Chem. Soc.* **2001**, *123*, 7194– 7195.

(66)   Sastri, C. V.; Lee, J.; Oh, K.; Lee, Y. J.; Lee, J.; Jackson, T. A.; Ray, K.; Hirao, H.; Shin, W.; Halfen, J. A.; Kim, J.; Que, L., Jr.; Shaik, S.; Nam, W. *Proc. Natl. Acad. Sci.,* **2007**, *104*, 19181– 19186.

(67)   Leising, R. A.; Norman, R. E.; Que, L., Jr. *Inorg. Chem.* **1990**, *29*, 2553– 2555

(68)   Kim, C.; Chen, K.; Kim, J.; Que, L., Jr. *J. Am. Chem. Soc.* **1997**, *119*, 5964– 5965

(69)   Rohde, J.-U.; Stubna, A.; Bominaar, E. L.; Münck, E.; Nam, W.; Que, L., Jr. *Inorg. Chem.* **2006**, *45*, 6435– 6445

(70)   Chen, K.; Que, L., Jr. *Chem. Commun.* **1999**, 1375– 1376

(71)   England, J.; Gondhia, R.; Bigorra-Lopez, L.; Petersen, A. R.; White, A. J. P.; Britovsek, G. J. P. *Dalton Trans.* **2009**, 5319– 5334

(72)   Sooknoi, T.; Limtrakul, *J. Appl. Catal., A* **2002**, *233*, 227– 237.

(73)   Shi, S.; Wang, Y.; Xu, A.; Wang, H.; Zhu, D.; Roy, S. B.; Jackson, T. A.; Busch, D. H.; Yin, G. *Angew. Chem., Int. Ed.* **2011**, *50*, 7321– 7324

(74)   Que, L., Jr. *Acc. Chem. Res.* **2007**, *40*, 493– 500.

(75)   Lee, Y.-M.; Hong, S.; Morimoto, Y.; Shin, W.; Fukuzumi, S.; Nam, W. *J. Am. Chem. Soc.* **2010**, *132*, 10668– 10670

(76)   Li, F.; Meier, K. K.; Cranswick, M. A.; Chakrabarti, M.; Van Heuvelen, K. M.; Münck, E.; Que, L., Jr. *J. Am. Chem. Soc.* **2011**, *133*, 7256– 7259

(77)   Mukherjee, A.; Cranswick, M. A.; Chakrabarti, M.; Paine, T. K.; Fujisawa, K.; Münck, E.; Que, L., Jr. *Inorg. Chem.* **2010**, *49*, 3618– 3628.

(78)   Martinho, M.; Blain, G.; Banse, F. *Dalton Trans.* **2010**, *39*, 1630– 1634.

(79)   Roelfes, G.; Lubben, M.; Hage, R.; Que, L., Jr.; Feringa, B. L. *Chem.—Eur. J.* **2000**, *6*, 2152– 2159.

(80)   Russell, G. A. *J. Am. Chem. Soc.* **1957**, *79*, 3871– 3877.

(81)   Roelfes, G.; Lubben, M.; Chen, K.; Ho, R. Y. N.; Meetsma, A.; Genseberger, S.; Hermant, R. M.; Hage, R.; Mandal, S. K.; Young, V. G., Jr.; Zang, Y.; Kooijman, H.; Spek, A. L.; Que, L., Jr.; Feringa, B. L. *Inorg. Chem.* **1999**, *38*, 1929– 1936.

(82)   Shearer, J.; Scarrow, R. C.; Kovacs, J. A. *J. Am. Chem. Soc.* **2002**, *124*, 11709– 11717.

(83)   Ho, R. Y. N.; Roelfes, G.; Hermant, R.; Hage, R.; Feringa, B.L.; Que, L., Jr. *Chem. Commun.* **1999**, 2161– 2162

(84)   Namuswe, F.; Hayashi, T.; Jiang, Y.; Kasper, G. D.; Narducci Sarjeant, A. A.; Moënne-Loccoz, P.; Goldberg, D. P. *J. Am. Chem. Soc.* **2009**, *132*, 157– 167

(85)   Bassan, A.; Blomberg, M. R. A.; Siegbahn, P. E. M.; Que, L., Jr. *J. Am. Chem. Soc.* **2002**, *124*, 11056– 11063.

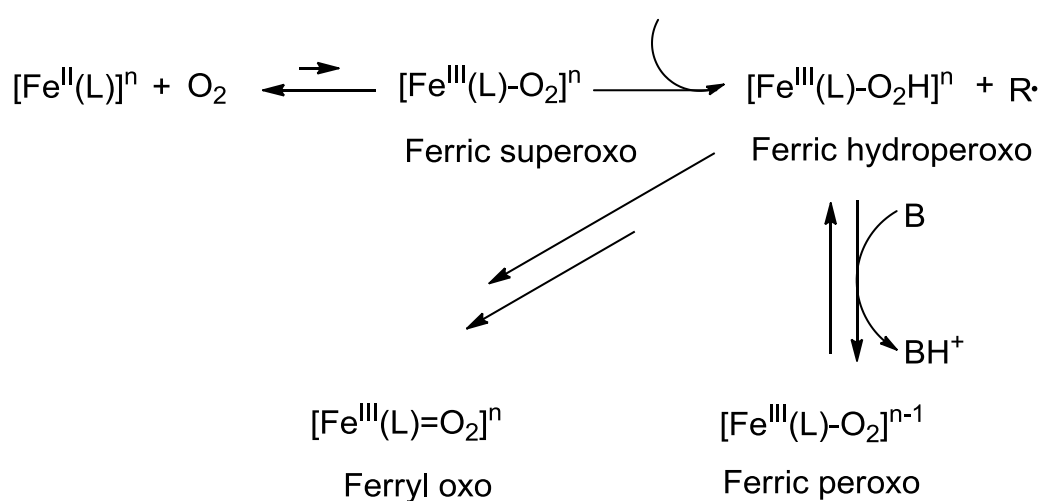(86)   Park, M. J.; Lee, J.; Suh, Y.; Kim, J.; Nam, W. *J. Am. Chem. Soc.* **2006**, *128*, 2630– 2634

Chapter 4

Observation of a Ferric Hydroperoxide Complex in Reactions between a Non-heme Ferrous Complex, O_2, and Hydrocarbon Substrates[*]

4.1 Introduction

Mononuclear non-heme iron enzymes have been investigated extensively over the past several decades and have garnered much attention due to their abilities to catalyze the oxidation of C-H bonds by O_2 through the use of an exceedingly abundant and inexpensive metal. The anticancer activity of the glycopeptide bleomycin is believed to degrade DNA through similar chemistry, with a ferric hydroperoxide species being the last observable intermediate before the rate-determining step of this reactivity.[1, 2] Although most functional small molecule analogs of these biomolecules use H_2O_2 or other two-electron acceptors as the terminal oxidant,[3-6] some recent work has focused on using O_2 in this capacity.[7-14] In much of this prior work, ferryl oxo species have been postulated, observed, and identified during the oxidations of the hydrocarbons. These Fe(IV)=O species are believed to be preceded by ferric superoxo and ferric hydroperoxide complexes (Scheme 4.1), but evidence for these is indirect. The intermediacy of Fe(III)-OOH species, for instance, is largely supported by the isolation and identification of their conjugate base ferric peroxo complexes under basic conditions.[8, 15, 16]

$$[Fe^{II}(L)]^n + O_2 \rightleftharpoons [Fe^{III}(L)\text{-}O_2]^n \longrightarrow [Fe^{III}(L)\text{-}O_2H]^n + R^\bullet$$

Ferric superoxo   Ferric hydroperoxo

$[Fe^{III}(L)=O_2]^n$ $[Fe^{III}(L)\text{-}O_2]^{n-1}$

Ferryl oxo   Ferric peroxo

Scheme 4.1 Mechanism of O_2 activation

One difficulty is that the known Fe(III)-OOH complexes tend to be extremely unstable.[15-18] Analysis of the proposed ferric superoxo complex, that is believed to serve as the initial metal-based oxidant, suffers in that the immediate product of the initial C-H activation does not accumulate. With some ligand systems, however, Fe(III)-OOH complexes are much more stable and are commonly observed instead of higher-valent iron species, such as Fe(IV)=O complexes.[19-23] Previously, two mononuclear Fe(III)-OOH complexes have been generated from reactions between O_2 and an Fe(II) precursor, but these use discrete proton and electron donors, as opposed to abstracting a hydrogen atom from an alkane or alkene substrate.[16, 24]

In prior work, we found that the [Fe(bbpc)(MeCN)$_2$]$^{2+}$ complex could catalyze the oxygenation of C-H bonds using H_2O_2 as the terminal oxidant.[19] The bbpc ligand differs from the more extensively studied 1,4,8,11-tetramethyl-1,4,8,11-tetraazacyclotetradecane (TMC)[8,15,17,25] in that it prefers to coordinate iron ions in a *cis-* rather than a *trans-* conformation and contains more strongly electron-withdrawing pyridine rings in place of two amine N-donors. When H_2O_2 is added to [Fe(bbpc)(MeCN)$_2$]$^{2+}$ in the absence of a hydrocarbon substrate, we found substantial evidence for a Fe(III)-OOH intermediate that could be stabilized through the addition of either acetic or perchloric acid.[19]

4.2 Experimental Section

Materials

Unless stated otherwise, all chemicals were purchased from Sigma-Aldrich and used without further purification. Anhydrous acetonitrile (MeCN) was stored under a dry N_2 atmosphere. 9,10-tetradeutero-9,10-dihydroanthracene (*d4*-DHA) was prepared through a previously reported procedure,[26] as were *N,N'*-di(phenylmethyl)-

N,N′-bis(2-pyridinylmethyl)- 1,2-cyclohexanediamine (bbpc) and [Fe(bbpc)(MeCN)$_2$](SbF6)$_2$.[19]

Instrumentation

A Varian Cary 50 spectrophotometer was used to acquire optical data. High resolution mass spectrometry (HR-MS) data were obtained at the Mass Spectrometer Center at Auburn University, using a Bruker microflex LT MALDI-TOF mass spectrometer operated in the positive ion mode. Electron paramagnetic resonance (EPR) spectra were collected on a Bruker EMX-6/1 X-band spectrometer operated in the perpendicular mode; all samples were run as frozen MeCN solutions in quartz tubes. The EPR data werer analyzed with the program Easyspin.

Stopped-Flow Kinetic Data

All kinetic data were collected at 23 ($\pm$0.1) ℃ on a Hi-Tec SF-51 Stopped-Flow Spectrophotometer with Olis 4300S data acquisition and analysis software. The reaction were monitored at 535 nm every 0.2 s, which displayed greatest change in absorbance during the reactions. The initial concentration of [Fe(bbpc)(MeCN)$_2$](SbF6)$_2$ was 0.5 mM for all experiments. All of the reported data are the averages of at least three independent experiments. The initial rates were calculated using the nine data points collected from 0.4 s – 2.0 s.

4.3 Results and Discussion

EPR Observation of a Ferric Hydroperoxide Intermediate

Although aerobic solutions of [Fe(bbpc)(MeCN)$_2$](SbF$_6$)$_2$ in MeCN are indefinitely stable in the absence of a hydrocarbon substrate, the addition of 9,10-dihydroanthracene (DHA), cyclohexene, *trans*-1,2-dimethylcyclohexane, or *cis*-1,2-dimethylcyclohexane leads to noticeable changes in the color of the solution.

Quenching the reaction with cyclohexene at 25 s and subsequently analyzing the sample by electron paramagnetic resonance (EPR) reveals that the Fe(II) is oxidized to a mixture of high-spin and low-spin Fe(III). The features in this spectrum are nearly identical to those observed in the previously studied reaction between H_2O_2 and $[Fe(bbpc)(MeCN)_2]^{2+}$ (Figure 4.1). The observed high-spin and low-spin Fe(III) features for the H_2O_2-oxidized iron were previously speculated to be a consequence of spin-crossover behavior.[19] Spin-crossover was also observed in other O_2 activation.[24] Consistent with this hypothesis, the ratio of the high-spin and low-spin components in the EPR data is not consistent for otherwise identically prepared samples; the rapid freezing of the samples apparently prevents the full equilibration of the $S = 5/2$ and $1/2$ states. Also, samples frozen and studied at lower temperatures tend to have more prominent low-spin features since the $S = 1/2$ electronic state is enthalpically favored over the $S = 5/2$.[26] For the samples oxidized by H_2O_2, we do not believe that the high-spin feature corresponds to a ferric end-product since its intensity increases and decreases at about the same rate as that of the low-spin signal (Figure 4A.4).

The oxidation of $[Fe(bbpc)(MeCN)_2]^{2+}$ by O_2 in presence of cyclohexene appears to proceed less cleanly. The high-spin signal is consistently more intense (Figure 4.1), and the mass spectrometry (MS) data associated with the intermediate contain several more m/z peaks, most of which are consistent with ligand decomposition (Figure 4A.6). Consequently, we believe that multiple high-spin Fe(III) species are present in the samples oxidized by O_2/cyclohexene mixtures. The EPR spectra of O_2-oxidized $[Fe(bbpc)(MeCN)_2]^{2+}$ also contain sharp peaks at $g \sim 2$, which are typical for organic radicals (Figure 4A.5). The reaction between a ferric superoxo species and an alkene substrate would be anticipated to generate an alkenyl radical in addition to the ferric hydroperoxo intermediate. This feature develops

gradually, reaching a peak intensity at about 5 min. The reaction between a ferric superoxo species and an alkene substrate would be anticipated to generate an allylic radical in addition to the ferric hydroperoxo intermediate. This radical would readily react with O_2, which is present at 8 mMin aerated MeCN at room temperatures,[27] to yield an organic peroxyl radical, which itself is capable of oxidizing the bbpc ligand.
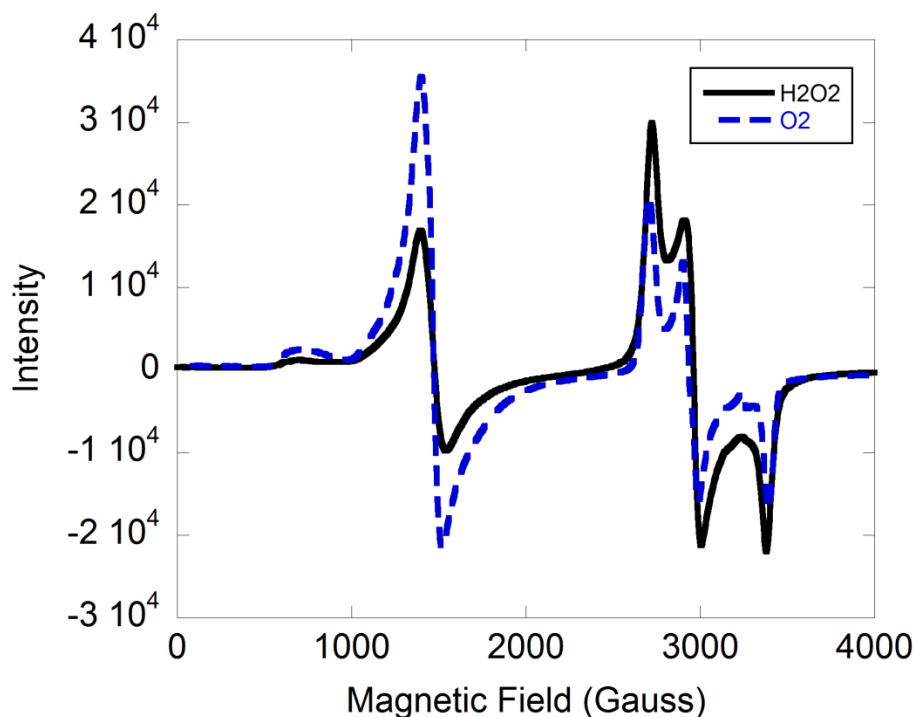

Figure 4.1 Comparative X-band EPR spectra of the species generated from the reactions between 1.0 mM $[Fe(bbpc)(MeCN)_2]^{2+}$ and A) 2.0 mM H_2O_2 in MeCN (black solid line, g = 4.28, 2.37, 2.19, 1.93) and B) 200 mM cyclohexene under air (blue dashed line, g = 4.27, 2.39, 2.21, 1.92). The EPR data were acquired at 20 K with samples that were frozen 25 s after the initial mixing of the reagents.

Mass Spectrometry Analysis of Intermediate

The MS of the H_2O_2- and air-derived intermediates share several features, in particular the 564.2 m/z peak corresponding to $[Fe(bbpc)(O_2)]^+$ (Figure 4A.6, Figure 4A.7). The addition of an acid, such as perchloric acid or acetic acid, has no influence on the g values for the high-spin and low-spin Fe(III) species but introduces additional features into the MS, including a m/z peak at 606.2 that is assigned as

[Fe(bbpc)(OOH)(MeCN)]$^+$ (Figure 4A.8). In order to confirm the incorporation of O_2 into the intermediate, we reacted the Fe(II) precursor with ^{18}O-labeled dioxygen and cyclohexene. Unexpectedly, we observed features consistent with ^{16}O-^{18}O incorporation in addition to those corresponding to $^{16}O_2$ and $^{18}O_2$ (Figure 4A.9). The $^{16}O_2$ adduct is anticipated, given the residual dioxygen contained in the mobile phase used for the MS measurements; It disappears as the $^{18}O_2$-treated samples are run. As for the ^{16}O-^{18}O adduct, we speculate that the oxygen atoms from adventitious water molecules are exchanging into the complex through an as yet uncharacterized equilibration process capable of breaking and reforming the O-O bonds. When the Fe(II) precursor is oxidized by either H_2O_2 or cyclohexene/air in the presence of 3 mM $H_2^{18}O$, more prominent m/z feature appears at 566.2 in the acid-free spectra and at 608.2 in the MS of the samples containing acetic acid (Figure 4.2, Figure 4A.11, Figure 4A.12). Previously, it has been speculated that O-O bonds in Fe(III)-OOH complexes can homolytically or heterolytically cleave to form high valent species (Scheme 4.2, with homolytic cleavage shown).[18,28] Substantial evidence suggests that the O atoms from H_2O can exchange into these high-valent species.[29-31] The MS data here may suggest that the O-O cleavage is reversible in certain instances. The availability of *cis* coordination sites and the relatively electron-withdrawing ligand would be anticipated to facilitate this reverse reaction by keeping the O atoms of the former –OOH ligand close to one another and by favoring lower metal oxidation states, respectively. The alternative mechanistic possibility, Lewis acid-catalyzed O atom exchange into an intact hydroperoxyl group, is unlikely.[32, 33]
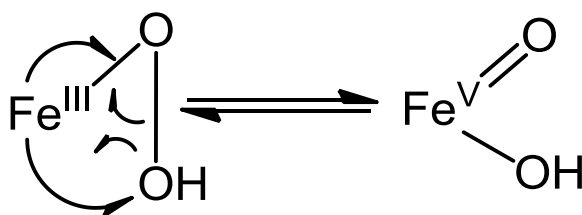
Scheme 4.2 Equilibrium between Fe^{III}-(OOH) and Fe^{V}=(O)OH)

Kinetic Analysis

The formation of the ferric hydroperoxide species was followed by stopped-flow kinetics. The reactions were run in O_2-saturated MeCN with a variable amount of hydrocarbon substrate present (Figure 4.3). When a substrate containing a weak C-H bond is present in high enough concentrations, a transient UV/Vis feature with a maximum absorbance a 650 nm is observed (Figure 4A.1, Figure 4A.2, Figure 4A.3). The intensity maximizes at about 25 s, after which a λ_{max} of 535 nm slowly develops. The kinetic data cannot be fit to a simple single or double-exponential model (Figure 4A. 13, Figure 4A.14). Instead, we approximate the initial rates, which should correspond largely to the formation of the Fe (III)-OOH species. The initial rates were measured from 0.4 to 2.0 s, which should minimize the influence of decomposition reactions and catalytic turnover on the analysis. The changes in absorbance over this time scale linearly with the concentration of the hydrocarbon, indicating that the initial oxidation of the iron is first-order with respect to the hydrocarbon. The rate of formation also depends on the bond dissociation energies (BDEs) of the weakest C-H bonds in the substrates. DHA (BDE = 77 kcal mol^{-1}) leads to faster oxidation than cyclohexene (BDE = 81 kcal mol^{-1}), which in turn oxidizes the Fe(II) more quickly than cycloheptene (BDE = 83 kcal mol^{-1}).[34] The reactivity with deuterated DHA was also assessed. The k_H/k_D ratio of 6.8 is consistent with a primary kinetic isotope effect and implicates C-H bond cleavage in the rate-determining step. The results are consistent with the mechanism proposed in Scheme 4.1: hydrogen atom abstraction

from the hydrocarbon by a ferric superoxo complex or isoelectronic species to form

an Fe(III)-OOH complex.
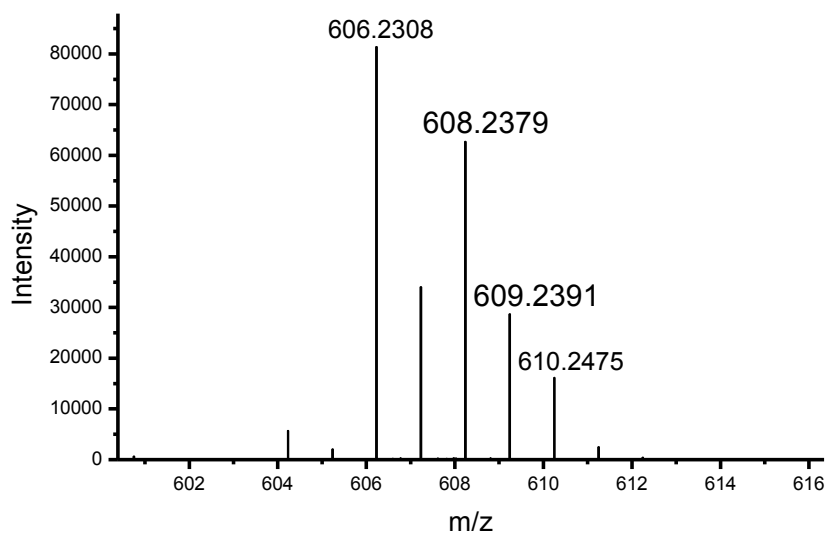
Figure 4.2 Mass spectrum of the species generated from the reaction between 1.0 mM [Fe(bbpc)(MeCN)$_2$](SbF$_6$)$_2$, 400 mM cyclohexene, 100 mM AcOH in aerobic MeCN and 3 mM H$_2$^{18}O present as additives. The new features at 608.2 is assigned to [Fe(bbpc)(^{18}O^{16}OH)(CH$_3$CN)]$^+$.
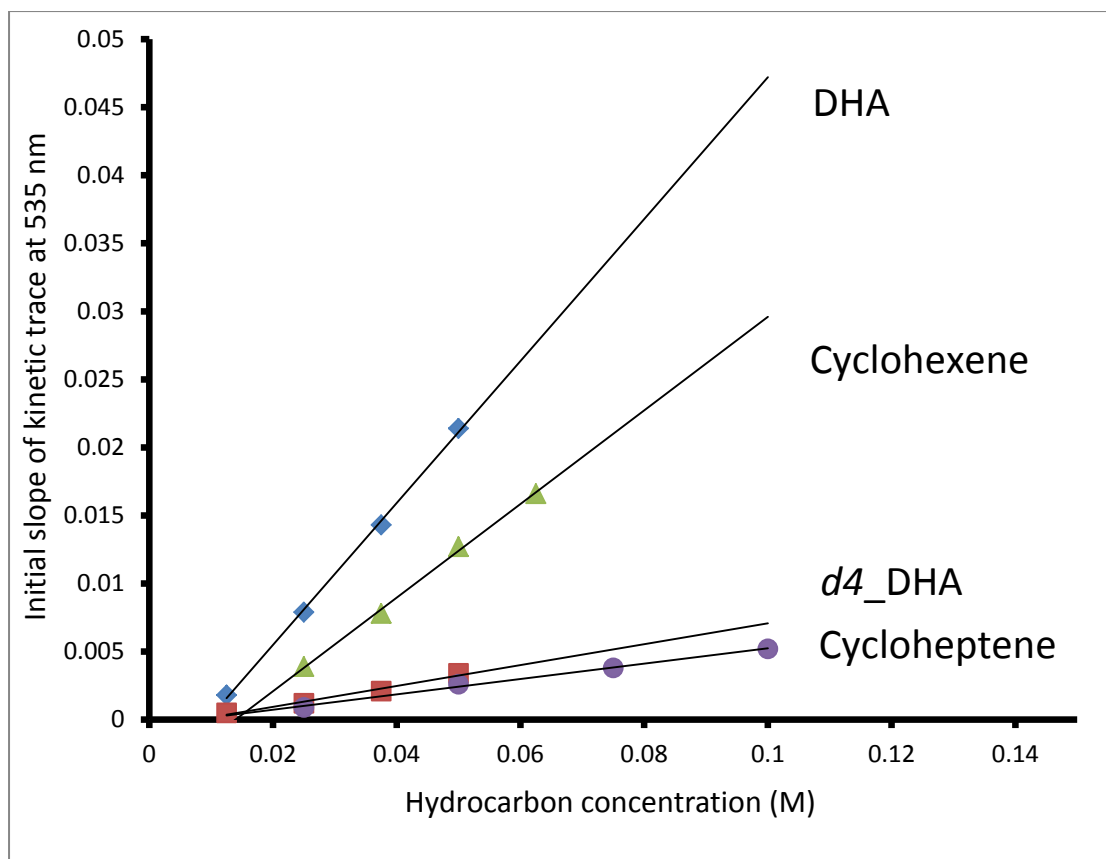
Figure 4.3 Initial slope of the kinetic trace, which follows the changes in absorbance at 535 nm from 0.4 to 2.0 s for the reaction between 0.5 mM $[Fe(bbpc)(MeCN)_2]^{2+}$ with a variety of hydrocarbon substrate in O_2 saturated MeCN at 295 K. These changes correlate to the initial rates of the reactions. The data are well fit by linear functions; in all four cases, R>0.99. The slopes are 0.52 (DHA), 0.077 (d4_DHA), 0.34 (cyclohexene), and 0.056 (cycloheptene).
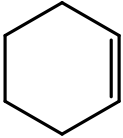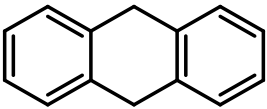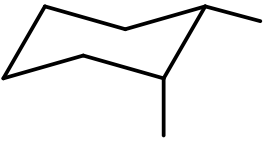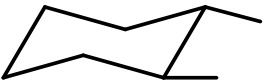
Substrate	Products (TON)
	2-Cyclohexen-1-one (20) 2-Cyclohexen-1-ol (4)
	Anthracene (30) Anthrone (11) Anthroquinone (trace)
	No reaction
  cis	*trans*-1,2-Dimethylcyclohexanol (1.0) *cis*-1,2-Dimethylcyclohexanol (0.7) *cis*-3,4-Dimethylcyclohexanone/ol (0.4)[a] *cis*-2,3-Dimethylcyclohexanone/ol (0.1)[a]
  trans	*trans*-3,4-Dimethylcyclohexanone/ol (0.8)[a] *trans*-2,3-Dimethylcyclohexanone/ol (0.4)[a] *cis*-1,2-Dimethylcyclohexanol (0.6) *trans*-1,2-Dimethylcyclohexanol (0.2)

Table 4.1 Turnover numbers for the $[Fe(bbpc)(MeCN)_2]^{2+}$-catalyzed oxidation of organic substrates by O_2 in MeCN. All reactions were run in MeCN under air at 295 K. Yields were measured by GC at 2 h. The initial substrate concentration was 500 mM. The initial concentration of $[Fe(bbpc)(MeCN)_2](SbF_6)_2$ was 1.0 mM. [a]Secondary carbon oxidation products are inseparable mixtures of the alcohol and ketone.

Hydrocarbon Reactivity

The reactions between $[Fe(bbpc)(MeCN)_2]^{2+}$, O_2, and hydrocarbons turn over, albeit slowly. When the catalyst and substrate are placed under N_2, oxidation of neither iron nor hydrocarbon is observed; the EPR spectra corresponding to these

anaerobic solutions are featureless. Over the course of 2 h, the Fe(II) catalyzes 20 turnovers for the conversion of cyclohexene to 2-cyclohexenol and 2-cyclohexenone by air (Table 4.1). The chemistry differs from the previously reported catalysis of cyclohexene by H_2O_2 in that the ketone is the favored product. In contrast with the TMC system, no dehydrogenation is observed. 9,10-Dihydroanthracene (DHA), conversely, is dehydrogenated to anthracene, with a substantial amount of anthrone as a secondary product. The alkanes *trans*- and *cis*-1,2-dimethylcyclohexanes are oxidized to mixtures of ketones and alcohols, with the catalyst turning over slightly over 2 times over the course of 2 h. To our best knowledge, this represents the first instance of aliphatic C-H bonds being oxidized by O_2 with a non-heme iron compound serving as the catalyst; previously reported chemistry activated thermodynamically weaker benzylic or allylic C-H bonds. The 59% (*cis*) and 75% (*trans*) retentions of regioselectivity for the tertiary alcohol products are low relative to most non-heme iron oxidants, with the notable inclusion of $[Fe(bbpc)(OOH)]^{2+}$.[19, 35, 36] These numbers may suggest a longer-lived organic radical intermediate. Another significance is that the oxidation of 1,2-dimethylcycohexane substrates by O_2 occurs on the tertiary carbons to a greater extent than that by H_2O_2.[19] Tertiary oxidation accounts for 77% (*cis*) and 40% (*trans*) of the organic products of the O_2 reactions; when H_2O_2 is the terminal oxidant, these percentages are 58% and 17, respectively.

Aliphatic C-H bonds on primary and secondary carbons are more difficult to activate, and substrates containing exclusively these sorts of C-H bonds cannot initiate the reactivity. Aerobic solutions of $[Fe(bbpc)(MeCN)_2]^{2+}$ and cyclohexane, for instance, are indefinitely stable, with no alkane oxidation observed over 3 d. We attribute the observed secondary carbon oxidation in Table 4.1 to Fe(III)-OOH species. The observed reactivity therefore relies on at least two oxidants, with the first, tentatively

a ferric superoxo species, being relatively weak. That detectable levels of [Fe(bbpc)(OOH)(MeCN)]$^{2+}$ accumulate and persist suggests that the Fe(III)-OOH species and/or its successors oxidizes substrates more slowly, even though the relevant metal-based oxidant(s) is capable of activating more robust C-H bonds.

4.4 Conclusions

In summary, we have identified a ferric hydroperoxide complex that forms during the catalysis of hydrocarbon oxidation by O_2. The formation of this species relies upon the presence of a substrate with one or more weak C-H bonds (tertiary alkane or weaker). The [Fe(bbpc)(MeCN)$_2$]$^{2+}$ compound catalyzes the oxidation of many hydrocarbons by O_2. We speculate that the initial metal-based oxidant is either a ferric superoxo complex or an isoelectronic species.

Appendix
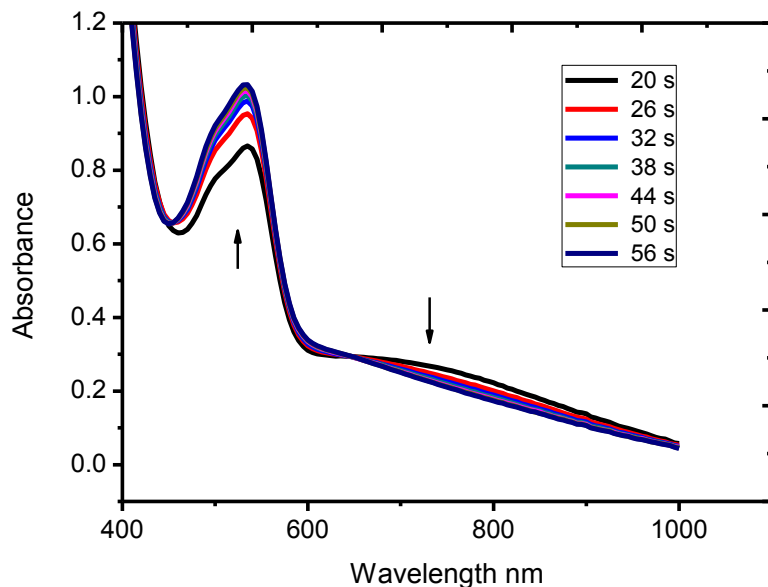
Figure 4A.1 UV-Vis spectrum of 0.89 mM [Fe(bbpc)(MeCN)$_2$](SbF$_6$)$_2$, 139 mM cyclohexene in O$_2$ saturated CH$_3$CN (~8 mM at room temperature, 1 atm.)
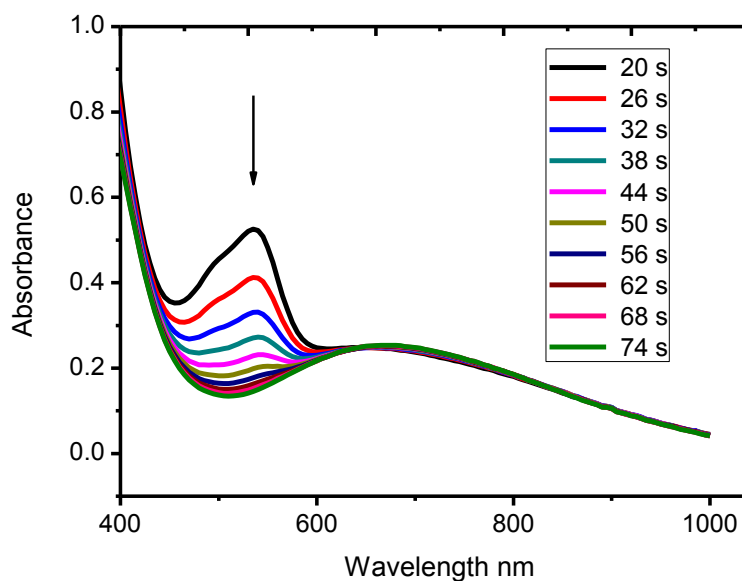
Figure 4A.2 HClO$_4$ added into the solution monitored in Figure 4.A1. The initial concentrations are 0.8 mM [Fe(bbpc)(MeCN)$_2$](SbF$_6$)$_2$, 125 mM cyclohexene, 25 mM HClO$_4$.
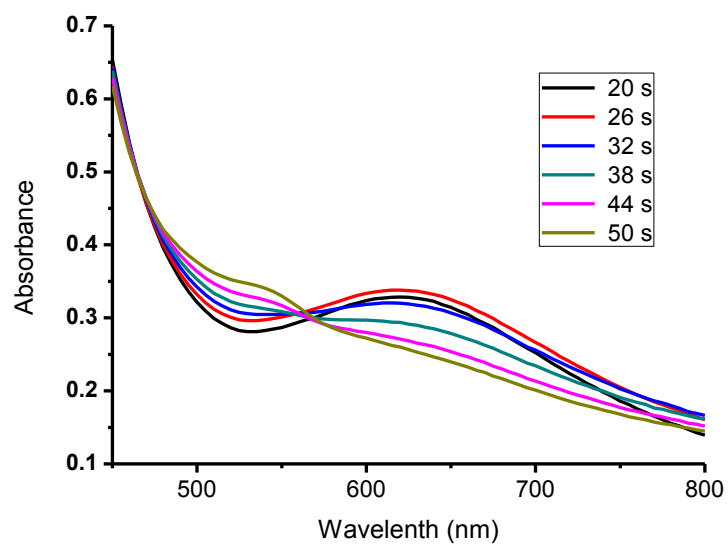
Figure 4A.3 UV-Vis spectrum of 0.5 mM [Fe(bbpc)(MeCN)$_2$](SbF$_6$)$_2$, 500 mM cyclohexene in O$_2$ saturated CH$_3$CN. The UV/Vis feature at ~650 nm is much more prominent when the initial concentration of cyclohexene is high.
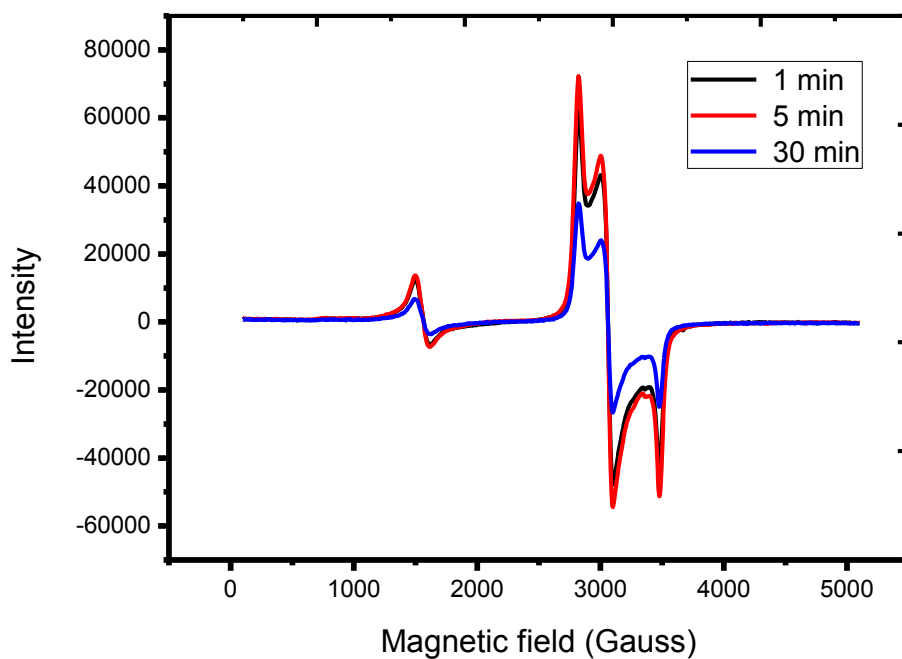
Figure 4A.4 Time-dependence X-band EPR analysis of the reaction between 1.0 mM
$[Fe(bbpc)(MeCN)_2]^{2+}$ and 4.0 mM H_2O_2 in MeCN. At 1 min (black), 5 min (red), and
30 min (blue), aliquots were frozen and analyzed at 20 K. The high-spin components
of each spectrum ($g = 4.28$) were integrated over the 100-2200 Gauss region. The
low-spin components of each spectrum ($g = 2.37, 2.19, 1.93$) were integrated over the
2200-5100 Gauss region. The ratios of the intensities of the low-spin: high-spin
components were: 3.3 (1 min), 3.5 (5 min), and 3.0 (30 min). These ratios are within
experimental error of each other. The overall intensity of the Fe(III) signal decreases
by ~45% from 5 to 30 min.
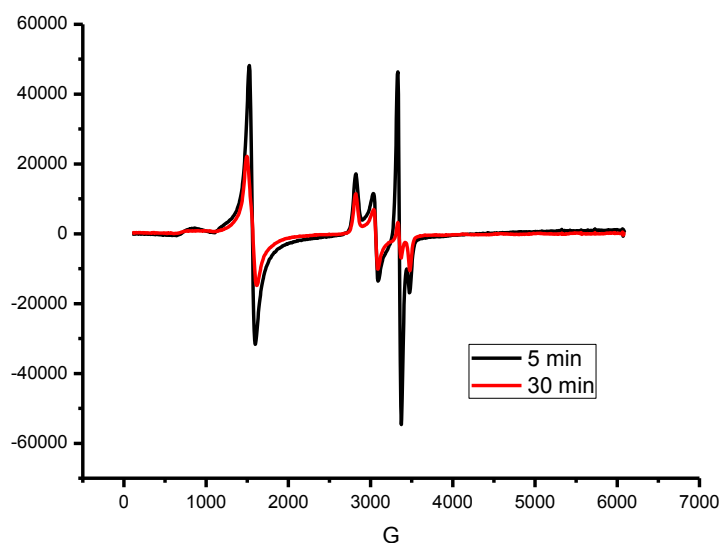
Figure 4A.5 Time-dependence X-Band EPR spectra depicting the reaction between 1 mM [Fe(bbpc)(MeCN)$_2$](SbF$_6$)$_2$ and 250 mM cyclohexene under air at 295 K. At 5 min (black) and 30 min (red), Aliquots were frozen at 20 K. Of note is the additional feature at 3350 Gauss (g=2.00), which may correspond to an organic radical.
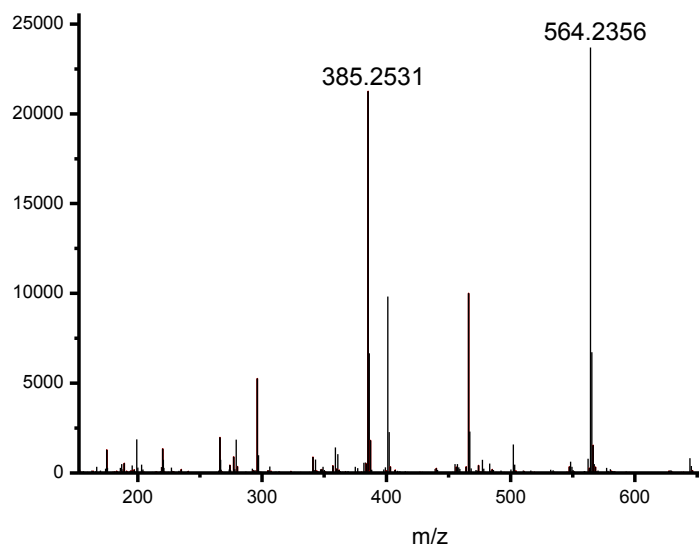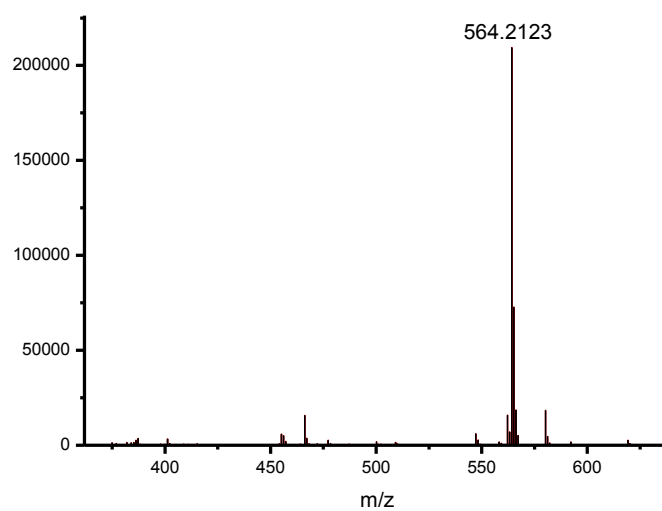

Figure 4A.6 Mass spectrum of the species generated from the reaction between 1.0 mM [Fe(bbpc)(MeCN)$_2$](SbF$_6$)$_2$ and 400 mM cyclohexene in MeCN under air at 295 K. The spectrum was acquired 20 s after the reagents were mixed. The m/z feature at 564.2 is assigned to [Fe(bbpc)(O$_2$)]$^+$, the conjugate base of [Fe(bbpc)(OOH)]$^{2+}$. The 385.3 m/z feature is tentatively assigned to oxidatively degraded ligand (bbpc − picolyl arm has MW = 385.2).

Figure 4A.7 Mass spectrum of the species generated from the reaction between 1.0 mM [Fe(bbpc)(MeCN)$_2$](SbF$_6$)$_2$ and 3.0 mM H$_2$O$_2$ in MeCN under air at 295 K. The spectrum was acquired 20 s after the reagents were mixed. The m/z feature at 564.2 is assigned to [Fe(bbpc)(O$_2$)]$^+$, the conjugate base of [Fe(bbpc)(OOH)]$^{2+}$.
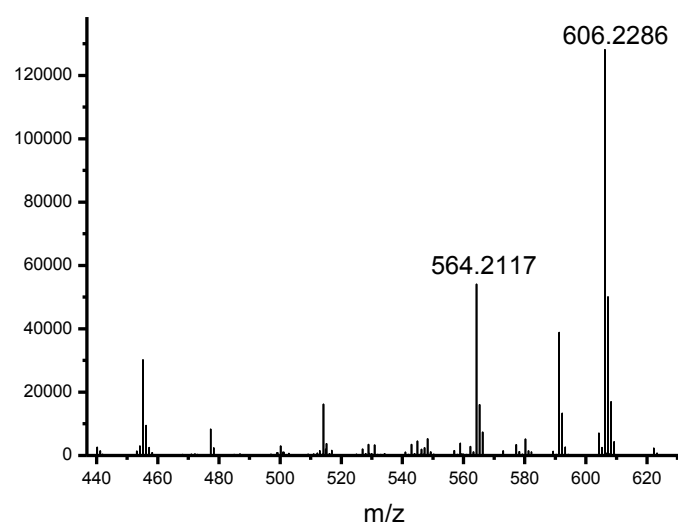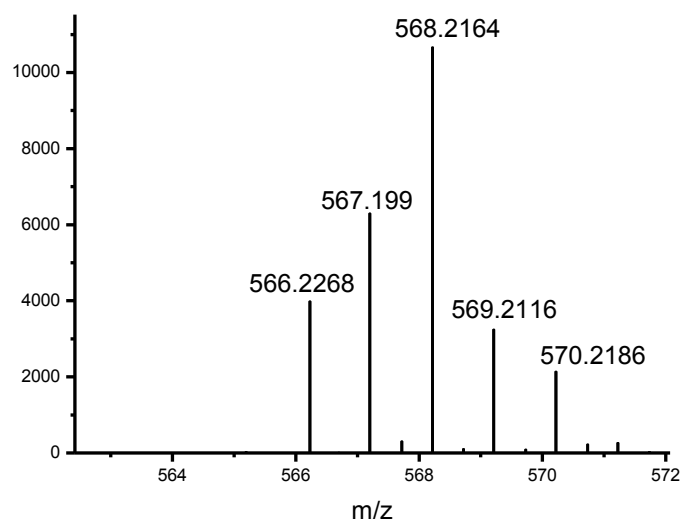
Figure 4A.8 Mass spectrum of the species generated from the reaction between 1.0 mM [Fe(bbpc)(MeCN)$_2$](SbF$_6$)$_2$, 400 mM cyclohexene and 100 mM AcOH in MeCN under air at 295 K. The spectrum was acquired 20 s after the reagents were mixed. The m/z feature at 606.2 is assigned to [Fe(bbpc)(OOH)(CH$_3$CN)]$^+$.

Figure 4A.9 Mass spectrum of the species generated from the reaction between 1.0 mM [Fe(bbpc)(MeCN)$_2$](SbF$_6$)$_2$, 200 mM cyclohexene and ^{18}O$_2$ at 295 K. The spectrum was acquired 20 s after the reagents were mixed. The m/z feature at 566.2 is assigned to [Fe(bbpc)(^{16}O^{18}O)]$^+$. The m/z feature at 568.2 is assigned to [Fe(bbpc)(^{18}O^{18}O)]$^+$.

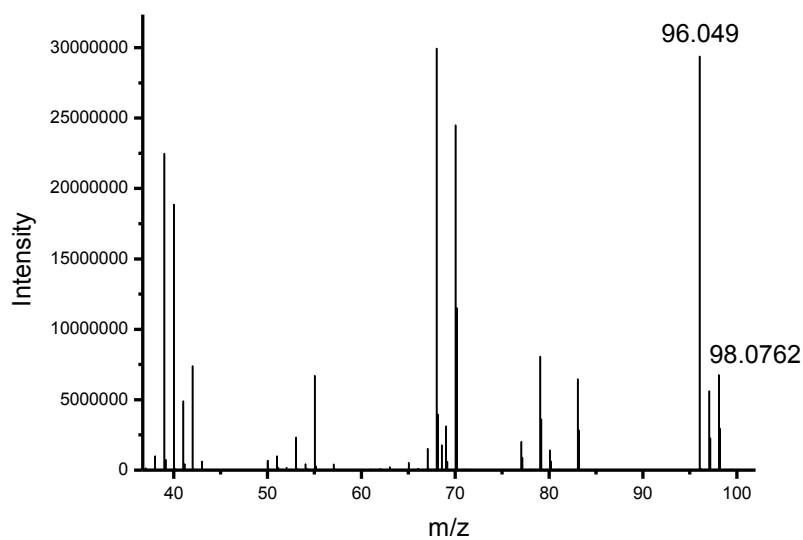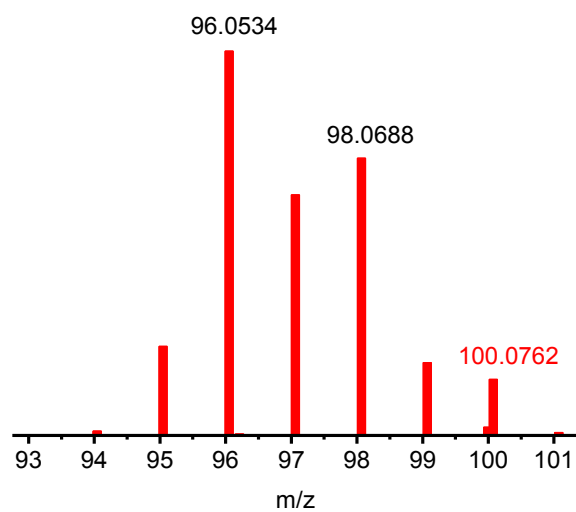**Figure 4A.10** GC/MS spectra of $^{18}O_2$ (top) and $^{16}O_2$ (bottom) oxidized cyclohexene products. The top spectrum is an expanded view in the m/z region 93-101. The m/z feature at 96.0534 is assigned to $C_6H_8{}^{16}O$; the one at 98.0688 is assigned to the mixture of $C_6H_9{}^{16}OH$ and $C_6H_8{}^{18}O$; the one at 100.0762 is assigned to $C_6H_9{}^{18}OH$.
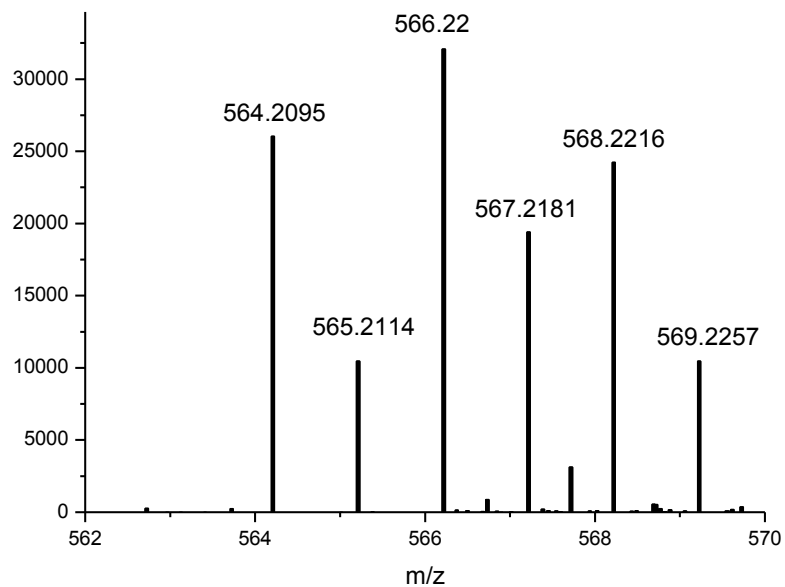
Figure 4A.11 Mass spectrum of the species generated from the reaction between 1.0 mM [Fe(bbpc)(MeCN)$_2$](SbF$_6$)$_2$, 400 mM cyclohexene and 3 mM H$_2$^{18}O in MeCN under air at 295 K. ^{18}O could be introduced into the reactive intermediate via water. The spectrum was acquired 20 s after the reagents were mixed. The m/z feature at 564.2 is assigned to [Fe(bbpc)(O$_2$)]$^+$, the conjugate base of [Fe(bbpc)(OOH)]$^{2+}$. The new features at 566.2 and 568.2 are assigned to [Fe(bbpc)(^{18}O^{16}O)]$^+$ and [Fe(bbpc)(^{18}O^{18}O)]$^+$, respectively.
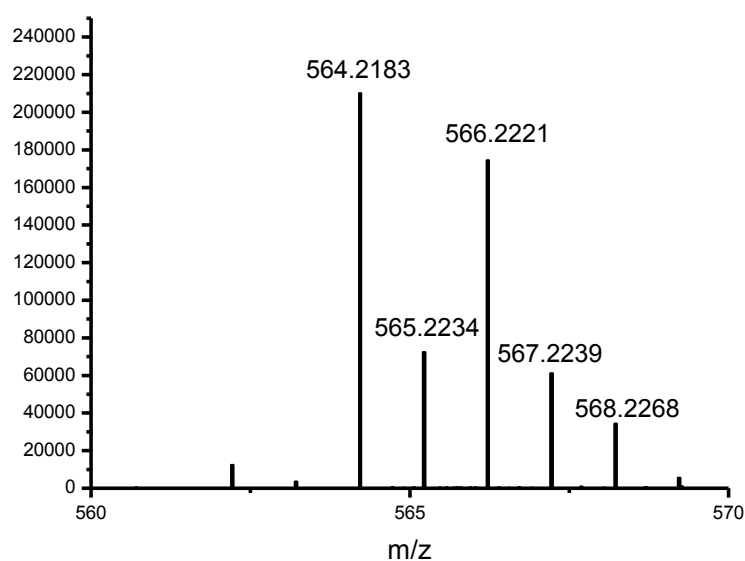
Figure 4A.12 Mass spectrum of the species generated from the reaction between 1.0 mM [Fe(bbpc)(MeCN)$_2$](SbF$_6$)$_2$ and 3.0 mM H$_2$O$_2$ in MeCN under air at 295 K. 3 mM H$_2$^{18}O was added to the sample to assess whether ^{18}O could be introduced via water. The spectrum was acquired 20 s after the reagents were mixed. The m/z feature at 564.2 is assigned to [Fe(bbpc)(O$_2$)]$^+$, the conjugate base of [Fe(bbpc)(OOH)]$^{2+}$. The new features at 566.2 and 568.2 are assigned to [Fe(bbpc)(^{18}O^{16}O)]$^+$ and [Fe(bbpc)(^{18}O$_2$)]$^+$, respectively. Note that the H$_2$O$_2$ was added as a 30 wt% solution in water, accounting for the lesser ^{18}O incorporation relative to the experiment described in **Figure 4.A11**.
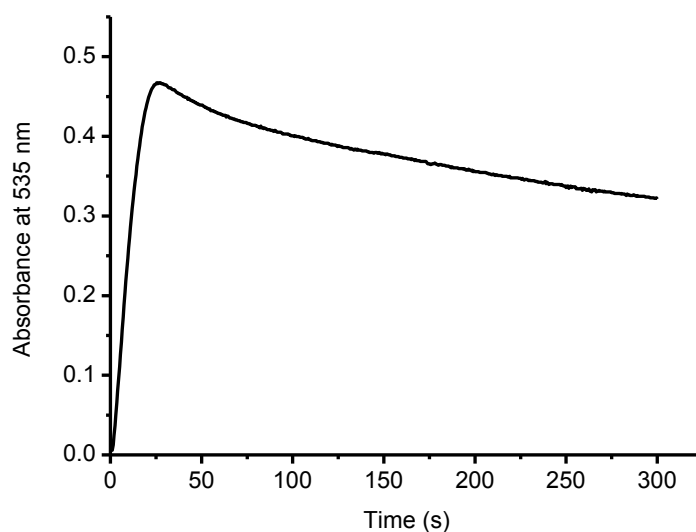
Figure 4A.13 Sample kinetic run showing the reaction between 0.5 mM [Fe(bbpc)(MeCN)$_2$]$^{2+}$ and 200 mM cyclohexene in aerated MeCN at 295 K. When the concentration of cyclohexene is high enough, a noticeable peak in the absorbance occurs between 20-30 s. The data could not be adequately fit to a single (A→B) or double (A→B→C) exponential model.

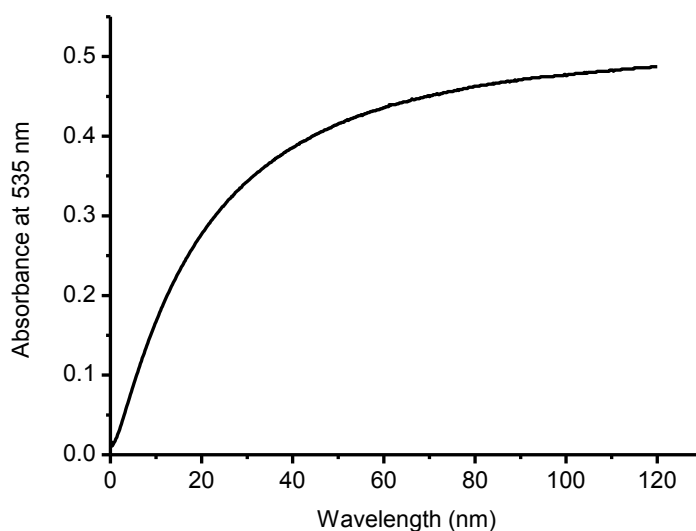**Figure 4A.14** Sample kinetic run showing the reaction between 0.5 mM [Fe(bbpc)(MeCN)$_2$]$^{2+}$ and 50 mM cyclohexene in aerated MeCN at 295 K. In this case, the concentration of cyclohexene is too low to observe the peak found in **Figure 4A.13**. The data could not be adequately fit to a single (A→B) or double (A→B→C) exponential model.

105

References

(1) Burger, R. M.; Peisach, J.; Horwitz, S. B. *J. Biol. Chem.* **1981**, *256*, 11636-11644.

(2) Decker, A.; Chow, M. S.; Kemsley, J. N.; Lehnert, N.; Solomon, E. I. *J. Am. Chem. Soc.* **2006**, *128*, 4719-4733.

(3) Costas, M.; Mehn, M. P.; Jensen, M. P.; Que, L., Jr. *Chem. Rev.* **2004**, *104*, 939-986.

(4) England, J.; Gondhia, R.; Bigorra-Lopez, L.; Petersen, A. R.; White, A. J. P.; Britovsek, G. .J. P. *Dalton Trans.* **2009**, 5319-5334.

(5) Que, L.,Jr. *Acc. Chem. Res.* **2007**, *40*, 493-500.

(6) Nam. W. *Acc. Chem. Res.* **2007**, *40*, 522-531.

(7) Jaafar, H.; Vileno, B.; Thibon, A.; Mandon, D. *Dalton Trans.* **2011**, *40*, 92-106.

(8) Lee, Y.-M.; Hong, S.; Morimoto, Y.; Shin, W.; Fukuzumi, S.; Nam, W. *J. Am. Chem. Soc.* **2010**, *132*, 10668-10670.

(9) Mandon, D.; Jaafar, H.; Thibon, A. *New J. Chem.* **2011**, *35*, 1986-2000.

(10) Mukherjee, A.; Martinho, M.; Bominaar, E. L.; Münck, E.; Que, L., Jr. *Angew. Chem. Int. Ed.* **2009**, *48*, 1780-1783.

(11) Mukherjee, A.; Cranswick, M. A.; Chakrabarti, M.; Paine, T. K.; Fujisawa, K.; Münck, E.; Que, L., Jr. *Inorg. Chem.* **2010**, *49*, 3618-3628.

(12) Gupta, R.; Borovik, A. S. *J. Am. Chem. Soc.* **2003**, *125*, 13234-13242.

(13) Borovik, A. S. *Acc. Chem. Res.* **2005**, *38*, 54-61

(14) Mukherjee, J.; Lucas, R. L.; Zart, M. K.; Powell, D. R.; Day, V. W.; Borovik, A. S. *Inorg. Chem.* **2008**, *47*, 5780-5786.

(15)   Cho, J.; Jeon, S.; Wilson, S. A.; Liu, L. V.; Kang, E. A.; Braymer, J. J.; Lim, M. H.; Hedman, B.; Hodgson, K. O.; Valentine, J. S.; Solomon, E. I.; Nam, W. *Nature* **2011**, *478*, 502-505.

(16)   Hong, S.; Lee, Y.-M.; Shin, W.; Fukuzumi, S.; Nam, W. *J. Am. Chem. Soc.* **2009**, *131*, 13910-13911.

(17)   Li, F.; Meier, K. K.; Cranswick, M. A.; Chakrabarti, M.; Van Heuvelen, K. M.; Münck, E.; Que, L., Jr. *J. Am. Chem. Soc.* **2011**, *133*, 7256-7259.

(18)   Chen, K.; Que, L., Jr. *J. Am. Chem. Soc.* **2001**, *123*, 6327-6337.

(19)   He, Y.; Gorden, J. D.; Goldsmith, C. R. *Inorg. Chem.* **2011**, *50*, 12651-12660.

(20)   Ho, R. Y. N.; Roelfes, G.; Hermant, R.; Hage, R.; Feringa, B. L.; Que, L., Jr. *Chem. Commun.* **1999**, 2161-2162.

(21)   Mialane, P.; Nivorojkine, A.; Pratviel, G.; Azéma, L.; Slany, M.; Godde, F.; Simaan, A.; Banse, F.; Kargar-Grisel, T.; Bouchoux, G.; Sainton, J.; Horner, O.; Guilhem, J.; Tchertanova, L.; Meunier, B.; Girerd, J.-J. *Inorg. Chem.* **1999**, *38*, 1085-1092.

(22)   Roelfes, G.; Lubben, M.; Chen, K.; Ho, R. Y. N.; Meetsma, A.; Genseberger, S.; Hermant, R. M.; Hage, R.; Mandal, S. K.; Young, V. G., Jr.; Zang, Y.; Kooijman, H.; Spek, A. L.; Que, L., Jr; Feringa, B. L. *Inorg. Chem.* **1999**, *38*, 1929-1936.

(23)   Roelfes, G.; Lubben, M.; Hage, R.; Que, L., Jr.; Feringa, B. L. *Chem. Eur. J.* **2000**, *6*, 2152-2159.

(24)   Martinho, M.; Blain, G.; Banse, F. *Dalton Trans.* **2010**, *39*, 1630-1634.

(25)   Rohde, J.-U.; In, J.-H.; Lim, M. H.; Brennessel, W. W.; Bukowski, M. R.; Stubna, A.; Münck, E.; Nam, W.; Que, L., Jr. *Science* **2003**, *299*, 1037-1039.

(26)   Goldsmith, C. R.; Jonas, R. T.; Stack, T. D. P. *J. Am. Chem. Soc.* **2002**, *124*, 83-96.

(27)   Achord, J. M.; Hussey, C. L. *Anal. Chem.* **1980**, *52*, 601-602.

(28)   Bassan, A.; Blomberg, M. R. A.; Siegbahn, P. E. M.; Que, L., Jr. *J. Am. Chem. Soc.* **2002**, *124*, 11056-11063.

(29)   Comba, P.; Maurer, M.; Vadivelu, P. *Inorg. Chem.* **2009**, *48*, 10389-10396.

(30)   Seo, M. S.; In, J.-H.; Kim, S. O.; Oh, N. Y.; Hong, J.; Kim, J.; Que, L., Jr.; Nam, W. *Angew. Chem. Int. Ed.* **2004**, *43*, 2417-2420.

(31)   Meknouche, Y.; Ménage, S.; Toia-Duboc, C.; Fontecave, M.; Galey, J.-B.; Lebrun, C.; Pécaut, J. *Angew. Chem. Int. Ed.* **2001**, *40*, 949-952.

(32)   Anbar, M.; Guttmann, S. *J. Am. Chem. Soc.* **1961**, *83*, 2035-2037.

(33)   Anbar, M. *J. Am. Chem. Soc.* **1961**, *83*, 2031-2035.

(34)   Luo, Y.-R. *Handbook of Bond Dissociation Energies in Organic Compounds*; CRC Press: Boca Raton, FL, **2003**.

(35)   Chen. K.; Que, L., Jr. *J. Am. Chem. Soc.* **2001**, *123*, 6327-6337.

(36)   Gómez, L.; Garcia-Bosch, I.; Company, A.; Benet-Buchholz, J.; Polo, A.; Sala,X; Ribas, X.; Costas, M. *Angew. Chem. Int. Ed.* **2009**, *48*, 5720-5723.

(37)   Russell, G. A. *J. Am. Chem. Soc.* **1957**, *79*, 3871-3877.

(38)   Stoll, S.; Schweiger, A. *J. Magn. Reson.* **2006**, *178*, 42-55.